2009

Dynamic Analysis of a Rotor Bearing System

Sandi Elhibir
Cleveland State University

DYNAMIC ANALYSIS OF A ROTOR-BEARING SYSTEM

SANDI ELHIBIR

Bachelor of Science in Mechanical Engineering

Cleveland State University

August, 1997

submitted in partial fulfillment of requirements for the degree

MASTER OF SCIENCE IN MECHANICAL ENGINEERING

at the

CLEVELAND STATE UNIVERSITY

May, 2009

This thesis has been approved

for the Department of ENGINEERING

and the College of Graduate Studies by

_____

Thesis Chairperson, Dr. Majid Rashidi

_____

Department & Date

_____

Dr. John Frater

_____

Department & Date

_____

Dr. Paul Lin

_____

Department & Date

DEDICATION

To the four women who have shaped the person I have become: my grandmother, Fatima Gafurovic, my mother, Zinka Elhibir, my mother-in-law, Riva Reznichenko, and last but not least, my wife, Liora Reznichenko.

ACKNOWLEDGEMENTS

I would like to thank my academic advisor, Dr. Rashidi, for his support. His encouragement and guidance is greatly appreciated in the development of this thesis. I also would like to thank the members of my committee: Dr. Frater and Dr. Lin for their time and advice.

My sincerest gratitude goes out to my two brothers, Hany and Riemy Elhibir, my father, Mahmoud Elhibir, my friends and work colleagues for their continued support throughout my academic career. I am especially grateful to my father-in-law, Yury Reznichenko, and my work supervisor, Brian Honeck, for their help and encouragement during the pursuit of my master's degree. Without their continued support, my success would have not been possible.

DYNAMIC ANALYSIS OF A ROTOR-BEARING SYSTEM

SANDI ELHIBIR

ABSTRACT

This thesis presents the results of the finite element analysis (FEA) approach for designing a Permanent Magnet Alternator (PMA). The PMA is configured as a cantilever hollow shaft supported by two identical rolling contact bearings. The performance requirements of the PMA are a maximum operating speed of 16,000 *rpm*, with a maximum shaft displacement of less than 0.010 *in* at its free end.

The static and dynamic results of a cantilever beam was predicted by closed form solutions and verified to those results obtained from FEA for code validation. A mathematical model of a rotor-bearing system was proposed and analyzed for its dynamic unbalance response when subjected to a harmonic excitation force at the free end. The proposed design for a rotor-bearing geometry was modeled by SolidWorks, and then analyzed in COSMOSWorks using second order tetrahedral solid elements.

Lastly, the FEA results of six parametric studies of a rotor-bearing system are presented. In these parametric studies, the rotor-bearing configuration from parametric study No.5 proved to satisfy the PMA first natural frequency and displacement requirements. The first natural frequency was determined to be 358,171 *rpm*, which is 22 times of the maximum operating speed of the PMA. Additionally, the maximum steady-state UX and UY displacements were obtained at 2.35E-06 *in* and 1.06E-05 *in*, respectively, which is less than the maximum allowable shaft displacement.

TABLE OF CONTENTS

LIST OF TABLES

Table Page

LIST OF FIGURES

Figure Page

NOMENCLATURE

A	Area
A.C.	Alternating current
α_n	Mode shape constant
$\beta_n l$	Frequency parameter
$\delta_{Closed\ form\ solution}$	Static deflection using closed form solution
δ_{FEA}	Static deflection using FEA
e	Eccentricity
E	Young's modulus
FEA	Finite element analysis
FEM	Finite element method
f_x	External force in the x-direction
f_y	External force in the y-direction
I	Moment of inertia
ID	Internal diameter
in	Inches
k	Stiffness
Kg	Kilograms
K_{xx1}	Stiffness in the x-direction for bearing No.1
K_{xx2}	Stiffness in the x-direction for bearing No.2
K_{yy1}	Stiffness in the y-direction for bearing No.1
K_{yy2}	Stiffness in the y-direction for bearing No.2
l	Length
lbf	Pound force
M	Mass
m	Meters
No.	Number
^{o}	Degree
$\varnothing$	Diameter
OD	Outside Diameter
P	Point Load
PM	Permanent Magnet
PMA	Permanent Magnet Alternator
ρ	Density
rad/sec	Radians per second
RPM	Revolutions per minute
sec	Seconds

t	Time
UX	X-axis displacement
UY	Y-axis displacement
UZ	Z-axis displacement
ω	Angular velocity
ω_n	n^{th} natural frequency of the system
$Y_r(x)$	Mode shape
Ω	Rotor angular speed
%	Percentage

CHAPTER I

INTRODUCTION

1.1 Historical Background

Various studies have incorporated foundation effects in rotor-bearing system analyses. Kirk and Gunter [1] analyzed the steady state and transient responses of the Jeffcott rotor for elastic bearings mounted on damped and flexible supports. They disregarded the rotor flexibility and the disk gyroscopic effects in the formulation of the governing equations of motion, and provided design charts for both turned and off-turn support conditions to minimize the foundation characteristics of the rotor amplitude and force transmitted over a given speed range. Smith [2] investigated the Jeffcott rotor with internal damping to include a mass less, damped and flexible support system. Lund [3] and Gunter [4] showed that damped and flexible support might also improve the stability of high-speed rotors. In addition, Lund and Sternlicht [5], Dowrski [6], and Gunter [7] demonstrated that a significant reduction in transmitted force could be achieved through proper design of a bearing support system. Pilkey [8] presented an efficient two-stage procedure for optimizing suspension systems of rotors. From these studies, the dynamic

performance problems in association with the foundation effects on mass, damping, and stiffness of the Jeffcott rotor incorporating the bearing support systems, could be found.

Gasch [9] explored rotating shafts of large turbo-rotors by way of finite element analysis. He introduced foundation dynamics into the rotor equations via reacceptance analysis, which was obtained from modal testing and modal analysis. Vance [10] provided comparison results for computer predictions and experimental measurements on a rotor-bearing test apparatus, modeling the rotor-bearing system to include foundation impedance effects by using the transfer matrix method. Stephenson and Rouch [11] have utilized the finite element method to analyze rotor-bearing foundation systems. They provided a procedure using modal analysis techniques, which when applied, could measure the frequency response functions to include the dynamic effects of the foundation structure.

Many finite element procedures developed have been implemented and geared toward generalizing and improving the formulation of the rotor-bearing system, such as by Ruhl and Booker [12]. In their early investigation, the effects of rotary inertia, gyroscopic moments, shear deformation, axial load, and internal damping have been neglected. Nelson and McVaugh [13] have utilized the Raleigh beam finite to formulate the rotor-bearing systems by including the additional effects mentioned above. Zorzi and Nelson [14] in 1977 and 1980 [15] worked on the generalization of a similar model by including internal damping and axial torque respectively. Further, Nelson [16] and Greenhill [17] utilized the Timoshenko beam shape functions to establish the shaft element formulation. Ozguven and Ozkan [18] additionally improved the shaft finite element model by including the effect of internal hysteric and viscous damping.

There are many software packages available today for analyzing dynamic responses, natural frequencies and modal characteristics of rotor-bearing systems [19, 20]. However, the software may be limited if the involved foundation is very complex.

These brief histories of “rotordynamics” help justify the premise that behavior of rotating machinery is best achieved through interplay between theory and practice. Rotor dynamics is not unique in this regard but does offer an unusual number of vivid examples. Lately, the balance between analysis and experience has been affected by the emergence of modern computational tools. Lest a fascination with these tools replace the lessons of practice, we would be wise to heed the words of Dara Childs [21], "the quality of predictions from a computer code has more to do with the soundness of the basic model and the skill and physical insight of the rotor dynamicist than the particular algorithm used. Good engineers get good results from good models, leading to sound engineering judgments with a variety of algorithms or computer codes. Superior algorithms or computer codes will not cure bad models or a lack of engineering judgment."

1.2 Motivation for Research

The Jeffcott rotor model has been around for over 80 years and despite its age, is widely used by many rotor dynamicists in their research. However, removing computational burden still does not address a need a need to develop models, which reflect basic properties of real systems within limited range of frequencies. These models offer useful tools of analyzing the behavior of linear dynamic systems. Also, such models

represent useful educational tools designed for better understanding of dynamic systems in general.

So far, most of the analytical approaches to the Jeffcott rotor model have been identical and concrete as it relates to a complex analysis approach. It is possible to develop a simpler and more user-friendly model which can easily be adapted to become a design tool for use in aerospace applications. State of the art research has also failed to make adequate comparisons between theoretical models and FEA data, hence, providing room for research in this particular area.

The rotor-bearing system of modern rotating machines constitutes a complex dynamic system. The challenging nature of rotor-dynamic problems has attracted many engineers whose investigations have contributed to the impressive progress in the study of rotating systems. Modern machinery is bound to fulfill the increasing economic demands for larger machines; higher quality, environmental acceptance in production, as well as inevitably growing end-user product requirements and expectations and the advances in vibration technology require exact and complete consideration of vibration characteristics of the PMA design in its basic conception and definition.

1.3 Research Objectives

The main objective of this research paper is to investigate the dynamics of a rotor-bearing system that allows the development of the Permanent Magnet Alternator (PMA) free from vibrational problems detrimental to its performance. The steps for the study are summarized below:

- Compare the results predicted by analytical analysis for the simple cantilever beam with those results obtained from FEA analysis (COSMOSWorks).
- Propose a design for the rotor-bearing system and analyze its dynamic response under a harmonic excitation force at the free end using FEA analysis (COSMOSWorks).
- Perform a parametric study for the rotor-bearing system for an acceptable configuration that satisfies the performance requirements of the Permanent Magnet Alternator (PMA).

CHAPTER II

DESIGN CONFIGURATION OF THE PMA

Permanent Magnet Alternator (PMA) is a 3-phase A.C. machine operating at a maximum speed of 16,000*rpm* (1,675.52*rad/sec*). The PMA is essentially comprised of a rotating part, the rotor, and a non-rotating part, the stator. The rotor is a cantilevered hollow shaft integral with a gearbox, where as the stator is mounted to flange-face of gearbox. The gearbox has a two-bearing support arrangement and is driven with a gear-set. In this research, only the rotor system will be analyzed to ultimately ensure no rotor-to-stator mechanical contact due to rotor shaft deflection, which would ultimately compromise the performance of the PMA.

An alternator is simply a power-generating machine that produces a sinusoidal output when a mechanical input to its shaft is applied. Alternators are used for wind energy, down-hole drilling, auxiliary power generation, military and aerospace applications. Typically, a rotating hub/magnet/retaining band assembly called the PM rotor turns within a stationary set of conductors wound in coils on an iron core called the stator. As the mechanical input causes the rotor to turn, the magnetic field cuts across the

conductors in the stator and generates an electrical current. The rotor magnetic field induces an AC voltage in the stator windings. This induced voltage is reversed every 180°. First a north pole of the field cuts across one section of the stator winding while a south pole cuts across another section of the winding. After each 180° of rotation, this process is reversed, creating an alternating voltage in the stator windings.

There are three sets of stator windings called phase A, B and C, each physically offset to ensure the rotating field produces three phase alternating currents, displaced by one-third of a period with respect to each other.

The main function of this permanent magnet alternator machine is to provide continuous power to the flight control computer on an aircraft.

2.1 Design Parameters and Performance Requirements of the PMA

In this thesis, the Permanent Magnet Alternator (PMA) design parameters and performance requirements are considered to be critical factors in the analysis of the dynamic response of a rotor-bearing system.

The PMA constrained design parameters are:

- Shaft overall length
- Shaft outside diameter
- Bearing size and geometry

The PMA unconstrained design parameters are:

- Bearing-to-bearing axial distance
- Shaft internal diameter
- Bearing size and geometry

The PMA performance requirements are:

- First natural frequency (ω_1) > 20 times of the maximum operating speed of the PMA.
- The shaft UX and UY displacements < 0.010 inches to avoid a rotor-bearing system to stator mechanical contact.

After reviewing the Permanent Magnet Alternator (PMA) design parameters and performance requirements, a FEA code was validated to help design the PMA such that it meets the design and performance requirements. In order to validate the FEA code, a simple cantilever beam was analyzed using FEA software, COSMOSWorks. The results of COSMOSWorks analysis are compared with those predicted by closed form solutions. Appendix A contains the FEA code validation results for a cantilever beam. Appendix A includes the following results:

- Static deflection
- First four natural frequencies of vibration
- First four mode shapes of vibration
- Forced vibration

2.2 Results of the FEA Code Validation

Figure 2.1 shows a schematic view of the cantilever beam analyzed in Appendix A. Table 2.1 contains the physical parameters for this cantilever beam.

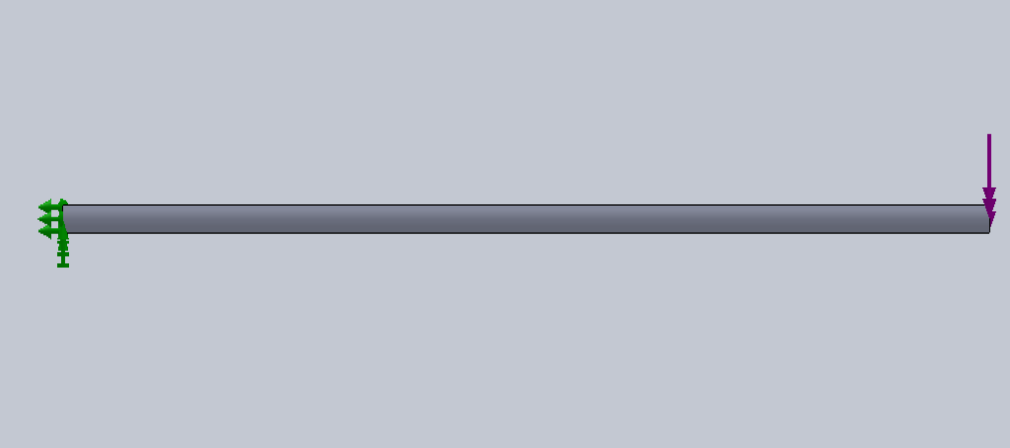

Figure 2.1– Schematic of a cantilever beam

Parameter	**Value**
Load (*P*)	20 *lbf*
Length (*l*)	24 *in*
Diameter (*d*)	0.5 *in*
Young's Modulus (*E*)	3.0E+07 lb/in^2
Density (ρ)	0.284 lb/in^3
Area (A)	0.196 in^2

Table 2.1– Physical parameters of a cantilever beam

Table 2.2 shows a comparison of the static deflection analysis of a cantilever beam obtained by the closed from solution approach and that of the FEA model.

$\delta_{Closed\ form\ solution}$ **(in)**	δ_{FEA} **(in)**	***% Error***
1.00065	0.985	1.6

Table 2.2– Summary of static deflection results

Table 2.3 shows a comparison of the first four natural frequencies of a cantilever beam obtained by the closed form solution approach and the FEA model.

Natural frequency	$\omega_{Closed\ form\ solution\ (rad/sec)}$	$\omega_{FEA\ (rad/sec)}$	Relative % error
ω_1	153.75	153.23	0.34
ω_2	970.84	959.41	1.18
ω_3	2,702	2,680.52	0.80
ω_4	5,301.11	5,236.22	1.22

Table 2.3 – Summary of natural frequency results

Table 2.4 shows a comparison of the first four mode shapes of a cantilever beam obtained by the closed form solution approach and the FEA model.

	Closed form solution			FEA			% Error		
Mode Shape	x/L_1	x/L_2	x/L_3	x/L_1	x/L_2	x/L_3	x/L_1	x/L_2	x/L_3
First	-	-	-	-	-	-	-	-	-
Second	0.78	-	-	0.76	-	-	2.56	-	-
Third	0.50	0.97	-	0.49	0.95	-	2.06	2.30	-
Fourth	0.36	0.64	0.91	0.35	0.63	0.89	2.78	1.56	2.20

Table 2.4 – Summary of mode shape results

Table 2.5 summarizes the displacement results of a cantilever beam FEA model when subjected to a harmonic excitation force at the free end.

Displacement Direction	Value (*in*)
UX	2.844E-4
UY	0.966
UZ	0.015

Table 2.5 – Forced vibration results of a cantilever beam using FEA

The results presented in Appendix A shows that the FEA prediction values for the static and dynamic response of a typical cantilever beam are close to the results obtained by the closed form solutions. The maximum error percentage was found to be 1.6% for the static deflection, 1.22% for the first four natural frequencies, and 2.78% for the fourth mode shape at x/L_1. Lastly, the maximum steady-state displacement of a cantilever beam was found to be 0.966 inches in the UY direction. The UY displacement value was expected to be higher than the UX and UZ directions, since the harmonic excitation force was applied in the UY direction.

CHAPTER III

MATHEMATICAL MODELING AND FINITE ELEMENT ANALYSIS OF A ROTOR-BEARING SYSTEM

According to Rao [30], a common source of such a sinusoidal force is unbalance in a rotating machine or, as in our case, the rotor-bearing system. Rotating machines include turbines, electric motors, fans, generators, or rotating shafts. Unbalance in rotating machinery is one of the main causes of vibration. A simplified model of such a machine is shown in Figure 3.1 below.

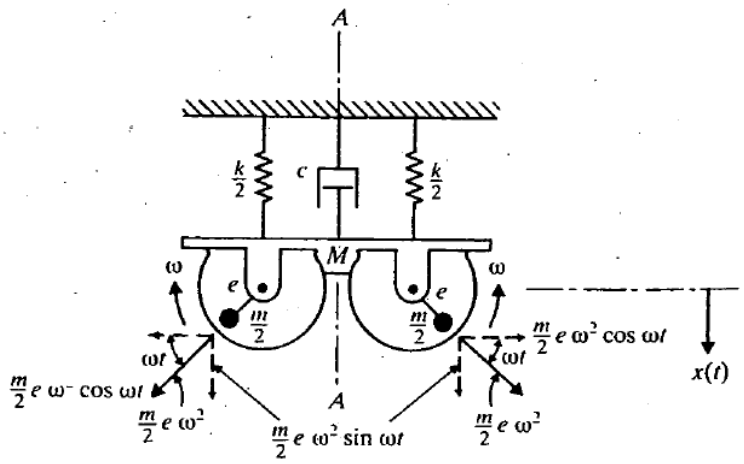

Figure 3.1 – Rotating unbalance masses [30]

The total mass of the machine is M, and there are two eccentric masses, $m/2$, rotating in opposite directions with a constant angular speed of rotation, ω. The centrifugal force $(me\omega^2)/2$ due to each mass will cause excitation of the mass M. We consider two equal masses $m/2$ rotating in opposite directions in order to have the horizontal components of excitation of the two masses cancels each other out. However, the vertical components of excitation add together and act along the axis of symmetry *A-A* in Figure 3.1. If the angular position of the masses is measured from a horizontal position, the total vertical component of the excitation is always given by [30]:

$$F(t) = me\omega^2 \sin \omega t \tag{3.1}$$

Therefore, the equation of motion is derived as [30]:

$$m\ddot{x} + c\dot{x} + kx = me\omega^2 \sin \omega t \tag{3.2}$$

Where, m is the unbalanced mass, e is the eccentricity, ω is the angular speed of the rotating shaft in radians per second and t is time is seconds.

This chapter describes a proposed design of a rotor-bearing system for analyzing its own behavior when subjected to a concentrated mass with a constant speed of rotation at its free end. This concentrated mass represents the mass of the rotating unbalanced PM rotor. The rotor shaft is hollow and supported by two identical ball bearings. The rolling element bearings are mechanical parts whose role is to support and locate the rotor shaft during operation. Each bearing contains two rings and between the rings, rolling elements (bearing balls). The rolling elements allow the relative motion between the rings as well as the correct positioning of them.

Additionally, there exists a cage whose main function is to keep the adequate angular separation of the rolling elements. The left end of the system is the drive end that incorporates gear teeth which mates with a pinion for driving the shaft. The shaft supports a PM rotor at the right end (free end) of the shaft.

3.1 Mathematical Model of a Rotor-Bearing System

The dynamic modeling of the rotor-bearing system is required to understand its dynamic behavior and the associated vibration problems. Early dynamic models of the rotor-bearing system were formulated either analytically or using the transfer matrix approach. The transfer matrix method solves dynamic problems in the frequency domain, which makes itself reasonable to analyze the steady-state responses of the rotor-bearing system. This method was first applied to the rotor-bearing system by Prohl [39] and was employed by Lund and Orcutt [40]. They constructed the transfer matrix of the rotor in sense of a continuous system and investigated the unbalance vibrations experimentally and analytically. In the 1970's the potential of finite element method was recognized. The first studies in this area were by Ruhl and Booker [12]. Based on various beam theories, many researchers have extended the capability of the rotor-bearing system analysis using the finite element method. Polk [41] presented a Rayleigh beam, Rayleigh [42], finite element in his work. Nelson and McVaugh [13] improved the Rayleigh beam theory in a finite rotating shaft element, which included the effects of translational and rotary inertia, axial load, and gyroscopic moments. Gash [43] refined the formulation by considering the destabilizing effect due to linear internal viscous damping. These

developments were subsequently generalized by Zorzi and Nelson [14]. Nelson [16] added shear deformation to the Rayleigh beam theory to develop a Timoshenko beam element. In this model, shear deformation effects was included but internal damping was neglected. Later, Özgüven and Özkan [18] extended these works by considering the effects of rotary inertia, axial load, gyroscopic moments, shear deformations, and internal hysteric and viscous damping in the same model.

Figure 3.2 shown below, illustrates a mathematical model of the external forces acting on a typical configuration of an unbalanced rotating machine, which consists of the components of a shaft, bearings, and foundation.

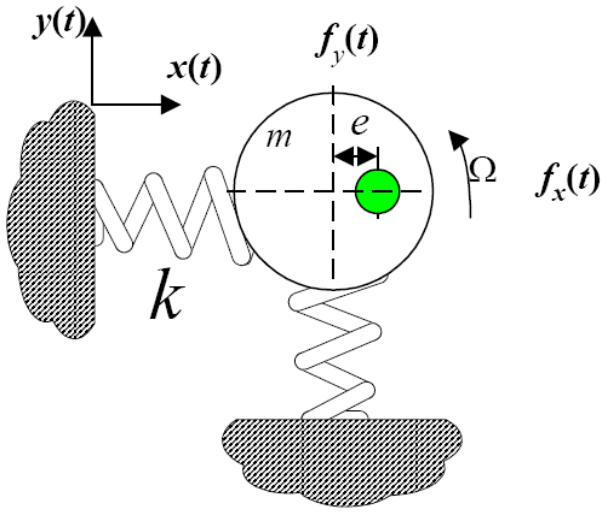

Figure 3.2 – Unbalanced rotating machine

From Figure 3.2, the equations of motion in the *x* and *y* directions are:

$$f_x(t) = m\ddot{x} + kx \tag{3.3}$$

$$f_y(t) = m\ddot{y} + ky \tag{3.4}$$

Solving for equations 3.3 and 3.4, the differential equation becomes:

$$\frac{d^2}{dt^2} m(x + e\cos\omega t) + kx = 0 \tag{3.5}$$

$$\frac{d^2}{dt^2} m(y + e\sin\omega t) + ky = 0 \tag{3.6}$$

Rearranging equations 3.5 and 3.6 and solving for equations 3.3 and 3.4, the external forces due to rotating unbalance with a constant speed of rotation are:

$$f_x(t) = me\omega^2 \cos\omega t \tag{3.7}$$

$$f_y(t) = me\omega^2 \sin\omega t \tag{3.8}$$

3.2 Finite Element Modeling of a Rotor-Bearing System

After reviewing the brief history of rotor-bearing systems and deriving the equations of motion for a typical unbalanced rotating machine, one may proceed with constructing a solid model in SolidWorks for the proposed rotor-bearing system. A SolidWorks model is the starting point to FEA analysis needed to study the dynamic behavior of the proposed rotor-bearing system when subjected to an eccentric mass rotating with a constant speed of rotation at the free end. Figure 3.3 depicts a schematic of the proposed rotor-bearing configuration.

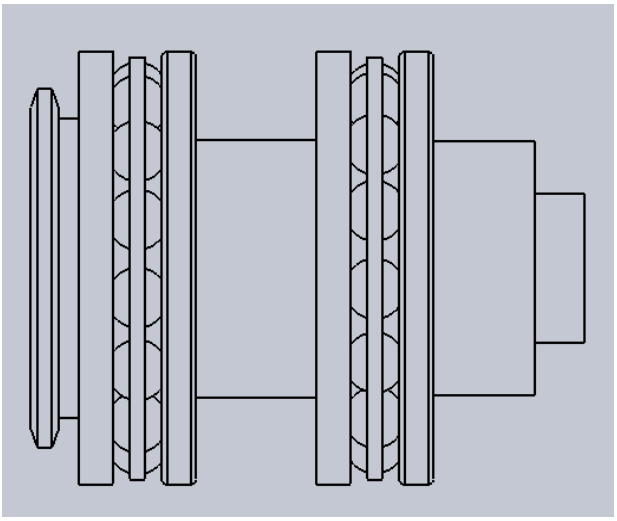

Figure 3.3 – Schematic of the proposed rotor-bearing system

Figure 3.4 depicts dimensional details of the proposed bearing races. The bearing race is designed with an OD of Ø3.188 *in*, ID of Ø2.00 *in,* and a Ø0.444 *in* groove for seating the ball bearings. The groove has an offset centerline distance of 1.297 *in*.

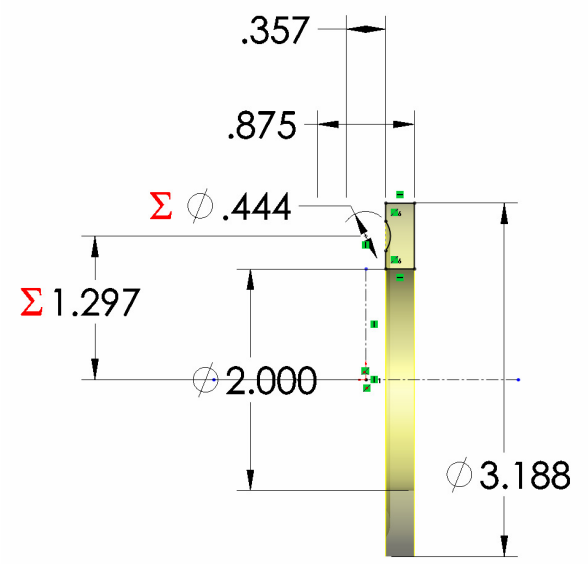

Figure 3.4 – Bearing race proposed configuration and dimensions

Figure 3.5 depicts dimensional details of the proposed bearing cage spine. The cage spine is designed with an OD of Ø3.114 *in,* ID of Ø2.074 *in,* and a thickness of 0.112 *in*.

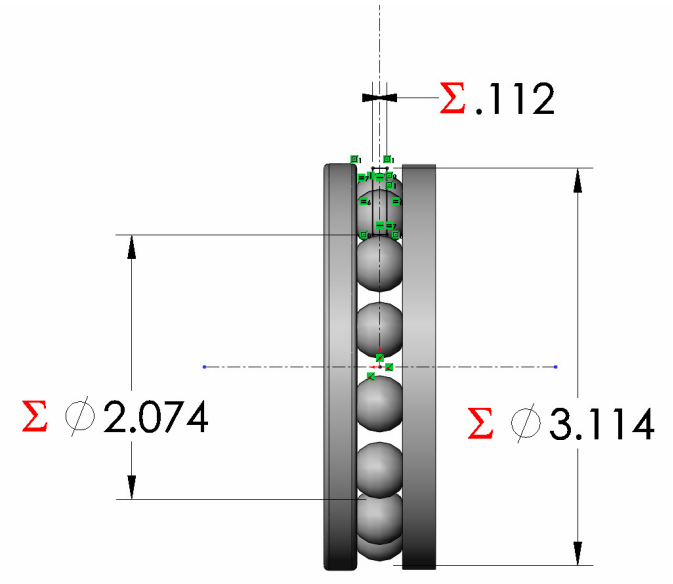

Figure 3.5 – Bearing cage spine proposed configuration and dimensions

Figure 3.6 depicts dimensional details of the proposed bearing ball. The bearing ball is designed with an OD of Ø0.466 *in* at an offset centerline distance of 1.297 *in*.

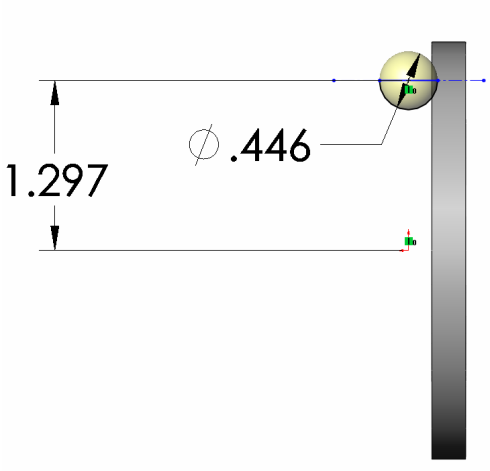

Figure 3.6 – Bearing ball proposed configuration and dimensions

Figure 3.7 depicts a dimensional detail of the proposed bearing assembly, and Figure 3.8 depicts a schematic of the proposed rotor-bearing system. The bearing to shaft radial clearance is designed to 0.000 *in* – 0.0003 *in*.

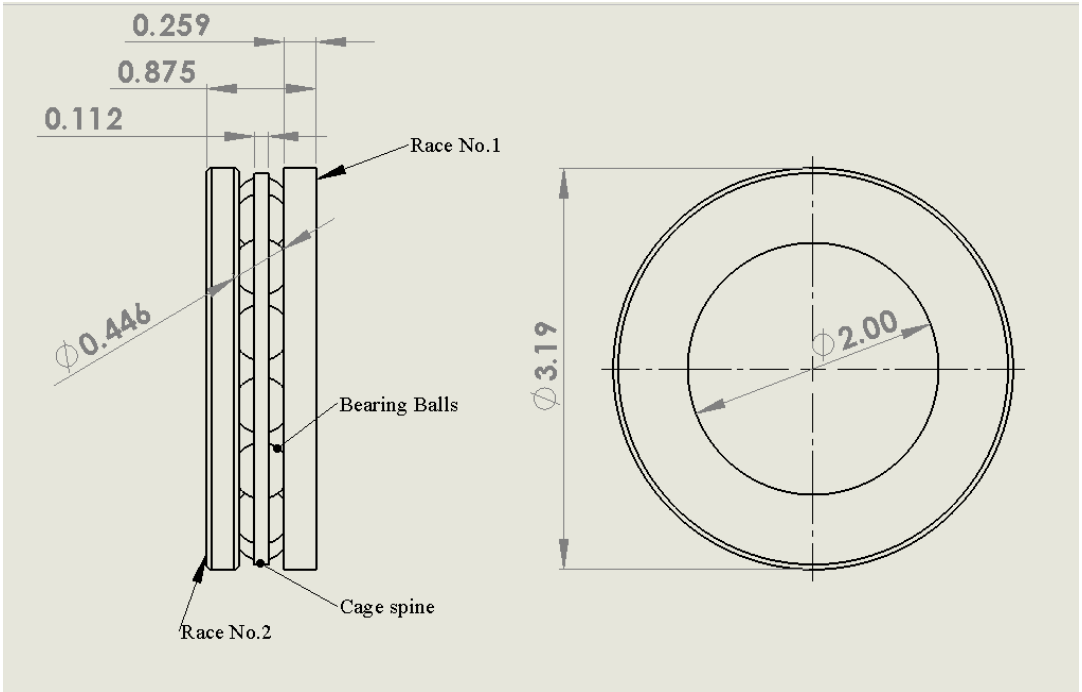

Figure 3.7 – Schematic of the proposed bearing assembly

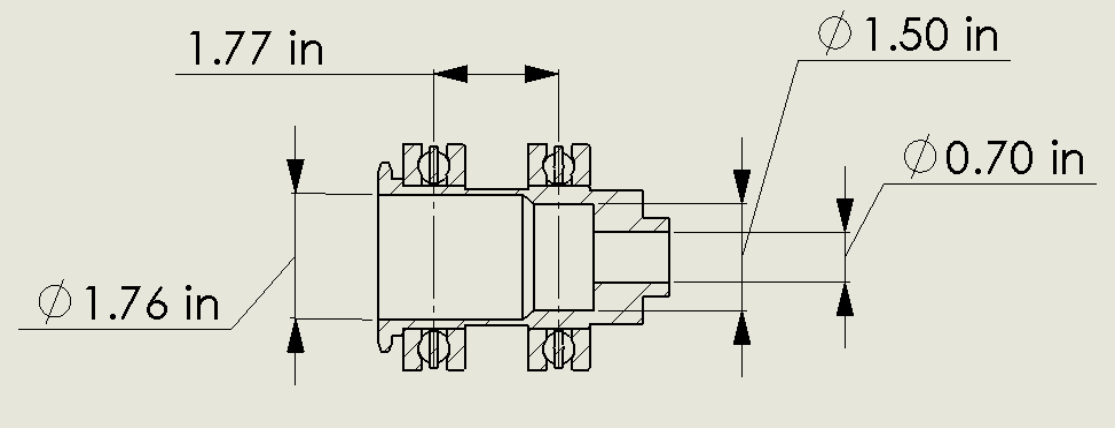

Figure 3.8 – Schematic of the proposed rotor-bearing system

The proposed rotor-bearing system is modeled using the physical parameters per Table 3.1 for the proposed rotor shaft and Table 3.2 for proposed bearings No.1 and No.2. The proposed rotor shaft is assigned with the material properties of alloy steel and the proposed bearings No.1 and No.2 with the material properties of stainless steel.

Rotor shaft	
Parameter	**Value**
Outside Diameter	Variable
Inside Diameter	Variable
Speed (Ω)	1,675.52*rad/sec*
Young's Modulus (E)	3.0E+07lb/in^2
Density (ρ)	0.284lb/in^3

Table 3.1 – Physical parameters of the proposed rotor shaft

Bearings No.1 and No.2	
Parameter	**Value**
Outside Diameter	3.19 *in*
Inside Diameter	2.00 *in*
Thickness	0.*875 in*
No. of Balls	14
Stiffness (K_{xx1}, K_{yy1}, K_{xx2}, $K_{yy2)}$	10E8 *lbf/in*
Young's Modulus (E)	2.80E07 lb/in^2
Density (ρ)	0.289 lb/in^3

Table 3.2 – Physical parameters of the proposed bearings

Next, the FEA model starts by defining a dynamic study/modal time history analysis type and the application of the appropriate loads and restraints. An immovable restraint is applied to the left end of the model; only translational degrees of freedom are constrained while rotational degrees of freedom remain unconstrained as shown in Figure 3.9.

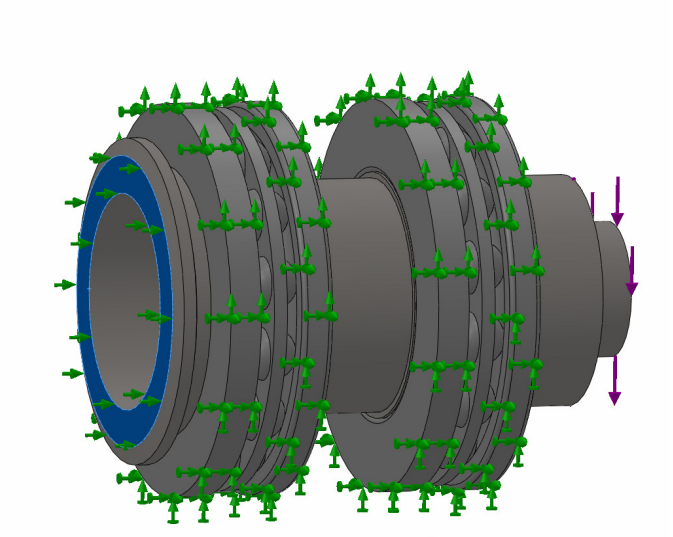

Figure 3.9 – Immovable restraint applied to a rotor-bearing system

A fixed restraint is applied to the bearing races; all translational and all rotational degrees of freedom remain unconstrained as shown in Figure 3.10.

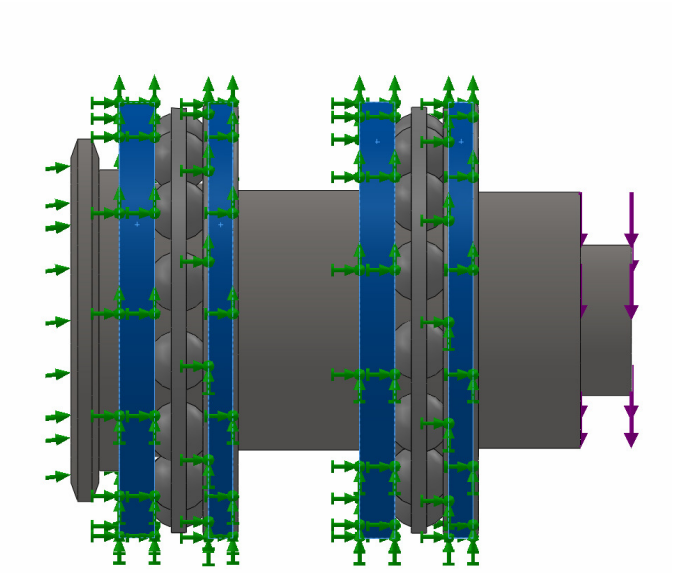

Figure 3.10 – Fixed restraint applied to a rotor-bearing system

The rolling element (bearing balls) is not restrained and thus is free to rotate. Finally, a harmonic loading as a function of time is applied uniformly over the face of the free end as shown in Figure 3.11.

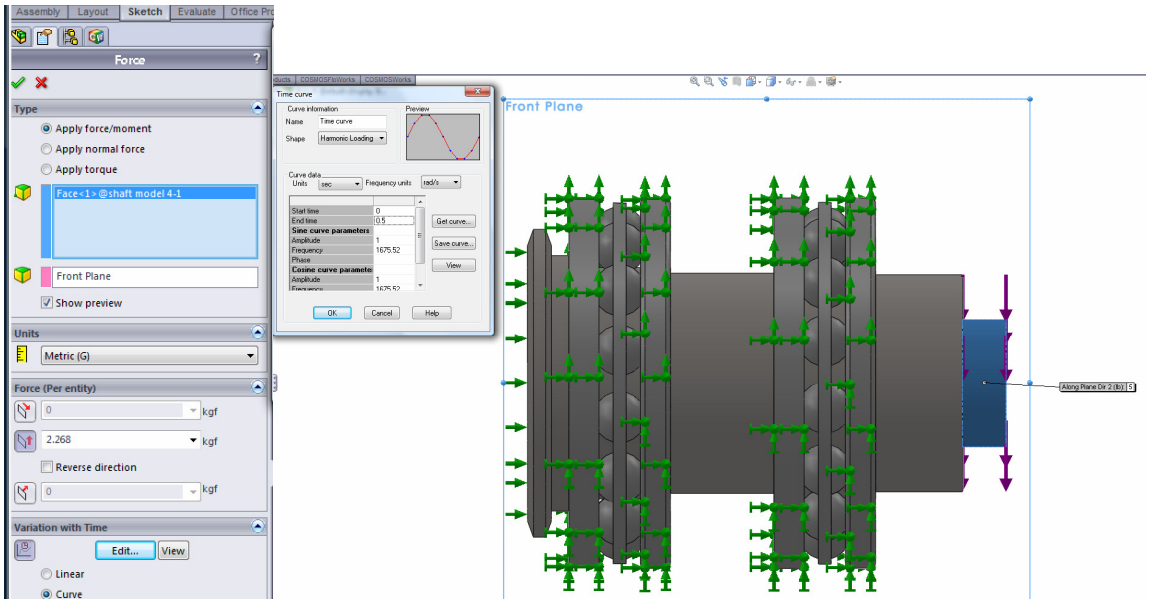

Figure 3.11 – Harmonic loading applied at the free end of a rotor-bearing system

This Harmonic loading force represents the unbalanced PM rotor. In the variation with time folder, a harmonic loading type is selected for the time history curves. The sine and cosine curve parameters for the study are defined per equations 3.7 and 3.8. The PM rotor is unbalanced such that the unbalance effect is equivalent to a mass (m) of 2.27 kg located at a distance (e) of 3.60E-7 m from the center of rotation, rotating at an angular speed (ω) of 1,675.52 *rad/sec*. Therefore, the force magnitude, $F_o = me\omega^2$, at the free end is:

$$F_o = (2.27)(3.60E-7)(1{,}675.52^2) = 2.30Kg$$

Substituting the force magnitude into equations 3.7 and 3.8, the resulting forces in the *x* and *y* directions as a function of time are:

$$f_x(t) = 2.30\cos(1{,}675.52) \times t$$

$$f_y(t) = 2.30\cos(1{,}675.52) \times t$$

In the dynamic options folder, the properties of the time history study are selected as zero (0) *sec* for the start time and one-half (0.5) *sec* for the end time in increment of 0.0005 *sec* as shown in Figure 3.12.

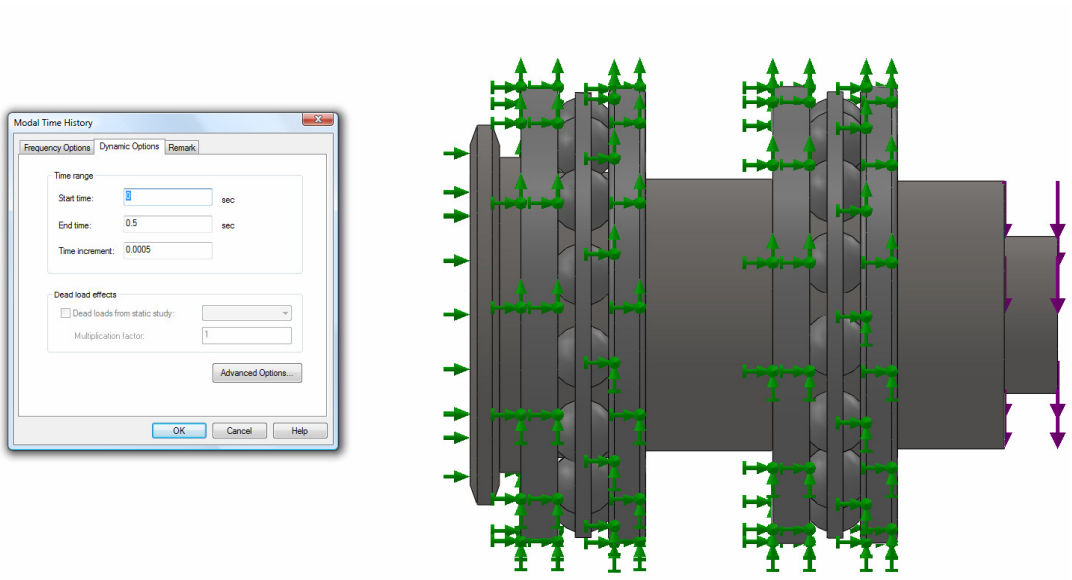

Figure 3.12 – Time range applied to a rotor-bearing system

In the results option folder, the tip of the free end was selected as the node location for the time response graphs in the UX, UY and UZ directions as shown in Figure 3.13. In the solution step option, 1 and 1,600 were selected as the start and end number of solution steps in increments of 20. The Damping in this study is negligible, thus the value for modal damping is set as zero.

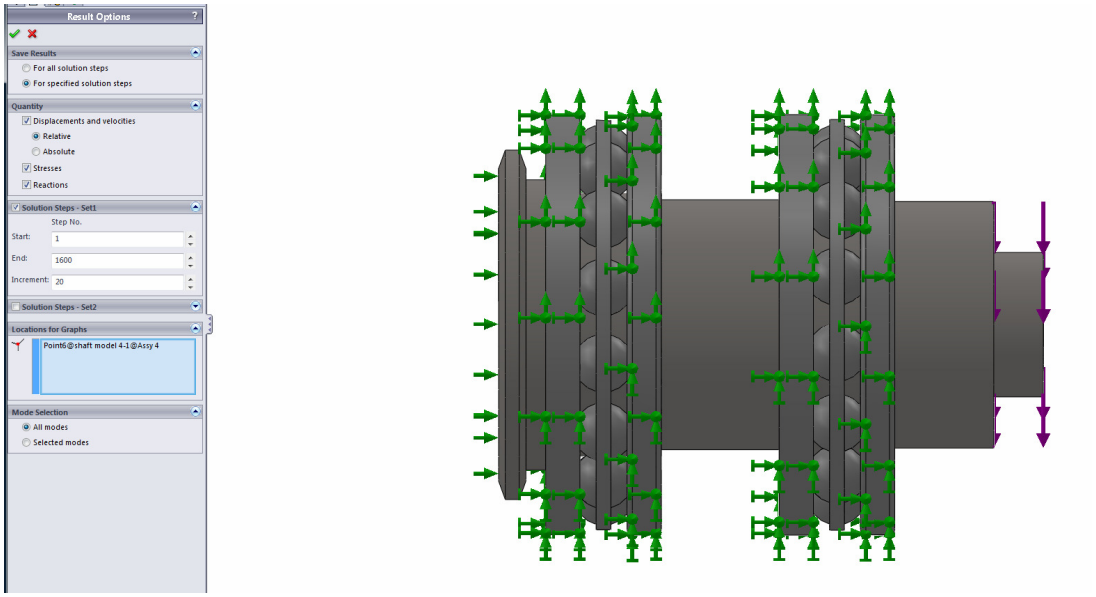

Figure 3.13 – Result options of a rotor-bearing system

The proposed rotor-bearing system is primed for meshing. A solid mesh type is selected to create a finite element mesh. Under Meshing Parameters, the slider bar is set to medium mesh density for meshing our beam model as shown in Figure 3.14.

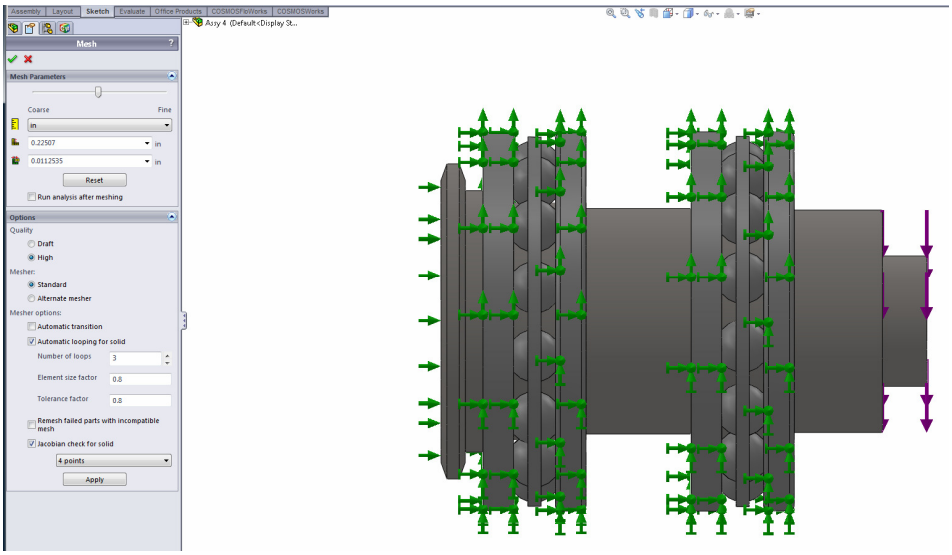

Figure 3.14 – Mesh parameters of a rotor-bearing system

The global element size is set to 0.225 *in* and the mesh tolerance set to 0.011 *in.* Both values are established automatically based on the volume, surface area, and other geometric features of a cantilever beam model. The global element size is the characteristic element size in the mesh and the element size tolerance is the allowable variance of the actual element sizes in the mesh.

Under Meshing Options, high quality mesh is selected for the study. The high quality mesh prompts the automatic mesher generate parabolic tetrahedral solid elements. Four corner nodes, six mid-side nodes, and six edges define a parabolic tetrahedral element. In general, parabolic elements yield better results because: 1) they represent curved boundaries more accurately, and 2) they produce better mathematical approximations. The mesher type is set to standard. This mesher is faster than the alternate mesher and hence is used in this study. In the mesher options, automatic looping for a solid was selected with 3 as the number of loops, 0.8 as the element size and tolerance factors. Automatic looping instructs the mesher to automatically retry to mesh the model using a smaller global element size. The maximum number of trials allowed is controlled by the designer and the ratio by which the global element size and tolerance are reduced each time. Additionally, the Jacobian check on 4 Gaussian points is selected. The Jacobian check is based on a number of points located within each element to be used in checking the distortion level of high order tetrahedral elements.

Lastly, the interfacing surfaces between the rolling elements and the bearing races bearings were modeled with a global contact condition, set to touching faces with no penetrations, and a local contact condition set to surface-to-surface contact. The contact formulation of the surface-to-surface contact with no penetration contact type prevents

interference between source and target entities during loading, but allows them to move away from each other to form gaps. The shaft to the bearing races interface was modeled with a global contact condition set to touching faces (bonded/no clearance), and a local contact condition set to node-to-node contact. The bonding contact type allows the program bond the source and target entities. The entities may be touching or within a small distance from each other.

The mesh parameters of the proposed rotor-bearing system model are now defined and ready for meshing. Figure 3.12 shows a meshed model of the proposed rotor-bearing system.

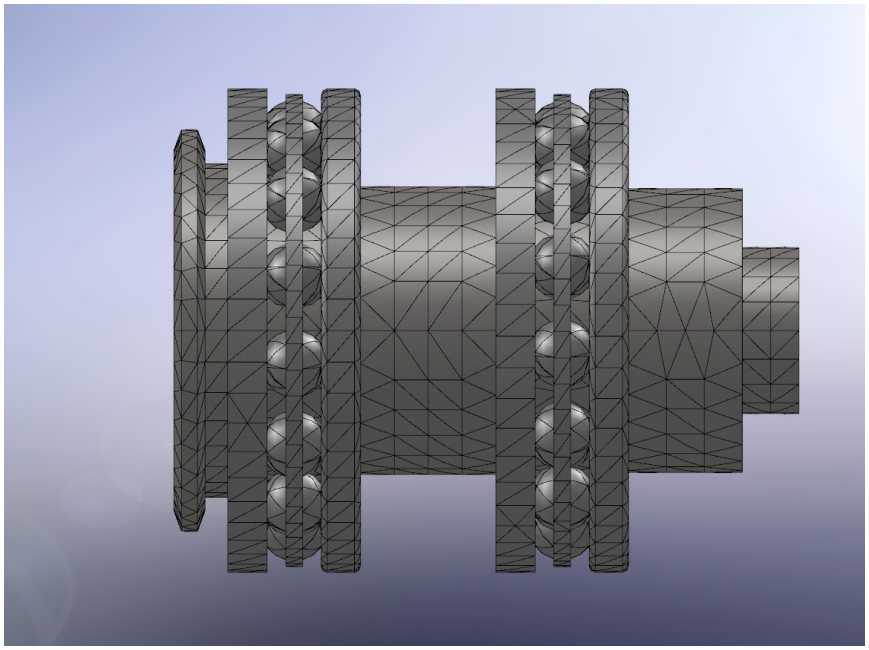

Figure 3.15 –Mesh model of the rotor-bearing system

With the mesh created, the rotor-bearing dynamic analysis is now ready to run. In the next chapter, parametric studies of six different rotor-bearing configurations will be examined for its dynamic behavior when subjected to a harmonic loading at the tip of the free end.

CHAPTER IV

PARAMETRIC STUDY OF A ROTOR-BEARING SYSTEM

Having defined the physical parameters and the FEA features of the proposed rotor-bearing system, various configurations of the rotor-bearing system may be used for performing a parametric study of the model to provide an acceptable configuration that satisfies the performance requirements of the PMA. The acceptable configuration of the parametric study will have a maximum shaft UX and UY displacements of less than 0.010 *in*, and a first natural frequency close to 20 times of the maximum operating speed of the PMA. The displacement and first natural frequency are two very important design requirements to avoid a rotor to stator collision that could lead wear and tear, deterioration, and even a catastrophic failure.

Several dimensional changes of the proposed rotor-bearing system will be used in performing the parametric studies. The axial distance between the bearings 'A' and the shaft's internal diameters 'ØB', 'ØC', and 'ØD' as shown in Figure 4.1 are the geometric dimensions used for the parametric studies. The procedure for generating the FEA dynamic study results for all six parametric studies is the same as outlined in Chapter 3.2.

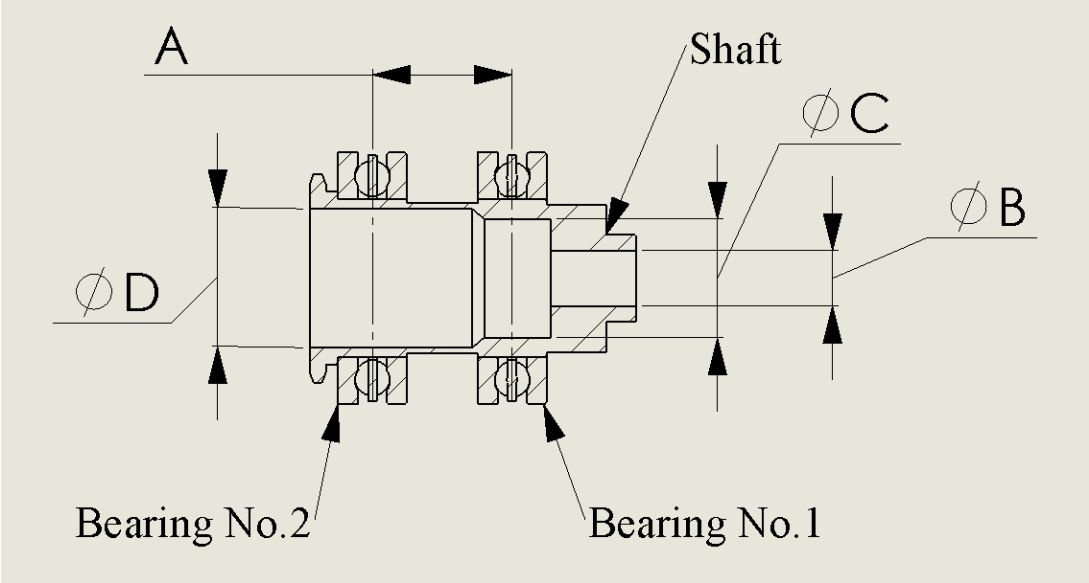

Figure 4.1– Proposed dimensions used for parametric study

In parametric study No.1, the internal diameter dimensions are Ø0.070 *in*, Ø1.50 *in*, Ø1.76 *in*, and the bearings axial distance is 1.77 *in* as shown in Figure 4.2.

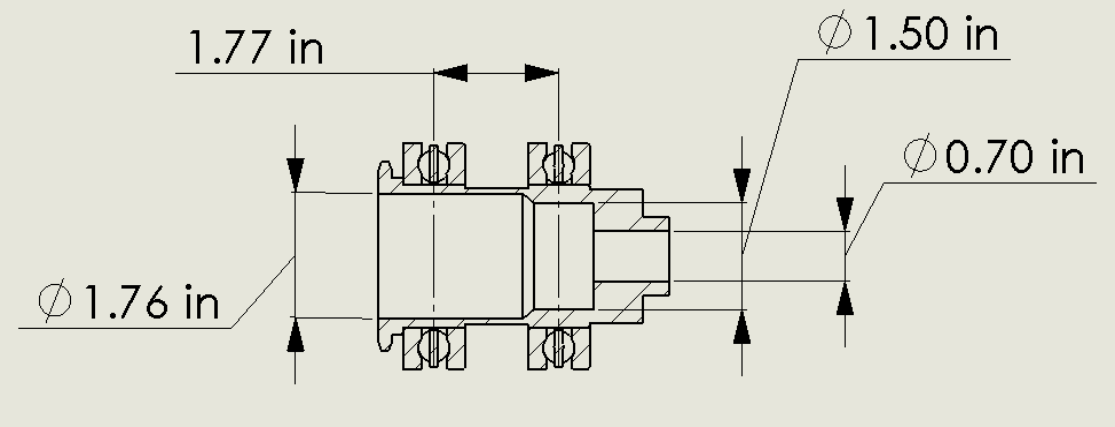

Figure 4.2 –Parametric study No.1 configuration

The dynamic study results of the parametric study No.1 are presented in Appendices G, H, and I. Appendix G shows the calculated data for the time history plots.

Appendix H shows the time history plots for UX, UY and UZ displacements. Appendix I shows the mode shapes and the associated frequencies.

A summary of the FEA dynamic study for the proposed rotor-bearing system is presented in Table 4.1 and Table 4.2. Table 4.1 summarizes the maximum steady-state UX, UY and UZ displacements, and Table 4.2 summarizes the frequencies associated with the first four mode shapes of vibration.

Displacement direction	**Value (*in*)**
UX	5.77E-7
UY	2.85E-6
UZ	3.28E-9

Table 4.1 - Maximum displacement results of parametric study No.1

Mode shape	**Frequency (*rad/sec*)**
First	84,883.33
Second	161,542.22
Third	166,216.77
Fourth	172,663.12

Table 4.2 – Frequency results of parametric study No.1

In parametric study No.2, the internal diameter dimensions remain unchanged, however, the bearings axial distance is reduced from 1.77 *in* to 1.02 *in* as shown in Figure 4.3.

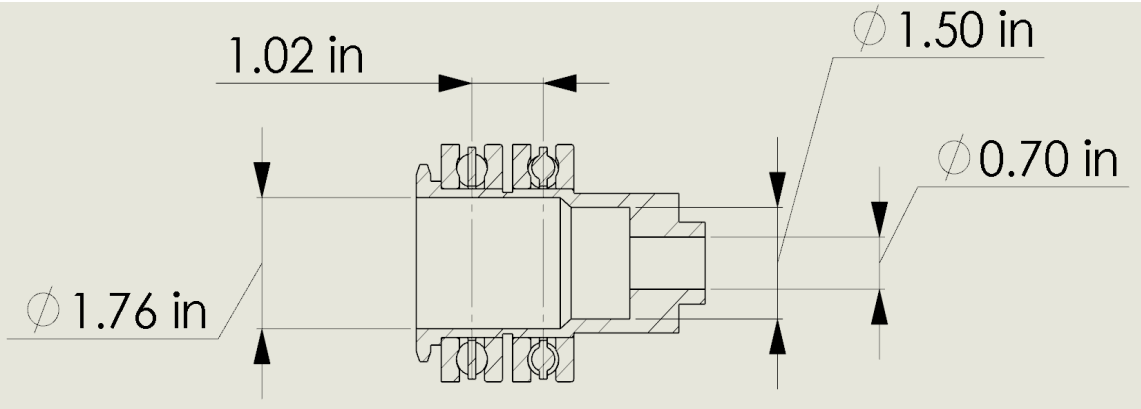

Figure 4.3 – Parametric study No.2 configuration

The dynamic study results of parametric study No.2 are presented in Appendices, J, K and L. The tabulated data for the time history plots are shown in Appendix J. The time history plots for the UX, UY and UZ displacements are shown in Appendix K. The mode shapes and the associated frequencies are shown in Appendix L. A summary of the FEA dynamic study results for parametric study No.2 is presented in Table 4.3 and Table 4.4. Table 4.3 summarizes the maximum steady-state UX, UY and UZ displacements, and Table 4.4 summarizes the frequencies associated with the first four mode shapes of vibration.

Displacement direction	**Value (*in*)**
UX	1.81E-06
UY	7.61E-06
UZ	4.44E-09

Table 4.3 – Displacement results of parametric study No.2

mode shape	Frequency (*rad/sec*)
First	46,249.163
Second	103,166.86
Third	128,939.73
Fourth	141,323.52

Table 4.4 – Frequency results of parametric study No.2

In parametric study No.3, the internal diameter dimensions remain unchanged, however, the bearings axial distance is increased from 1.77 *in* to 2.27 *in* as shown in Figure 4.4.

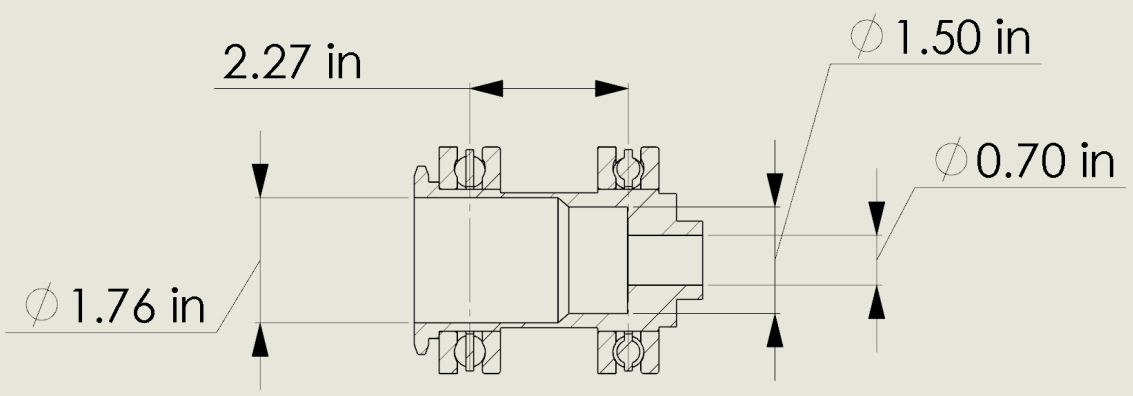

Figure 4.4 – Parametric Study No.3 configuration

The dynamic study results of parametric study No.3 are presented in Appendices M, N, and P. The tabulated data for the time history plots are shown in Appendix M. The time history plots for the UX, UY and UZ displacements are shown in Appendix N. The mode shapes and the associated frequencies are shown in Appendix P. A summary of the FEA dynamic study results for parametric study No.3 is presented in Table 4.5 and Table 4.6. Table 4.5 summarizes the maximum steady-state UX, UY and UZ displacements,

and Table 4.6 summarizes the frequencies associated with the first four mode shapes of vibration.

Displacement direction	Value (*in*)
UX	3.97E-07
UY	6.21E-07
UZ	9.46E-08

Table 4.5 – Displacement results of parametric study No.3

Mode shape	Frequency (*rad/sec*)
First	107,489.60
Second	138,910.85
Third	142,297.38
Fourth	154,341.90

Table 4.6 – Frequency results of parametric study No.3

In parametric study No.4, the bearing axial distance is the same as in parametric study No.1 at 1.77 *in*, however, the internal diameters are increased from Ø0.070 *in* to Ø1.00 *in,* Ø1.50 *in* to Ø1.70 *in* and Ø1.76 *in* to Ø1.80 *in* as shown in Figure 4.5.

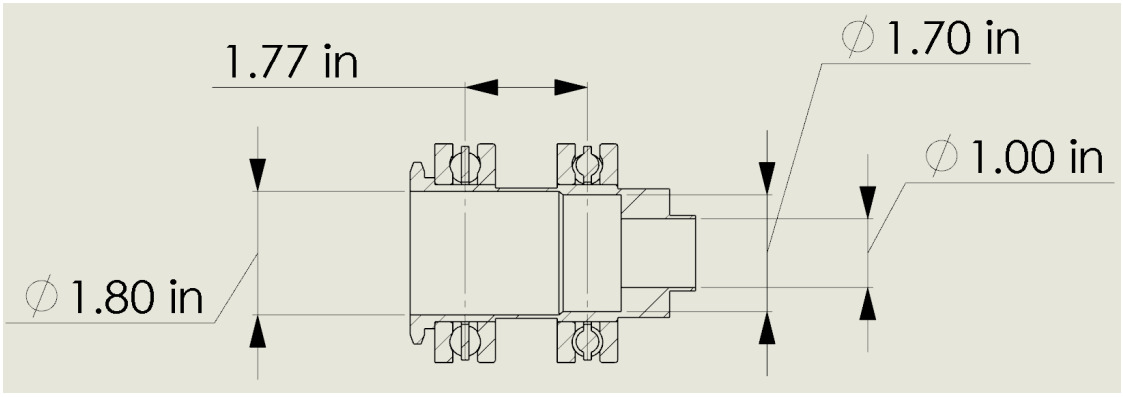

Figure 4.5 – Parametric study No.4 configuration

The dynamic study results of parametric study No.4 are presented in Appendices Q, R and S. The tabulated data for the time history plots are shown in Appendix Q. The time history plots for the UX, UY and UZ displacements are shown in Appendix R. The mode shapes and the associated frequencies are shown in Appendix S. A summary of the FEA dynamic study results for parametric study No.4 is presented in Table 4.7 and Table 4.8. Table 4.7 summarizes the maximum steady-state UX, UY and UZ displacements, and Table 4.8 summarizes the frequencies associated with the first four mode shapes of vibration.

Displacement direction	**Value (*in*)**
UX	5.13E-07
UY	2.25E-06
UZ	1.30E-09

Table 4.7 – Displacement results of parametric study No.4

Mode shape	**Frequency (*rad/sec*)**
First	96,406.35
Second	144,263.96
Third	148,398.20
Fourth	153,858.10

Table 4.8 – Frequency results of parametric study No.4

In parametric study No.5, the bearing axial distance is same as in parametric study No.2 at 1.02 *in;* however, the internal diameters are increased from Ø0.070 *in* to Ø1.00 *in*, Ø1.50 *in* to Ø1.70 *in* and Ø1.76 *in* to Ø1.80 *in* as shown in Figure 4.6.

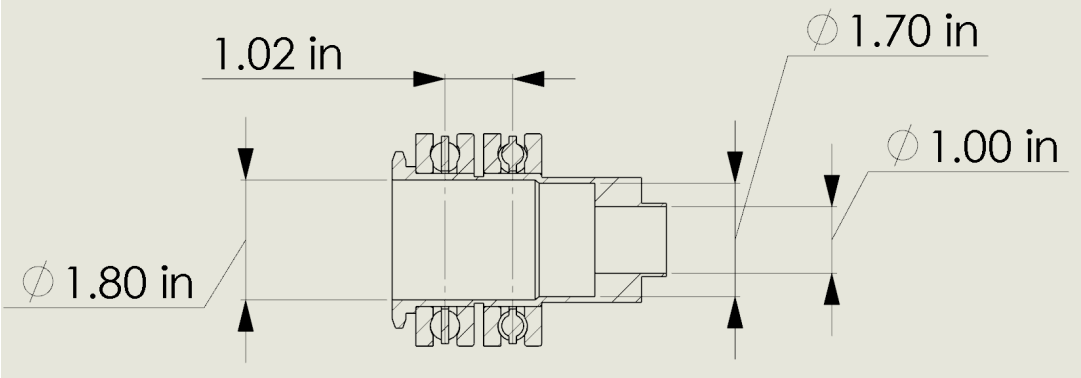

Figure 4.6 – Parametric study No.5 configuration

The dynamic study results of parametric study No.5 are presented in Appendices T, U and V. The tabulated data for the time history plots are shown in Appendix T. The time history plots for the UX, UY and UZ displacements are shown in Appendix U. The mode shapes and the associated frequencies are shown in Appendix V. A summary of the FEA dynamic study results for parametric study No.5 is presented in Table 4.9 and Table 4.10. Table 4.9 summarizes the maximum steady-state UX, UY and UZ displacements, and Table 4.10 summarizes the frequencies associated with the first four mode shapes of vibration.

Displacement direction	**Value (*in*)**
UX	2.35E-06
UY	1.06E-05
UZ	1.63E-08

Table 4.9 – Displacement results of parametric study No.5

Mode shape	Frequency (*rad/sec*)
First	37,507.63
Second	77,852.65
Third	115,902.50
Fourth	116,782.12

Table 4.10 – Frequency results of parametric study No.5

In parametric study No.6, the bearing axial distance is same as in parametric study No.3 at 2.27 *in*; however, the internal diameters are increased from Ø0.070 *in* to Ø1.00 *in*, Ø1.50 *in* to Ø1.70 *in* and Ø1.76 *in* to Ø1.80 *in* as shown in Figure 4.7.

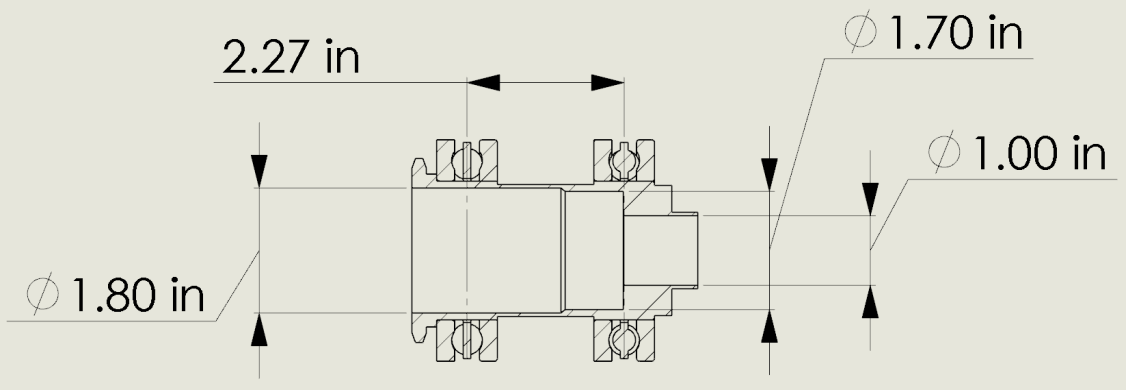

Figure 4.7 – Parametric study No.6 configuration

The dynamic study results of parametric study No.6 are presented in Appendices W, X and Y. The tabulated data for the time history plots are shown in Appendix W. The time history plots for the UX, UY and UZ displacements are shown in Appendix X. The mode shapes and the associated frequencies are shown in Appendix Y. A summary of the FEA dynamic study results for parametric study No.6 is presented in Table 4.11 and Table 4.12. Table 4.11 summarizes the maximum steady-state UX, UY and UZ displacements, and Table 4.12 summarizes the frequencies associated with the first four mode shapes of vibration.

Displacement direction	Value (*in*)
UX	1.92E-07
UY	2.00E-07
UZ	2.52E-07

Table 4.11 – Displacement results of parametric study No.6

Mode shape	Frequency (*rad/sec*)
First	117,479.53
Second	122,323.73
Third	129,88.20
Fourth	146,035.77

Table 4.12 – Frequency results of parametric study No.6

We conclude the parametric study by summarizing the steady-state maximum UX & UY displacements and the first natural frequency of a rotor-bearing system as presented in Table 4.13. The first natural frequency is the lowest frequency resonance of a rotor-bearing system.

Configuration	UX Displacement	UY Displacement	First natural frequency (rad/sec)
Parametric study No.1	5.77E-7	2.85E-06	84,883.33
Parametric study No.2	1.81E-06	7.61E-06	46,249.16
Parametric study No.3	3.97E-07	6.21E-07	107,489.60
Parametric study No.4	5.13E-07	2.25E-06	96,406.35
Parametric study No.5	2.35E-06	1.06E-05	37,507.63
Parametric study No.6	1.92E-07	2.00E-07	117,479.53

Table 4.13 - Summary of the parametric study results

As shown in Table 4.13, the maximum steady-state UX displacement was obtained in parametric study No.2 at 1.81E-06 *in*, while the maximum steady-state UY displacement was obtained in parametric study No.5 at 1.06E-05 *in*. Parametric study No.2 used the closest bearing-to-bearing axial distance (1.02 *in*), and a rotor shaft with the smallest internal diameters (Ø0.70, Ø1.50, Ø1.76). Parametric study No.5 used the closest bearing-to-bearing axial distance (1.02 *in*) as in parametric study No.2, however, a rotor shaft with the largest internal diameters (Ø1.00, Ø1.70, Ø1.80). The aforementioned results prove that a rotor-bearing system with the shortest bearing-to-bearing axial distance will result in the largest UX and UY displacements due to the cantilevered configuration of the system.

Furthermore, the highest first natural frequency was obtained in parametric study No.6 at 117,479.53 *rad/sec,* while the lowest first natural frequency was obtained in parametric study No.5 at 37,507.63 *rad/sec*. Parametric study No.6 used the longest bearing-to-bearing axial distance (2.27 *in*), and a rotor shaft with the largest internal diameters (Ø1.00, Ø1.70, Ø1.80). Parametric study No.5 used the shortest bearing-to-bearing axial distance (1.02 *in*), and a rotor shaft with the largest internal diameters (Ø1.00, Ø1.70, Ø1.80). The aforementioned results are as expected as the closest bearing-to-bearing axial distance yields the lowest first natural frequency, while the longest bearing-to-bearing axial distance yields the highest first natural frequency of a system.

CHAPTER V

CONCLUSIONS AND SUGGESTED FUTURE WORK

As hypothesized, the cantilever beam deflection, natural frequencies and mode shapes were analyzed using the closed from solution approach. The accuracy of the closed form predictions was verified when compared to those obtained from the FEA model; close agreement has been obtained.

A mathematical model of a rotor-bearing system was proposed and analyzed for its dynamic unbalance response at the free end using COSMOSWorks. A parametric study of six rotor-bearing configurations was used to plot the steady-state maximum UX and UY displacements at the free end in response to the dynamic unbalance. One parametric study changed the bearing-to-bearing axial distance, while the other study increased the internal diameter of the rotor shaft. Both parametric studies proved critical to the PMA design to ensure no rotor-to-stator mechanical contact occurred during operation. The shaft's maximum steady-state UX displacement was obtained in parametric study No.2 at 1.81E-06 *in*, while the maximum steady-state UY displacement was obtained in parametric study No.5 at 1.06E-05 *in.* The aforementioned shaft

displacements are almost negligible and hence have no affect on the designed rotor-bearing system to stator radial clearance of 0.010 *in.* Parametric study No.2 used the closest bearing-to-bearing axial distance (1.02 *in*) and a rotor shaft with the smallest internal diameters (Ø0.70, Ø1.50, Ø1.76). Parametric study No.5 used the same bearing-to-bearing axial distance (1.02 *in*) as in parametric study No.2, however, a rotor shaft with the largest internal diameters (Ø1.00, Ø1.70, Ø1.80).

Furthermore, the first natural frequency of parametric study No.5 was determined to be 37,507.63 *rad/sec* (358,171 *rpm*), which is 22 times of the PMA maximum operating speed of 1,675.52 *rad/sec* (16,000 *rpm*). It is desired that the first natural frequency of a rotor-bearing system be close to 20 times of the maximum operating speed of the PMA.

For future work, the following topics would be areas of interest for investigation:

- The thermal effects of rotor-to-stator rub, and their influence on the rotor vibrational response.
- The effects of rotary inertia, gyroscopic moments, internal viscous and hysteretic damping, shear deformations, and axial torque on the dynamic response of a rotor-bearing system.
- The stiffness effects on the dynamics of rotor-bearing foundation systems.
- Experimental validation of the rotor-bearing system to the analytical and FEA results.

In conclusion, the rotor-bearing configuration from parametric study No.5 proved to be the best design configuration satisfying the shaft deflection and first natural frequency requirements of the permanent magnet alternator.

REFERENCES

[1] R.G. Kirk and E.J. Gunter, 1972, ASME *Journal of Engineering for Industies*, Vol. 94, pp.221-232. The effect of support flexibility and damping on the synchronous response of a single-mass flexible Rotor.

[2] D.M Smith, 1933, Preceedings of the Royal Society, Series A 142, pp.92. The motion of a Rotor carried by a flexible shaft in flexiible Bearing.

[3] J.W. Lund, 1965, *Jourrnal of Apllied Mechanics*, Vol.32, Transactions ASME, Series E 87, pp.911-920. The stability of anelastic Rotor in journal Bearings with flexible, damped supports.

[4] E.J. Gunter, 1967, *Journal of Engineering for Industry*. Transactions ASME, Series B 89, pp.683-688. The influence of internal friction on the stability of hig speed Rotors.

[5] J.W. Lund and B. Sternlicht, 1962, *Journal of Basic Engineering*, Transactions ASME Series D84, pp.491-502. Rotor-Bearing dynamics with emphasis on attenuation.

[6] J. Dworksi, 1964, *Journal of Engineering for Power*. Transactions ASME Series A 86, pp.149-160. High speed Rotor suspension formed by fully floating hydronamic radial and thrust Bearings.

[7] E.J. Gunter, 1970, *Journal of Lubrication Technology*, Transactions ASME, Series F92, pp.59-75. Influence of Flexibly mounted rolling element Bearing on Rotor response, Part I - linear analysis.

[8] W.D. Pilkey, B.P. Wang and D. Vannoy, 1976, ASME *Journal of Engineering for Industries* pp.1026-1029. Efficient optimal design of suspesnion systems for rotating shafts.

[9] R. Gasch, 1976, *Journal of Sound and Vibration*, Vol. 47, pp.53-73. Vibration of large turboRotors in fluid-film Bearing on an elastic foundation.

[10] J.M. Vance, B.T. Murphy and H.A. Tripp, 1987, ASME *Journal of Vibration Acoustics*, *Stress*, *Reliabaility in Design*, Vol. 109, pp.8-14. Critical speeds of turbomachinery: computer predictions vs. experimental measurements – Part II: effect of tilt-pad Bearing and foundation dynamics.

[11] R.W. Stephenson and K.E. Rouch, 1992, *Journal of Sound and Vibration*, Vol. 154, pp.467-484. Generating matrices of the foundation structure of a Rotor system from test data.

[12] R. L. Ruhl and J.F. Booker, 1972, ASME *Journal of Engineering for Industry*, Vol. 94, pp.126-132. A finite element models for distributed parameter turboRotor systems.

[13] H.D. Nelson and J.M. McVaugh, 1976, ASME *Journal of Engineering for Industries*, Vol. 98, pp.593-600. The dynamics of Rotor-Bearing systems using finite elements.

[14] E. S. Zorzi and H. D. Nelson, 1977, ASME *Journal of Engineering for Power*, Vol. 99, pp.71-76. Finite element simulation of Rotor-Bearing systems with internal damping.

[15] E. S. Zorzi and H. D. Nelson, 1980, ASME *Journal of Engineering for Power*, Vol. 102, pp.158-161. The dynamics of Rotor-Bearing systems with axial torque - a finite element approach.

[16] H.D. Nelson, 1980, ASME *Journal of Mechanical Design*, Vol. 102, pp.793-803. A finite rotating shaft element using Timoshenko beam theory.

[17] L. M. Greenhill, W.B. Bickford and H. D. Nelson, 1985, ASME *Journal of Vibration Acoustics*, *Stress*, *Reliability in Design*, Vol. 107, pp.421-430. A conical beam finite element for Rotor dynamic analysis.

[18] H.N. Özgüven, and L. Z. Özkan, 1984, ASME *Journal of Vibration, Acoustics, Stress, and Reliability in Design*, Vol.106, pp.72-79. "Whirl Speeds and Unbalance Response of MultiBearing Rotors Using Finite Elements,"

[19] N.F. Rieger, 1976, Machine Design, Vol. 22, pp.89-95. A comprehensive guide to computer programs for analysis of Rotor systems.

[20] R. Firoozian and R. Stanway, 1989, *Journal of Sound and Vibration*, Vol.134, pp.115-137. Design and application of a finite element package for modeling turbomachinery vibrations.

[21] D. Childs, Turbomachinery Rotordynamics, 1993, Wiley & Sons, p.430.

[22] W.H. Liu and C.C. Haung, 1988, *Journal of Sound and Vibration*, Vol.123, pp.139-207. Free Vibration of beams with elastically restrained edges and intermediate concentrated masses.

[23] W.H. Liu and C.C. Haung, 1988, *Journal of Sound and Vibration*, Vol.123, pp.31-42. Free Vibration of restrained beam carrying concentrated masses.

[24] L Ercoli, and P.A.A. Laura, 1987, *Journal of Sound and Vibration*, Vol.114, pp.519-533. Analytical and experimnetal investigation on continuous beams carrying elastically mounted masses.

[25] R.G. Jacquot, and J.D. Gibson, 1972, *Journal of Sound and Vibration*, Vol.23, pp.237-244. The effects of discrete masses and elastic supports on continuous beam natural frequency.

[26] C.W. Bert, 1984, Industrial Mathematics, Vol.34, pp.65-67. Use of symmmetry in applying Rayleigh-Schmidt method to static and free vibration problem.

[27] W.H. Liu and F.H. Yeh, 1987, *Journal of Sound and Vibration*, Vol.117, pp.555-570. Free vibration of restrained non-uniform beam with intermediate masses.

[28] R.P. Goel, 1973, *Journal of Apllied Mathematics*, Vol.40, pp.821-822. Vibration of a beam carrying concentrated mass.

[29] A.N. Kounadis, 1975, *Journal of Engineering Mechanics Division*, ASME, 101 EMS: pp.695-706. Dynamics response of cantilevers with attached masses.

[30] S. S. Rao, Mechanical Vibrations, Addison-Wesley Publishing Company, 1986.

[31] S. Dunkerley, 1894, *Philosiphical Transactions of the Royal Society of London*, Series A, Vol. 185, Part I, pp.279-360. On the whirling and vibration of shafts.

[32] B.Atzori, 1974, *Journal of Sound and Vibration,* Vol.36, pp.563-564. Letter to the editor, Dunkerley's formula for finding the lowest frequency of vibration of elastic systems.

[33] H.H. Jefcott, 1919, *Proceedings of the Royal Society of London*. Vol.95, No.A666, pp.106-115. The periods of lateral vibration of loaded shafts – The rational deviation of Dunkerley's empirical rule for determining whirling speed.

[34] G. Temple and W.G. Bickly, 1956, *Rayleigh's Principle and Its Applications to Engineering*, Dover, New York.

[35] H. Holzer, *Die Berechnung der Drehschwin gungen*, Julius Springer, Berlin, 1921.

[36] H.E. Fettis, Journal f the Aeronautical Sciences, October 1949, pp.625-634; May 1954, pp.359-360. A modification of the Holzer method for comuting uncoupled torsion and bending modes.

[37] C. M. Harris and A. G. Piersol, Harris' Shock and Vibration Handbook, McGraw – Hill Companies, 5th Edition, 2002.

[38] A. Muszynska, Rotordynamics, Taylor and Francis Group, 2005.

[39] M.A. Prohl, 1945, ASME *Journal of Applied Mechanics*, Vol.67, pp.142. A General Method for Calculating Critical Speeds of Flexible Rotors.

[40] J.W. Lund, and F.K. Orcutt, 1967, ASME *Journal of Engineering for Industry*, Vol.89, pp. 785-796. Calculations and Experiments on the Unbalance of a Flexible Rotor.

[41] S.R. Polk, 1974, MSE Engineering Report, Arizona State University. Finite Element Formulation and Solution of Flexible Rotor Rigid Disc Systems for Natural Frequencies and Critical Whirl Speeds.

[42] L. Rayleigh, 1945, Dover Publications, New York. Theory of Sound.

[43] R. Gash, 1976, *Journal of Sound and Vibration*, Vol.120, pp.175-182. Vibration of Large Turbo-Rotors in Fluid Film Bearings on an Elastic Foundation.

APPENDICES

APPENDIX A

FEA code validation

ANALYTICAL ESTIMATES OF A CANTILEVER BEAM

The bending linear vibrations of an elastically retrained beam element carrying a concentrated mass at the tip of the free end is a subject of practical engineering interest and has been the objective of many recent theoretical investigations. Closed form solutions for this type of a system are generally difficult to obtain, and a number of researchers have considered various approximate methods for a variety of situations. Liu and Haung [22] used Laplace transformation method to calculate the eigenvalues and eigenfucntions for beam hinged at both ends by rotational springs and carrying arbitrary located concentrated masses. Liu and Haung [23] used the Laplace transformation method to study the free vibration of a beam hinged by a rotational spring at one end and carrying a concentrated mass at the tip, and another at an intermediate point. Ercoli and Laua [24] used the Jacquot's method [25], Ritz method, and Rayleigh Schmidt approach [26] to study the effect of an elastically mounted concentrated mass on the fundamental mode of a beam for various end conditions. Liu and Yeh [27] used the Rayleigh-Ritz method in conjunction with beam functions satisfying all end conditions to study the free vibration of a restrained non-uniform beam with intermediate masses. Goel [28] studied the free vibration of a cantilever beam carrying a concentrated mass at an arbitrary

intermediate location, and Kounadis [29] studied the free and forced vibrations of a restrained cantilever beam with attached masses. We note here that in all the aforementioned investigations the concentrated element located at the free end was treated as a concentrated load on the beam.

Static Analysis

In this section, the static deflection of a cantilever beam at its free end is analyzed by using the closed form solution approach. A schematic of the cantilever beam for the static deflection analysis is illustrated in Figure 2.2.

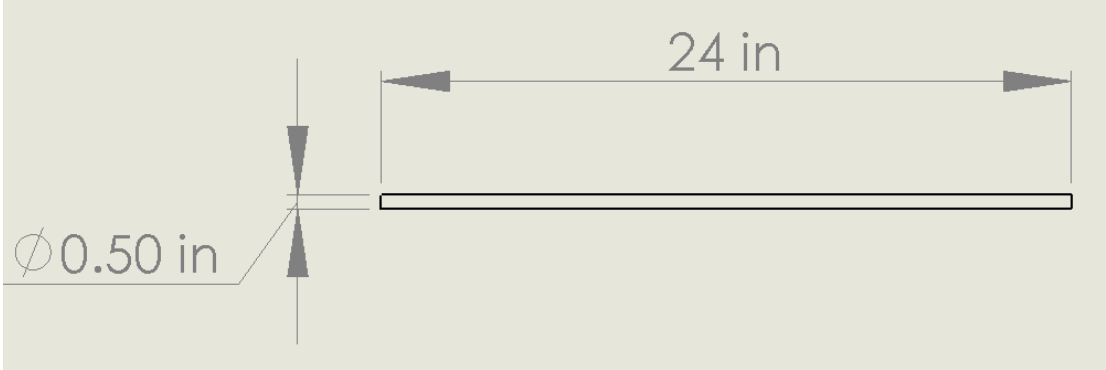

Figure 2.2 – Dimensional details of a cantilever beam

Table 2.6 lists the size and mechanical properties of the cantilever beam with assigned material properties of alloy steel. A fixed restraint is applied to the left face meaning all translational and rotational degrees of freedom is equal to zero, and a 20 *lbf* load is applied at the tip of the right face (free end), acting in a direction parallel to the y-axis as shown in Figure 2.3.

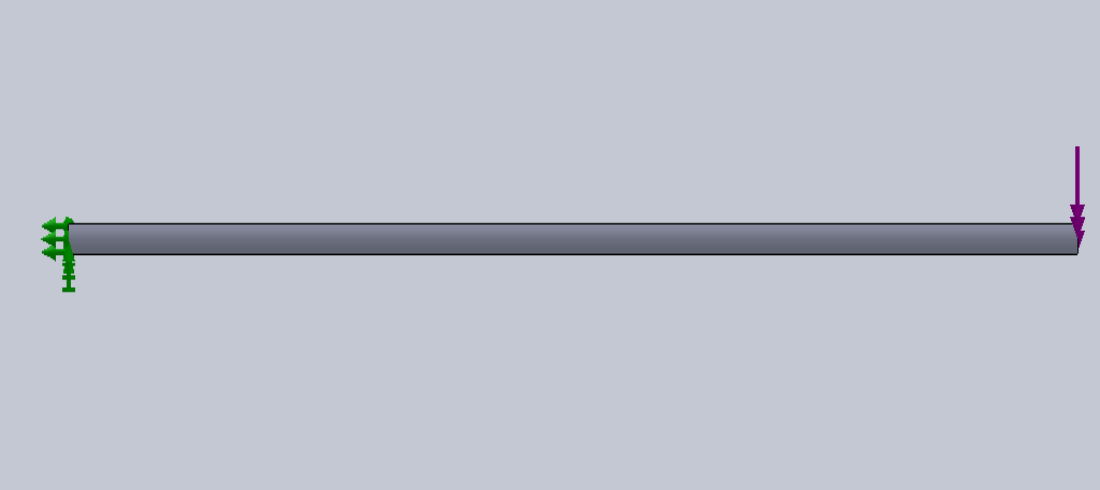

Figure 2.3 – Schematic of a cantilever beam with load/restraint applied

Parameter	**Value**
Load (*P*)	20 *lbf*
Length (*l*)	24 *in*
Diameter (*d*)	0.5 *in*
Young's Modulus (*E*)	3.0E+07 lb/in^2
Density (ρ)	0.284 lb/in^3
Area (A)	0.196 in^2

Table 2.6 – Physical parameters of a cantilever beam

To determine the maximum deflection of the simple cantilever beam, the beam's moment of inertia is first calculated using the following equation:

$$I = \frac{\pi d^4}{64} \tag{2.1}$$

Substituting the value of *d* from Table 1.0 into Eq. (2.1):

$$I = \frac{\pi(0.5)^4}{64} = 0.00307 in^4$$

And from Strength of Materials, the expression for maximum deflection (δ) at the free end of the beam due to a point load at the free end is:

$$\delta = \frac{Pl^3}{3EI} \tag{2.2}$$

Substituting the values of *P*, *l*, *E* and *I* from Table 2.1 into Eq. (2.2):

$$\delta_{Calculated} = \frac{(20)(24)^3}{3*(3.0E+07)(0.00307)} = 1.00065in$$

Natural Frequency Analysis

From Rao [30], we see if a system is disturbed and allowed to vibrate on its own, the frequency with which it oscillates without external forces or damping is known as its natural frequency. A vibratory system having '*n*' degrees of freedom will have, in general, '*n*' distinct natural frequencies of vibration. Several analytical and numerical methods have been developed to compute the natural frequencies of multi-degree of freedom systems such as Dunkerly's formula, Rayleigh's method, Holzer's method, the Matrix iteration method, and Jacobi's method.

Dunkerely's method is used to give the approximate value of the composite system fundamentals in terms of natural frequencies of its components parts. It's derived by making use of the fact that the higher natural frequencies of most vibratory systems are large compared to their fundamental frequencies [31-33]. The Rayleigh method is used to find the natural frequency of single degree of freedom systems. His method can be extended to find the natural frequency of a discrete system [34]. In addition, Holzer's method is essentially a trial and error method used to find the natural frequencies of

undamped, damped, semi-definite, fixed, or branched vibrating systems involving in linear and angular displacements [35, 36]. The Holzer method can also be programmed for solving problems using a computer. The matrix iteration method finds one natural frequency at a time, usually starting from the lowest value. The method can thus be terminated after finding the required number of natural frequencies [30]. When all natural frequencies are required, then, Jacobi's method can be used to find all eigenvalues and eigenvectors of a real symmetric matrix [*D*].

In this section, the natural frequencies of the simple cantilever beam are analyzed by using the closed form solution method. For the lateral vibration of beams, the differential equation of motion is simply expressed as [30]:

$$-\frac{\partial^2 M}{\partial x^2}(x,t) + f(x,t) = \rho A(x)\frac{\partial^2 w}{\partial t^2}(x,t) \tag{2.3}$$

Where $M(x,t)$ is the bending moment, $f(x,t)$ is the external force per unit length of the beam, and $w(x,t)$ is the transverse displacement in the z-direction. Adopting Bernoulli-Euler's classical theory of bending beams, the relationship between bending moment and deflection is expressed as [30]:

$$M(x,t) = EI(x)\frac{\partial^2 w}{\partial x^2}(x,t) \tag{2.4}$$

Where, $I(x)$ is the moment of inertia of the beam cross section about the y-axis. Inserting Eq. (2.4) into Eq. (2.3), the equation of motion for free vibration [$f(x, t) = 0$] of a uniform beam, becomes [30]:

$$c^2\frac{\partial^4 w}{\partial x^4}(x,t) + \frac{\partial^2 w}{\partial t^2}(x,t) = 0 \tag{2.5}$$

Where,

$$c = \sqrt{\frac{EI}{\rho A}} \tag{2.6}$$

Thus, the free vibration solution is found using the standard method of separation of variables as:

$$w(x,t) = W(x)T(t) \tag{2.7}$$

Substituting Eq. (2.7) into Eq. (2.5), the constant (β) is found as [30]:

$$\beta^4 = \frac{\omega^2}{c^2} = \frac{\rho A \omega^2}{EI} \tag{2.8}$$

Therefore, Eq. (2.8) yields the general expression for the natural frequency of a beam [22]:

$$\omega = \beta^2 \sqrt{\frac{EI}{\rho A}} \tag{2.9}$$

For a Fixed-Free beam, the frequency equation is expressed as [30]:

$$\cos\beta_n l \cosh\beta_n l = -1 \tag{2.10}$$

From the tables of hyperbolic and trigonometric functions, the non-dimensional frequency parameters ($\beta_n l$) for the first four modes of vibration for a cantilever beam are [37]:

$\beta_1 l$	1.875104
$\beta_2 l$	4.694091
$\beta_3 l$	7.854757
$\beta_4 l$	10.995541

Table 2.7 – Frequency parameters ($\beta_n l$) for a cantilever beam

Given the beam length (l) from Table 2.1, and the constant values of $\beta_n l$ from Table 2.7, the values of β_1, β_2, β_3, β_4 are calculated as follows:

$$\beta_1 l = 1.875104 \Rightarrow \beta_1 = \frac{1.875104}{24} = 0.078$$
$$\beta_2 l = 4.694091 \Rightarrow \beta_2 = \frac{4.694091}{24} = 0.196$$
$$\beta_3 l = 7.854757 \Rightarrow \beta_3 = \frac{7.854757}{24} = 0.327$$
$$\beta_4 l = 10.995541 \Rightarrow \beta_4 = \frac{10.995541}{24} = 0.458$$

Substituting the values obtained for β_1, β_2, β_3, β_4 into Eq. (2.9), the first four natural frequency of vibration is calculated as follows:

$$\omega_1 = (0.078)^2 \sqrt{\frac{(30\times10^6)(0.00307)(386)}{(0.284)(0.196)}}$$
$$\therefore \omega_1 = 153.75 rad/\sec$$

$$\omega_2 = (0.196)^2 \sqrt{\frac{(30\times10^6)(0.00307)(386)}{(0.284)(0.196)}}$$
$$\therefore \omega_2 = 970.84 rad/\sec$$

$$\omega_3 = (0.327)^2 \sqrt{\frac{(30\times10^6)(0.00307)(386)}{(0.284)(0.196)}}$$
$$\therefore \omega_3 = 2{,}702 rad/\sec$$

$$\omega_4 = (0.458)^2 \sqrt{\frac{(30\times10^6)(0.00307)(386)}{(0.284)(0.196)}}$$
$$\therefore \omega_4 = 5{,}301.11 rad/\sec$$

Mode Shape Analysis

According to Muszynska [38], the term "mode" is a description of motion. There are various kinds of modes such as first, second, bending, and torsional. Modes associated with the natural frequencies of a system are the most important characteristics of all mechanical vibratory systems. At a natural frequency, a vibrating system moves in a "principal" or "natural" mode of free vibration. If the amplitude of one discrete mass is chosen to be one unit of displacement, this mode is called a "normal" mode.

These different mode descriptions imply that all parts of the mechanical system perform the same harmonic motion at a system natural frequency and with maximum displacement amplitudes at identical times. The values of these maximum displacements and their phases at each point of the system are then frozen in time and compared with each other. This frozen image represents a "mode shape" of the system at this particular frequency. Hence, a mode is a mutual relationship between amplitudes and phases of the harmonic motion of all points of the mechanical system's elements. Among these vibrating points, there exist points which do not move called "nodes". The number of nodal points determines the mode. Usually, the lowest modes at the lowest frequencies have the minimum number of nodal points.

From Rao [30], the first four mode shapes at normal function for a simple cantilever beam is found using the following fixed-free beam expression:

$$Y_r(x) = C_n[\sin\beta_n x - \sinh\beta_n x - \alpha_n(\cos\beta_n x - \cosh\beta_n x)] \qquad (2.11)$$

where,

$$\alpha_n = \left(\frac{\sin\beta_n l + \sinh\beta_n l}{\cos\beta_n l + \cosh\beta_n l}\right) \qquad (2.12)$$

And from mathematics, the hyperbolic sine "sinh" and hyperbolic cosine "cosh" are defined as:

$$\sinh(\beta_n l) = \frac{e^{(\beta_n l)} - e^{-(\beta_n l)}}{2} \tag{2.13}$$

$$\cosh(\beta_n l) = \frac{e^{(\beta_n l)} + e^{-(\beta_n l)}}{2} \tag{2.14}$$

Hence, $\sin(\beta_n l), \sinh(\beta_n l)$, $\cos(\beta_n l)$ and $\cosh(\beta_n l)$ are all calculated and tabulated independently of each other as shown below:

$\beta_n l$	sin ($\beta_n l$)	sinh ($\beta_n l$)	cos ($\beta_n l$)	cos ($\beta_n l$)
1.875	0.033	3.183	0.999	3.337
4.694	0.082	54.64	0.9697	54.64
7.854	0.137	1,288	0.991	1,288
10.996	0.191	29,817	0.9892	29,817

Table 2.8 – Calculated data of constant (α_n)

Substituting the values obtained in Table 2.8 into Eq. (2.12), the constants associated with each mode α_1, α_2, α_3, and α_4 are calculated as follows:

$$\alpha_1 = \frac{\sin(1.875) + \sinh(1.857)}{\cos(1.875) + \cosh(1.875)} = \frac{0.033 + 3.183}{0.999 + 3.337} = 0.742$$

$$\alpha_2 = \frac{\sin(4.694) + \sinh(4.694)}{\cos(4.694) + \cosh(4.694)} = \frac{0.082 + 54.64}{0.9697 + 54.64} = 0.983$$

$$\alpha_3 = \frac{\sin(7.854) + \sinh(7.854)}{\cos(7.854) + \cosh(7.854)} = \frac{0.137 + 1{,}288}{0.991 + 1{,}288} = 0.999$$

$$\alpha_4 = \frac{\sin(10.996) + \sinh(10.996)}{\cos(10.996) + \cosh(10.996)} = \frac{0.191 + 29{,}817}{0.9892 + 29{,}817} = 1$$

The calculated data for constants α_n and Table 2.8 are now substituted into Eq. (2.11) to obtain the first four mode shapes of a cantilever beam. Appendix B shows the tabulated numerical data used for the mode shape plots, and Appendix C shows the corresponding first four modal shapes of the beam cantilever beam.

In a normal mode, each element of the beam oscillates vertically at the same frequency. As shown in Appendix C, the amplitude varies along the beam for each of the first four normal modes. In the four mode plots, $Y_r(x)$ shows the shape of the beam at extreme oscillation when all points on the beam are instantaneously at rest. All points also go through zero displacement at the same time. In the first mode, all parts of the beam move, except at the fixed end. In the second mode, there is a stationary point (node), also known as the zero (0) crossing, away from the fixed end (at $x/L = 0.78$). In the third mode, there are two nodes (at $x/L = 0.50$ & 0.87). In the fourth mode, there are three nodes (at $x/L = 0.36$, 0.64, and 0.91).

FEA ANALYSIS OF THE CANTILEVER BEAM MODEL

Finite Element Method (FEM) is a numerical method used for solving a system governing equations over the domain of physical systems. The governing equations for FEM are taken from the field of continuum mechanics and the theory of elasticity. While FEM was initially developed for performing structural analysis, its use has spread to the field of heat transfer, acoustics, electro-magnetics, fluid mechanics and other areas. In mathematical terms, FEA is a numerical technique used for solving field problems described by a set of partial equations.

In the field of mechanical engineering, FEA is used for solving mathematical problems in terms of vibration, structural and thermal analysis. Due to its versatility and high numerical efficiency, FEA is dominating the engineering analysis software market, while other numerical methods have been relegated to niche applications. When implemented into modern commercial software, both FEA theory and numerical problem formulation have become completely transparent to users. As a powerful tool, FEA is used to solve very simple to highly complex problems. Today, engineers alike use FEA analysis to design and develop products from start to finish. Time constraints and limited availability of product data calls for simplification of analysis models. On the other hand,

engineering specialists utilize FEA to solve complex problems, such as vehicle and aircraft dynamics.

The main objective of using FEA in the analysis process is to improve the design process from repetitive cycles into a streamlined process where prototypes are not used as design tool, but rather, as final design verification means of the mathematical model. With the use of FEA, design iterations are moved for the physical space of prototyping and testing into virtual space of computer simulations.

This section analyzes the cantilever beam using FEA analysis (COSMOSWorks), and simultaneously comparing those results predicted by the closed form solutions in the previous section.

COSMOSWorks is a commercial implementation of FEA capable of solving problems commonly found in design engineering, such as analysis of stresses, natural frequencies, buckling and deformation. COSMOSWorks was developed by Structural Research and Analysis Corporation (SRAC). In 1995, SRAC partnered with SolidWorks Corporation and thus created COSMOSWorks, which became the top selling three-dimensional FEA product for SolidWorks Corporation. In 2001, Dassault Systems, parent of SolidWorks Corporation, acquired SRAC and currently owns 100% of its shares.

Static Analysis Using FEA

The starting point of FEA analysis with COSMOSWorks begins with building a mathematical model of the cantilever beam using SolidWorks. The cantilever beam is modeled using the physical parameters defined in Table 2.1 with the material properties of alloy steel. Next, the FEA model starts by defining a static study type as shown in Figure 2.4, and the application of the appropriate loads and restraints associated with it.

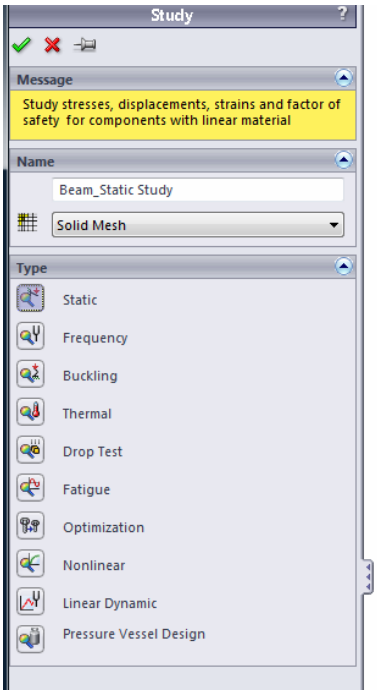

Figure 2.4 – Static study of a cantilever beam

The cantilever beam left face is assumed to be a rigid support by applying a fixed restraint as shown in Figure 2.5, and a 20*lb* force is applied at the tip of the free end perpendicular to the horizontal plane as shown in Figure 2.6.

Figure 2.5 – Fixed restraint applied to a cantilever beam

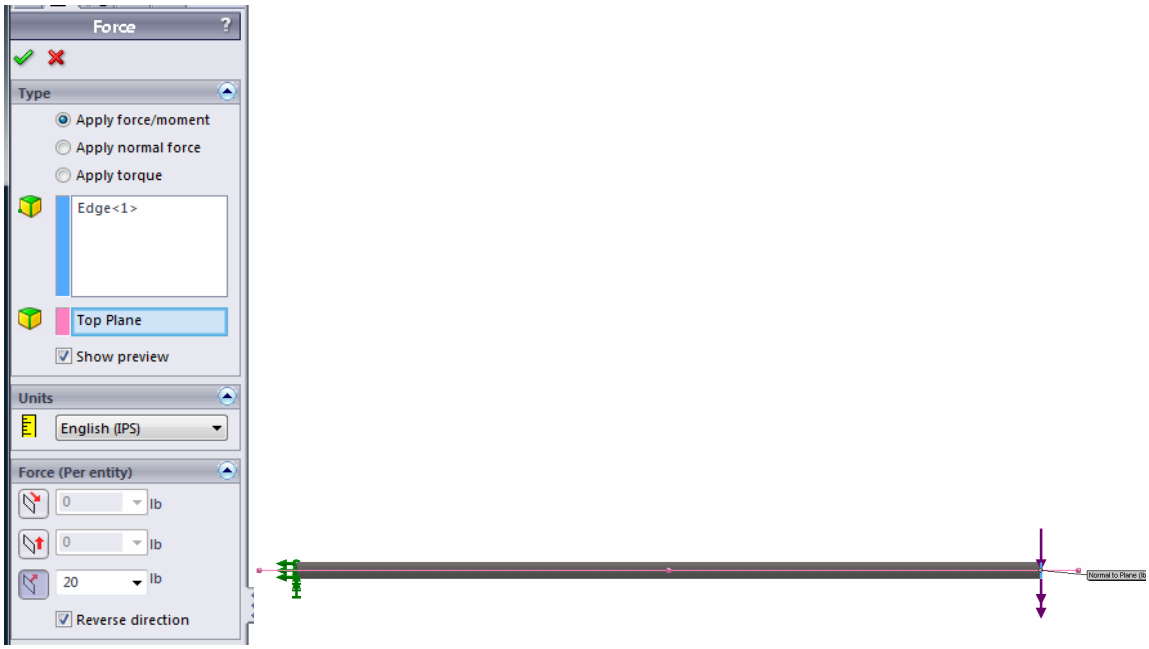

Figure 2.6 – 20*lbf* Load applied at the free end of a cantilever beam

This prepares the cantilever beam model for meshing. A solid mesh type is selected to create a finite element mesh. Under Meshing Parameters, the slider bar is set to medium mesh density for meshing our beam model as shown in Figure 2.7.

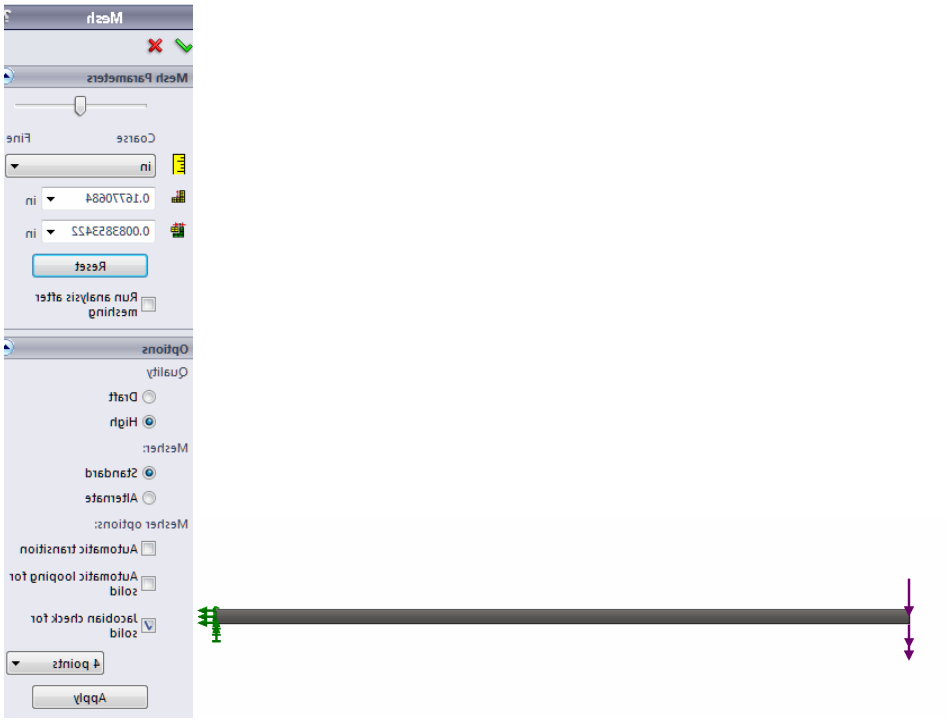

Figure 2.7 – Mesh parameters of a cantilever beam

Mesh density is essential in determining accurate results; the smaller the elements, the lower the discretization errors. It should be noted though; both meshing and solving times result in a less efficient timeline. The global element size is set to 0.167 *in* and the mesh tolerance set to 0.008 *in.* Both values are established automatically based on the volume, surface area, and other geometric features of a cantilever beam model. The global element size is the characteristic element size in the mesh and the element size tolerance is the allowable variance of the actual element sizes in the mesh.

Under Meshing Options, high quality mesh is selected for the study. The high quality mesh prompts the automatic mesher generate parabolic tetrahedral solid elements. Four corner nodes, six mid-side nodes, and six edges define a parabolic tetrahedral element. In general, parabolic elements yield better results because: 1) they represent

curved boundaries more accurately, and 2) they produce better mathematical approximations. The mesher type is set to standard. The standard mesher uses the Voronoi-Delaunay meshing scheme for subsequent meshing operations. This mesher is faster than the alternate mesher and hence is used in this study. In the mesher options, the Jacobian check on 4 Gaussian points is selected. The Jacobian check is based on a number of points located within each element to be used in checking the distortion level of high order tetrahedral elements. The mesh parameters of a cantilever beam model are now defined and ready for meshing.

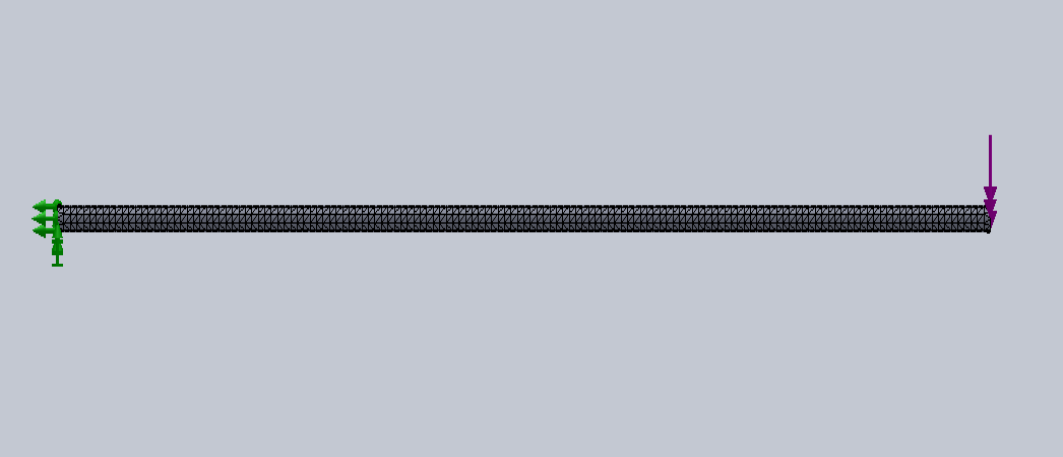

Figure 2.8 – Mesh model of a cantilever beam

Having created the mesh as shown in Figure 2.8, the cantilever beam static analysis is now ready to run. Figure 2.9 shows the FEA deformation plot of a cantilever beam where the maximum UY-deflection is taken directly off the displayed spectrum/range as δ_{FEA} = 0.985 *in*. Note that the undeformed shape of the beam is superimposed on the deformed shape. This option was selected as part of the plot settings.

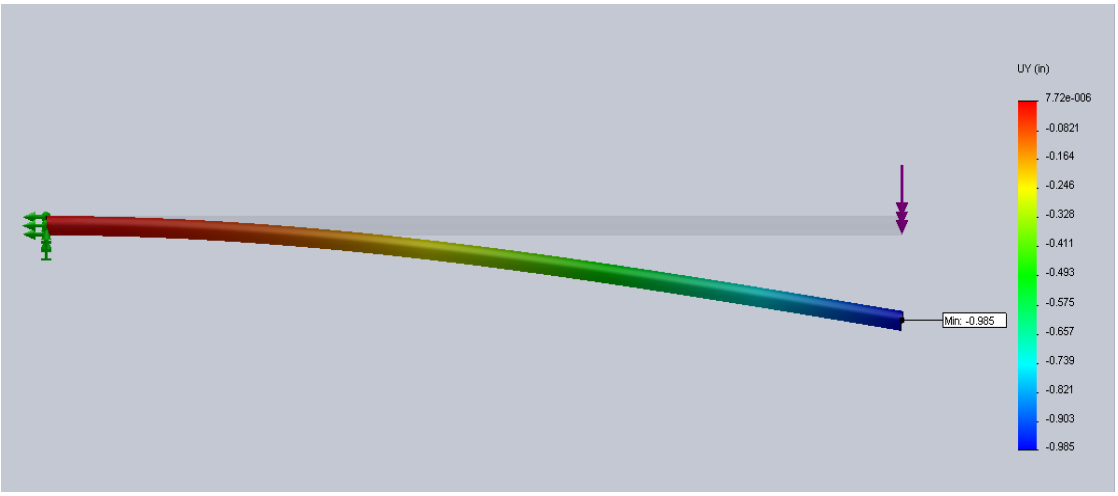

Figure 2.9 – Static deflection of a cantilever beam at the free end

We can conclude from this: our static deflection study of a cantilever beam by validating and comparing the closed form solution obtained using Eq. (2.2) to the COSMOSWorks FEA model.

This hypothesis is accomplished by calculating the relative percentage (%) error as follows:

$$\%Error = \frac{\delta_{Analytical} - \delta_{FEA}}{\delta_{Analytical}} \times 100\% \tag{2.15}$$

Hence, the % error is solved and tabulated as shown below:

$\delta_{Closed\ form\ solution}$ (in)	δ_{FEA} (in)	*% Error*
1.00065	0.985	1.6

Table 2.9 – Summary of static deflection results

Natural Frequency Analysis Using FEA

Having obtained the maximum static deflection of a cantilever beam with an end load applied at the tip of the free end, we now proceed to study the first four natural frequencies of a cantilever beam using COSMOSWorks. This study type requires a set up and run of a frequency study, also known as modal study in FEA terminology as shown in Figure 2.10.

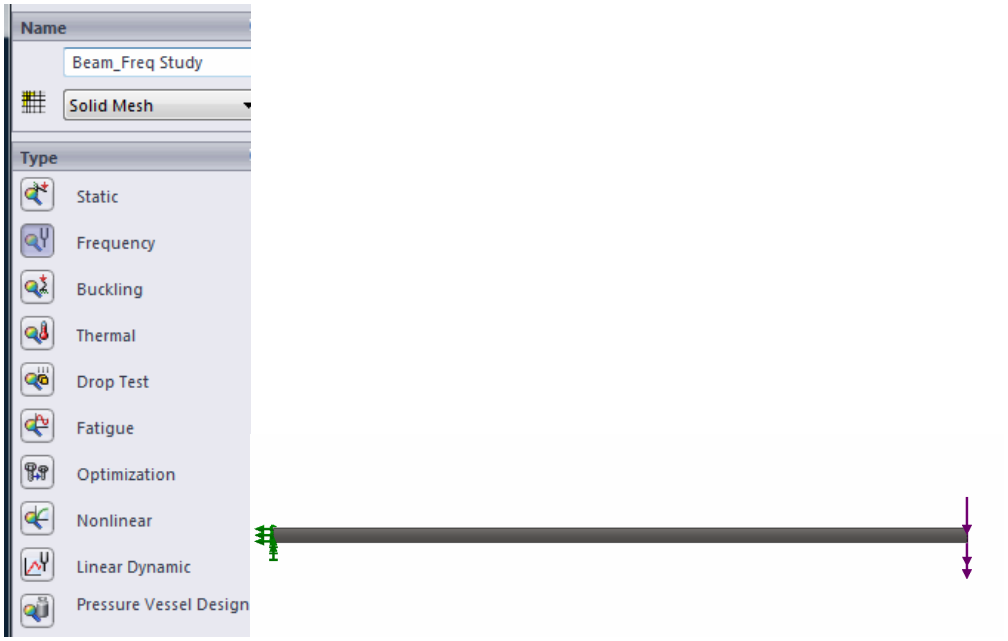

Figure 2.10 – Frequency study of a cantilever beam

The material definition from the static study is copied over to the frequency study. The same is performed for the end load and the fixed restraint. The mesh parameters selected are also the same as defined in the static study. Although the end load is defined in the frequency study, it has no effect. This is due to the frequency study only calculating the natural frequencies and associated modes of vibration of the model,

disregarding any effects of external loads unless a pre-load (i.e. centrifugal load) is defined by activating special options. Table 2.10 shows the frequency study FEA results for the first four natural frequencies of a cantilever beam in radians per second.

Natural frequency (ω_n)	***rad/sec***
ω_1	153.23
ω_2	959.41
ω_3	2,680.52
ω_4	5,236.22

Table 2.10 – Natural frequency results using FEA

The natural frequency analysis of a cantilever beam is finalized by validating and comparing the closed form solution obtained using Eq. (2.9) to the COSMOSWorks FEA model. This hypothesis is accomplished by calculating the relative percentage (%) error using Eq. (2.16):

$$\%Error = \frac{\omega_{closed\ form solution} - \omega_{FEA}}{\omega_{closed\ form solution}} \times 100\% \qquad (2.16)$$

Therefore, the relative percentage (%) error for the four natural frequencies is:

$$\omega_1 \%Error = \frac{153.75 - 153.23}{153.75} \times 100\% = 0.34\%$$

$$\omega_2 \%Error = \frac{970.84 - 959.41}{970.84} \times 100\% = 1.18\%$$

$$\omega_3 \%Error = \frac{2,702 - 2,680.52}{2,702} \times 100\% = 0.80\%$$

$$\omega_4 \%Error = \frac{5,301.11 - 5,236.22}{5,301.11} \times 100\% = 1.22\%$$

A comparison of the closed form solution and FEA results for the first four natural frequencies of a cantilever beam model is used to determine the accuracy of the equations and computing procedure used. A summary of the results is presented in Table 2.11:

Natural frequency	$\omega_{Closed\ form\ solution\ (rad/sec)}$	$\omega_{FEA\ (rad/sec)}$	**Relative % error**
ω_1	153.75	153.23	0.34
ω_2	970.84	959.41	1.18
ω_3	2,702	2,680.52	0.80
ω_4	5,301.11	5,236.22	1.22

Table 2.11 – Summary of natural frequency results

As seen above, the closed form solution and FEA results show a strong correlation. The deviation of the FEA from the closed form solutions is 0.34%, 1.18%, 0.80% and 1.22%. The second and forth natural frequency of the FEA model is only slightly greater than what is found for the closed form solution for the cantilever beam with 1.18 and 1.22 percent variation range. This slight difference is due to the greater stiffness, *k*, of the finite element model.

Mode Shape Analysis Using FEA

In the previous section, the first four natural frequencies for the cantilever beam were obtained. From the frequency study, two results folders were automatically created; displacement folder and deformation folder, both containing four plots corresponding to

these four frequencies. The displacement plots are ignored since they exhibit displacement magnitude, which has no quantitative importance in the frequency study. Displacement results are purely qualitative and only are used for comparison of displacements within the same mode of vibration. Relative comparison of displacements between different modes is invalid. The shape of the normal modes is presented in Appendix D, showing the profile of deformation associated with the given mode of vibration.

A comparison of the closed form solution and FEA results for the first four mode shapes of a cantilever beam model is used to determine the accuracy of the equations and computing procedure used. A summary of the results is presented in Table 2.12:

	Closed form solution			**FEA**			**% Error**		
Mode Shape	x/L_1	x/L_2	x/L_3	x/L_1	x/L_2	x/L_3	x/L_1	x/L_2	x/L_3
First	-	-	-	-	-	-	-	-	-
Second	0.78	-	-	0.76	-	-	2.56	-	-
Third	0.50	0.97	-	0.49	0.95	-	2.06	2.30	-
Fourth	0.36	0.64	0.91	0.35	0.63	0.89	2.78	1.56	2.20

Table 2.12 – Summary of mode shape results

In comparison to the closed form solution mode shapes as shown in Table 2.12, the normal modes and shapes of vibration are found to be similar in terms of the node locations (x/L) along the length of the beam. The minimum error percentage was 2.06% for the third mode shape at node location x/L_1, and the maximum error percentage was 2.78% for the fourth mode shape at node location x/L_1. Additionally, the first elastic mode of vibration, meaning the first mode requiring the cantilever beam to have elastic deformation is mode number one, has a frequency of 153.23*rad/sec*. This confirms what we were expecting to find as the fundamental mode of vibration for a cantilever beam.

Forced Vibration Analysis Using FEA

According to Rao [30], a dynamic system is often subjected to some type of external force or excitation, referred to as the forcing or exciting function. This excitation is usually time-dependent. It may be harmonic or non-harmonic but periodic, non-periodic, or random in nature. The response of a system to harmonic excitation is called harmonic response. The non-periodic excitation may have a long or short duration. The response of a dynamic system to suddenly applied non-periodic excitations is called transient response.

Harmonic excitation is often encountered in engineering systems. It is commonly produced by the unbalance in rotating machinery. Although pure harmonic excitation is less likely to occur than periodic or other type of excitation as mentioned above, learning the behavior of a system undergoing harmonic excitation is essential in understanding how the system will respond to more general types of excitation. Harmonic motion may be in the form of a force or displacement at some point in the system.

In this section, a cantilever beam is examined for its dynamic response under continuing excitation whose magnitude varies sinusoidally with time using the general equation of motion for the FEA model [30]:

$$m\ddot{x} + c\dot{x} + kx = F(t) \tag{3.3}$$

Where m, c, k are mass, damping and stiffness matrices, respectively, and $F(t)$ is the vector for external forces. Neglecting the influence of damping and expressing external load for a steady-state condition as [30]:

$$F(t) = F_o \sin \omega t \tag{3.4}$$

Where, F_o is the sinusoidal force subjected at the tip of the free end, ω is the frequency of the harmonic variation and *t* is time.

Having obtained the natural frequencies for a cantilever beam in the previous section, the results are copied to the linear dynamics study, modal history analysis. The material properties, restraints and results of the frequency study are also copied to the dynamic study. The properties of the dynamic study were selected as start time zero (0) *sec* and end time of one-half (0.5) *sec* in time increment of 0.0005 *sec*. The left face of a cantilever beam is fixed, and an oscillatory force in the vertical direction, $F_o = 20$ *lbf*, is subjected at the tip of the free end (right face) with a frequency of $\omega = 20$ *rad/sec*. In the results option, the tip of the free end was selected as the node for the time response graphs in the horizontal, vertical and longitudinal axis. After the analysis was run, three response time history plots were generated as shown in Appendix F and the corresponding data was tabulated in Appendix E.

Clearly, all three plots depict oscillations of the cantilever beam under a harmonic force. It's noted that the maximum dynamic UY displacement during transient-state is approximately 1.793 *in*. This value is greater than the 0.985 *in* which is the maximum static UY displacement of the beam. The maximum steady-state UX, UY and UZ displacements are summarized below in Table 2.13:

Displacement Direction	**Value (*in*)**
UX	2.844E-4
UY	0.966
UZ	0.015

Table 2.13 – Forced vibration results of a cantilever beam using FEA

APPENDIX B

Data points for mode shape plots of a cantilever beam

x	B_1x	$\sin(B_1x)$	$\sinh(B_1x)$	$\cos(B_1x)$	$\cosh(B_1x)$	x/L	$Y_r(x)$
0.00	0.00	0.00	0.00	1.00	1.00	0.00	0.00
0.50	0.04	0.04	0.04	1.00	1.00	0.02	0.00
1.00	0.08	0.08	0.08	1.00	1.00	0.04	0.00
1.50	0.12	0.12	0.12	0.99	1.01	0.06	0.01
2.00	0.16	0.16	0.16	0.99	1.01	0.08	0.02
2.50	0.20	0.19	0.20	0.98	1.02	0.10	0.03
3.00	0.23	0.23	0.24	0.97	1.03	0.13	0.05
3.50	0.27	0.27	0.28	0.96	1.04	0.15	0.06
4.00	0.31	0.31	0.32	0.95	1.05	0.17	0.08
4.50	0.35	0.34	0.36	0.94	1.06	0.19	0.11
5.00	0.39	0.38	0.40	0.92	1.08	0.21	0.13
5.50	0.43	0.42	0.44	0.91	1.09	0.23	0.16
6.00	0.47	0.45	0.49	0.89	1.11	0.25	0.20
6.50	0.51	0.49	0.53	0.87	1.13	0.27	0.23
7.00	0.55	0.52	0.57	0.85	1.15	0.29	0.28
7.50	0.59	0.55	0.62	0.83	1.18	0.31	0.32
8.00	0.63	0.59	0.67	0.81	1.20	0.33	0.37
8.50	0.66	0.62	0.71	0.79	1.23	0.35	0.42
9.00	0.70	0.65	0.76	0.76	1.26	0.38	0.48
9.50	0.74	0.68	0.81	0.74	1.29	0.40	0.55
10.00	0.78	0.70	0.86	0.71	1.32	0.42	0.61
10.50	0.82	0.73	0.92	0.68	1.36	0.44	0.68
11.00	0.86	0.76	0.97	0.65	1.39	0.46	0.76
11.50	0.90	0.78	1.02	0.62	1.43	0.48	0.84
12.00	0.94	0.81	1.08	0.59	1.47	0.50	0.93
12.50	0.98	0.83	1.14	0.56	1.52	0.52	1.02
13.00	1.02	0.85	1.20	0.53	1.56	0.54	1.12
13.50	1.05	0.87	1.26	0.49	1.61	0.56	1.22
14.00	1.09	0.89	1.33	0.46	1.66	0.58	1.33
14.50	1.13	0.91	1.39	0.42	1.71	0.60	1.44
15.00	1.17	0.92	1.46	0.39	1.77	0.63	1.56
15.50	1.21	0.94	1.53	0.35	1.83	0.65	1.69
16.00	1.25	0.95	1.60	0.32	1.89	0.67	1.82
16.50	1.29	0.96	1.68	0.28	1.95	0.69	1.96
17.00	1.33	0.97	1.75	0.24	2.02	0.71	2.10
17.50	1.37	0.98	1.83	0.20	2.09	0.73	2.26
18.00	1.41	0.99	1.92	0.16	2.16	0.75	2.41
18.50	1.45	0.99	2.00	0.13	2.24	0.77	2.58
19.00	1.48	1.00	2.09	0.09	2.32	0.79	2.75
19.50	1.52	1.00	2.19	0.05	2.40	0.81	2.93
20.00	1.56	1.00	2.28	0.01	2.49	0.83	3.12
20.50	1.60	1.00	2.38	-0.03	2.58	0.85	3.32
21.00	1.64	1.00	2.48	-0.07	2.68	0.88	3.52
21.50	1.68	0.99	2.59	-0.11	2.78	0.90	3.73
22.00	1.72	0.99	2.70	-0.15	2.88	0.92	3.95
22.50	1.76	0.98	2.81	-0.19	2.99	0.94	4.18
23.00	1.80	0.97	2.93	-0.22	3.10	0.96	4.42
23.50	1.84	0.97	3.06	-0.26	3.22	0.98	4.67
24.00	1.88	0.95	3.18	-0.30	3.34	1.00	4.93

Table 2.14 - Calculated data for first mode shape of a cantilever beam

x	B_2x	$\sin(B_2x)$	$\sinh(B_2x)$	$\cos(B_2x)$	$\cosh(B_2x)$	x/L	$Y_r(x)$
0.0	0.00	0.00	0.00	1.00	1.00	0.00	0.00
0.5	0.10	0.10	0.10	1.00	1.00	0.02	0.01
1.0	0.20	0.19	0.20	0.98	1.02	0.04	0.04
1.5	0.29	0.29	0.30	0.96	1.04	0.06	0.08
2.0	0.39	0.38	0.40	0.92	1.08	0.08	0.13
2.5	0.49	0.47	0.51	0.88	1.12	0.10	0.20
3.0	0.59	0.55	0.62	0.83	1.18	0.13	0.27
3.5	0.68	0.63	0.74	0.77	1.24	0.15	0.35
4.0	0.78	0.70	0.86	0.71	1.32	0.17	0.44
4.5	0.88	0.77	1.00	0.64	1.41	0.19	0.54
5.0	0.98	0.83	1.14	0.56	1.52	0.21	0.63
5.5	1.08	0.88	1.30	0.48	1.64	0.23	0.73
6.0	1.17	0.92	1.46	0.39	1.77	0.25	0.82
6.5	1.27	0.96	1.64	0.30	1.92	0.27	0.91
7.0	1.37	0.98	1.84	0.20	2.09	0.29	1.00
7.5	1.47	0.99	2.05	0.10	2.28	0.31	1.09
8.0	1.56	1.00	2.29	0.01	2.50	0.33	1.16
8.5	1.66	1.00	2.54	-0.09	2.73	0.35	1.23
9.0	1.76	0.98	2.82	-0.19	2.99	0.38	1.29
9.5	1.86	0.96	3.13	-0.28	3.28	0.40	1.34
10.0	1.96	0.93	3.46	-0.38	3.61	0.42	1.38
10.5	2.05	0.89	3.83	-0.46	3.96	0.44	1.40
11.0	2.15	0.84	4.24	-0.55	4.36	0.46	1.42
11.5	2.25	0.78	4.69	-0.63	4.79	0.48	1.42
12.0	2.35	0.71	5.18	-0.70	5.27	0.50	1.41
12.5	2.44	0.64	5.72	-0.77	5.81	0.52	1.39
13.0	2.54	0.56	6.32	-0.83	6.40	0.54	1.35
13.5	2.64	0.48	6.97	-0.88	7.04	0.56	1.30
14.0	2.74	0.39	7.70	-0.92	7.76	0.58	1.23
14.5	2.84	0.30	8.49	-0.95	8.55	0.60	1.16
15.0	2.93	0.21	9.37	-0.98	9.43	0.63	1.07
15.5	3.03	0.11	10.34	-0.99	10.39	0.65	0.96
16.0	3.13	0.01	11.41	-1.00	11.45	0.67	0.85
16.5	3.23	-0.09	12.58	-1.00	12.62	0.69	0.72
17.0	3.32	-0.18	13.88	-0.98	13.92	0.71	0.59
17.5	3.42	-0.28	15.31	-0.96	15.34	0.73	0.45
18.0	3.52	-0.37	16.89	-0.93	16.92	0.75	0.29
18.5	3.62	-0.46	18.62	-0.89	18.65	0.77	0.13
19.0	3.72	-0.54	20.54	-0.84	20.56	0.79	-0.03
19.5	3.81	-0.62	22.65	-0.78	22.67	0.81	-0.21
20.0	3.91	-0.70	24.98	-0.72	25.00	0.83	-0.39
20.5	4.01	-0.76	27.55	-0.65	27.57	0.85	-0.57
21.0	4.11	-0.82	30.38	-0.57	30.40	0.88	-0.75
21.5	4.21	-0.87	33.50	-0.49	33.52	0.90	-0.94
22.0	4.30	-0.92	36.95	-0.40	36.96	0.92	-1.13
22.5	4.40	-0.95	40.74	-0.31	40.76	0.94	-1.31
23.0	4.50	-0.98	44.93	-0.21	44.94	0.96	-1.50
23.5	4.60	-0.99	49.55	-0.12	49.56	0.98	-1.69
24.0	4.69	-1.00	54.64	-0.02	54.65	1.00	-1.88

Table 2.15 - Calculated data for second mode shape of a cantilever beam

x	B_4x	$sin(B_4x)$	$sinh(B_4x)$	$cos(B_4x)$	$cosh(B_4x)$	x/L	$Y_r(x)$
0.00	0.00	0.00	0.00	1.00	1.00	0.00	0.00
0.50	0.16	0.16	0.16	0.99	1.01	0.02	0.03
1.00	0.33	0.32	0.33	0.95	1.05	0.04	0.10
1.50	0.49	0.47	0.51	0.88	1.12	0.06	0.20
2.00	0.65	0.61	0.70	0.79	1.22	0.08	0.33
2.50	0.82	0.73	0.91	0.68	1.35	0.10	0.49
3.00	0.98	0.83	1.15	0.56	1.52	0.13	0.65
3.50	1.15	0.91	1.41	0.41	1.73	0.15	0.82
4.00	1.31	0.97	1.72	0.26	1.99	0.17	0.98
4.50	1.47	1.00	2.07	0.10	2.30	0.19	1.13
5.00	1.64	1.00	2.47	-0.07	2.67	0.21	1.26
5.50	1.80	0.97	2.94	-0.23	3.11	0.23	1.36
6.00	1.96	0.92	3.49	-0.38	3.63	0.25	1.44
6.50	2.13	0.85	4.14	-0.53	4.26	0.27	1.49
7.00	2.29	0.75	4.89	-0.66	4.99	0.29	1.51
7.50	2.45	0.63	5.78	-0.77	5.86	0.31	1.49
8.00	2.62	0.50	6.82	-0.87	6.89	0.33	1.43
8.50	2.78	0.35	8.04	-0.94	8.11	0.35	1.34
9.00	2.95	0.19	9.48	-0.98	9.54	0.38	1.22
9.50	3.11	0.03	11.18	-1.00	11.22	0.40	1.07
10.00	3.27	-0.13	13.17	-0.99	13.21	0.42	0.89
10.50	3.44	-0.29	15.52	-0.96	15.55	0.44	0.69
11.00	3.60	-0.44	18.29	-0.90	18.31	0.46	0.47
11.50	3.76	-0.58	21.54	-0.81	21.57	0.48	0.24
12.00	3.93	-0.71	25.38	-0.71	25.40	0.50	0.00
12.50	4.09	-0.81	29.89	-0.58	29.91	0.52	-0.23
13.00	4.25	-0.90	35.21	-0.44	35.22	0.54	-0.46
13.50	4.42	-0.96	41.47	-0.29	41.48	0.56	-0.68
14.00	4.58	-0.99	48.85	-0.13	48.86	0.58	-0.88
14.50	4.75	-1.00	57.53	0.03	57.54	0.60	-1.06
15.00	4.91	-0.98	67.76	0.20	67.77	0.63	-1.21
15.50	5.07	-0.94	79.81	0.35	79.82	0.65	-1.33
16.00	5.24	-0.87	94.00	0.50	94.00	0.67	-1.42
16.50	5.40	-0.77	110.71	0.63	110.72	0.69	-1.48
17.00	5.56	-0.66	130.40	0.75	130.40	0.71	-1.49
17.50	5.73	-0.53	153.58	0.85	153.58	0.73	-1.48
18.00	5.89	-0.38	180.89	0.92	180.89	0.75	-1.42
18.50	6.05	-0.23	213.05	0.97	213.05	0.77	-1.34
19.00	6.22	-0.06	250.92	1.00	250.93	0.79	-1.23
19.50	6.38	0.10	295.54	1.00	295.54	0.81	-1.09
20.00	6.55	0.26	348.08	0.97	348.08	0.83	-0.93
20.50	6.71	0.41	409.97	0.91	409.97	0.85	-0.77
21.00	6.87	0.56	482.85	0.83	482.85	0.88	-0.59
21.50	7.04	0.68	568.70	0.73	568.70	0.90	-0.42
22.00	7.20	0.79	669.81	0.61	669.81	0.92	-0.26
22.50	7.36	0.88	788.90	0.47	788.90	0.94	-0.11
23.00	7.53	0.95	929.15	0.32	929.15	0.96	0.01
23.50	7.69	0.99	1094.35	0.16	1094.35	0.98	0.10
24.00	7.85	1.00	1288.91	0.00	1288.91	1.00	0.15

Table 2.16 - Calculated data for third mode shape of a cantilever beam

x	B_4x	$sin(B_4x)$	$sinh(B_4x)$	$cos(B_4x)$	$cosh(B_4x)$	x/L	$Y_r(x)$
0.00	0.00	0.00	0.00	1.00	1.00	0.00	0.00
0.50	0.23	0.23	0.23	0.97	1.03	0.02	0.05
1.00	0.46	0.44	0.47	0.90	1.11	0.04	0.18
1.50	0.69	0.63	0.74	0.77	1.25	0.06	0.36
2.00	0.92	0.79	1.05	0.61	1.45	0.08	0.58
2.50	1.15	0.91	1.41	0.41	1.73	0.10	0.82
3.00	1.37	0.98	1.85	0.20	2.10	0.13	1.04
3.50	1.60	1.00	2.38	-0.03	2.59	0.15	1.23
4.00	1.83	0.97	3.05	-0.26	3.21	0.17	1.38
4.50	2.06	0.88	3.87	-0.47	3.99	0.19	1.48
5.00	2.29	0.75	4.89	-0.66	4.99	0.21	1.51
5.50	2.52	0.58	6.17	-0.81	6.25	0.23	1.48
6.00	2.75	0.38	7.78	-0.92	7.84	0.25	1.37
6.50	2.98	0.16	9.80	-0.99	9.85	0.27	1.20
7.00	3.21	-0.07	12.33	-1.00	12.37	0.29	0.97
7.50	3.44	-0.29	15.52	-0.96	15.55	0.31	0.70
8.00	3.67	-0.50	19.52	-0.87	19.54	0.33	0.39
8.50	3.89	-0.68	24.55	-0.73	24.57	0.35	0.07
9.00	4.12	-0.83	30.87	-0.56	30.89	0.38	-0.26
9.50	4.35	-0.94	38.83	-0.35	38.84	0.40	-0.57
10.00	4.58	-0.99	48.82	-0.13	48.83	0.42	-0.85
10.50	4.81	-1.00	61.39	0.10	61.40	0.44	-1.09
11.00	5.04	-0.95	77.20	0.32	77.21	0.46	-1.26
11.50	5.27	-0.85	97.08	0.53	97.08	0.48	-1.37
12.00	5.50	-0.71	122.07	0.71	122.07	0.50	-1.41
12.50	5.73	-0.53	153.49	0.85	153.50	0.52	-1.38
13.00	5.96	-0.32	193.01	0.95	193.01	0.54	-1.27
13.50	6.18	-0.10	242.70	1.00	242.70	0.56	-1.10
14.00	6.41	0.13	305.18	0.99	305.18	0.58	-0.87
14.50	6.64	0.35	383.74	0.94	383.74	0.60	-0.59
15.00	6.87	0.56	482.53	0.83	482.53	0.63	-0.29
15.50	7.10	0.73	606.75	0.68	606.75	0.65	0.03
16.00	7.33	0.87	762.94	0.50	762.95	0.67	0.35
16.50	7.56	0.96	959.35	0.29	959.35	0.69	0.64
17.00	7.79	1.00	1206.32	0.07	1206.32	0.71	0.90
17.50	8.02	0.99	1516.87	-0.16	1516.87	0.73	1.11
18.00	8.25	0.92	1907.36	-0.38	1907.36	0.75	1.26
18.50	8.48	0.81	2398.38	-0.58	2398.38	0.77	1.33
19.00	8.70	0.66	3015.81	-0.75	3015.81	0.79	1.33
19.50	8.93	0.47	3792.18	-0.88	3792.18	0.81	1.25
20.00	9.16	0.26	4768.42	-0.97	4768.42	0.83	1.10
20.50	9.39	0.03	5995.97	-1.00	5995.97	0.85	0.87
21.00	9.62	-0.20	7539.53	-0.98	7539.53	0.88	0.59
21.50	9.85	-0.41	9480.46	-0.91	9480.46	0.90	0.25
22.00	10.08	-0.61	11921.05	-0.79	11921.05	0.92	-0.13
22.50	10.31	-0.77	14989.93	-0.63	14989.93	0.94	-0.54
23.00	10.54	-0.90	18848.85	-0.44	18848.85	0.96	-0.95
23.50	10.77	-0.97	23701.17	-0.23	23701.17	0.98	-1.38
24.00	11.00	-1.00	29802.66	0.00	29802.66	1.00	-1.79

Table 2.17 - Calculated data for fourth mode shape of a cantilever beam

APPENDIX C

Modes shapes plots of a cantilever beam using closed form

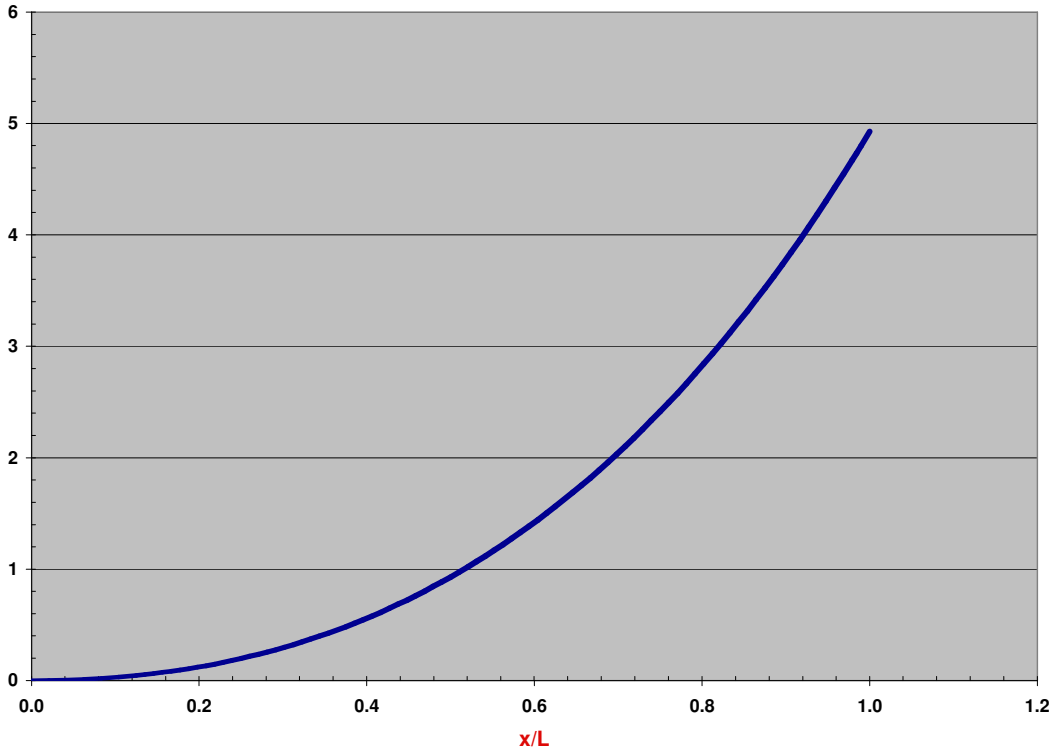

Figure 2.11 - First mode shape of a cantilever beam

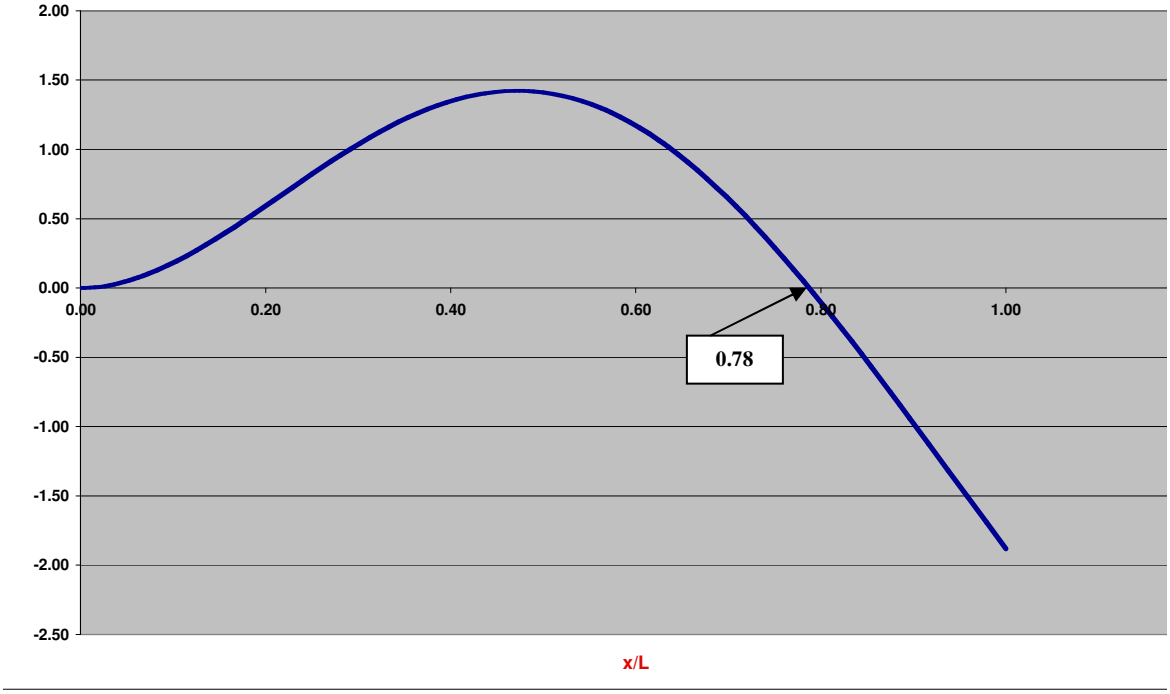

Figure 2.12 - Second mode shape of a cantilever beam

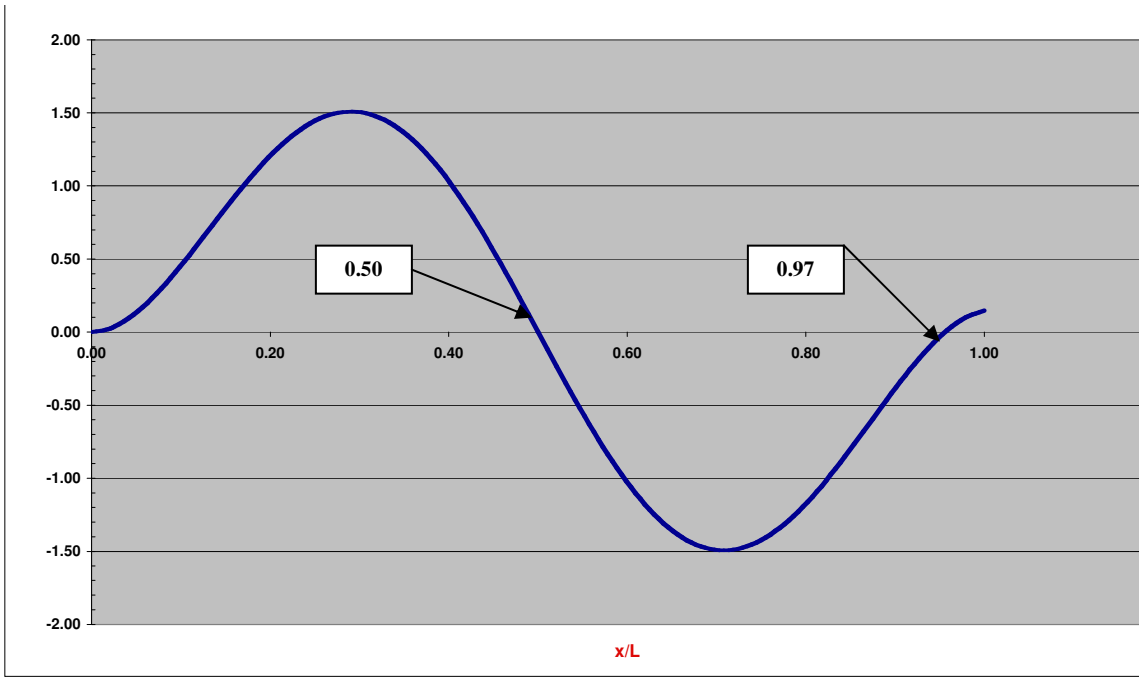

Figure 2.13 - Third mode shape of a cantilever beam

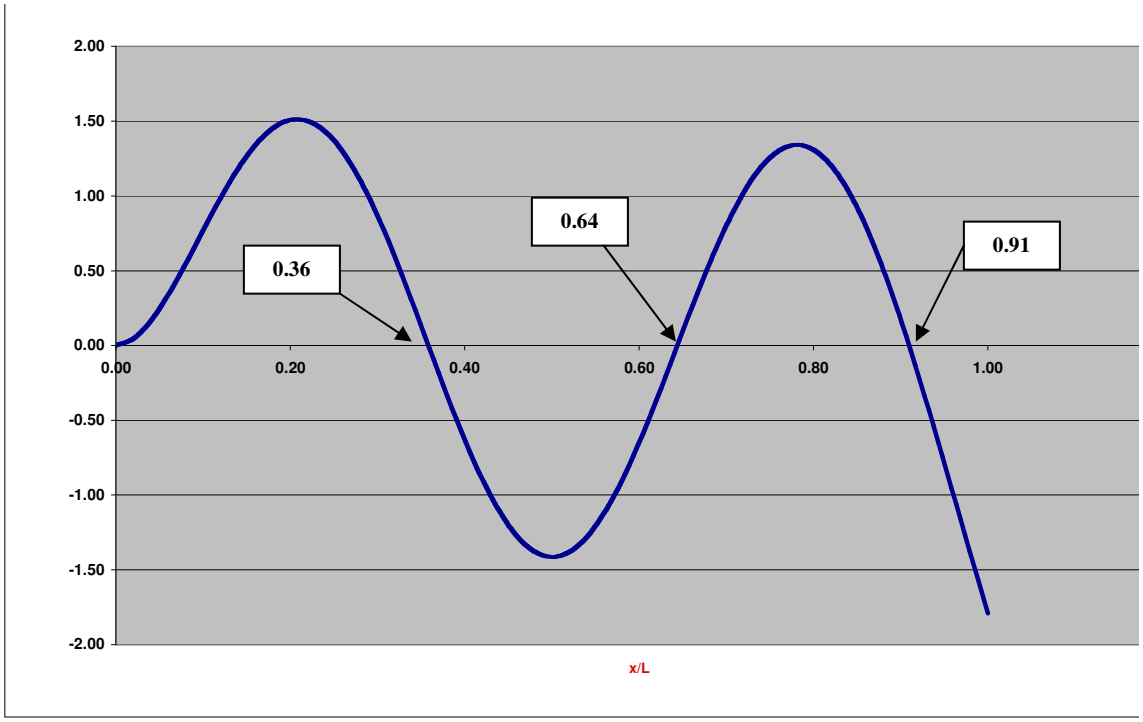

Figure 2.14 - Fourth mode shape of a cantilever beam

APPENDIX D

Modes shape plots of a cantilever beam using FEA

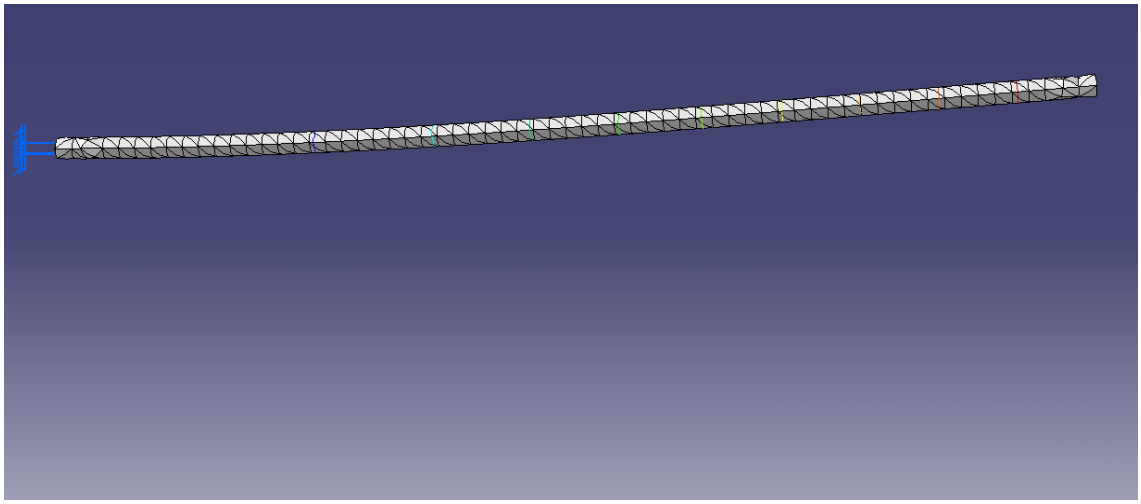

Figure 2.15 - First mode shape of a cantilever beam using FEA

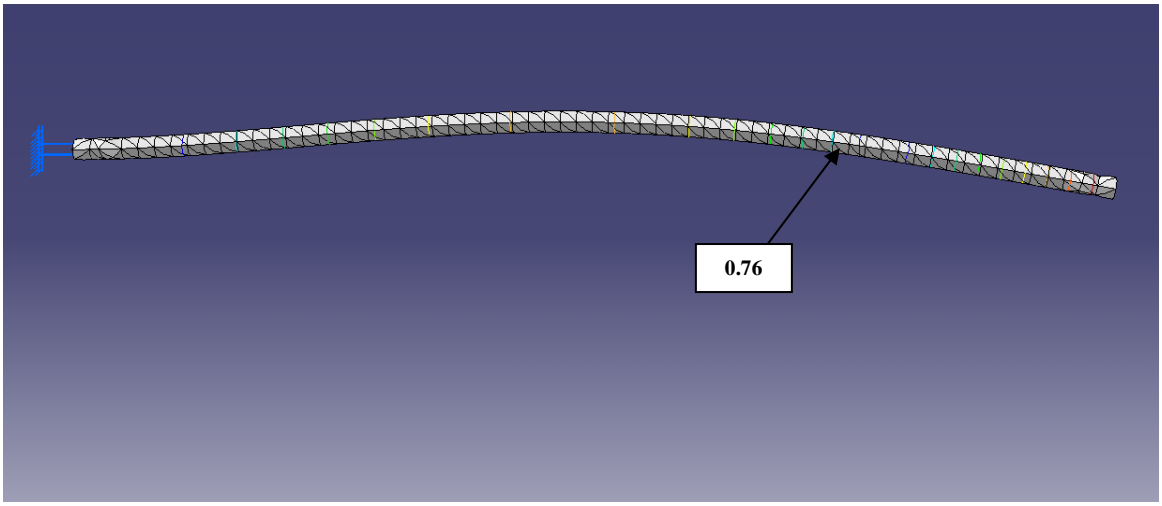

Figure 2.16 - Second mode shape of a cantilever beam using FEA

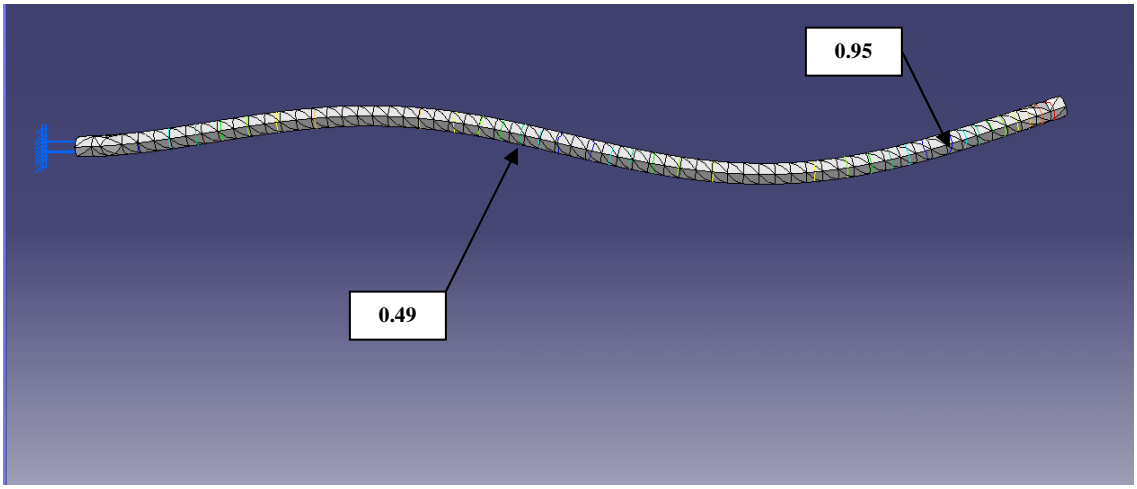

Figure 2.17 - Third mode shape of a cantilever beam using FEA

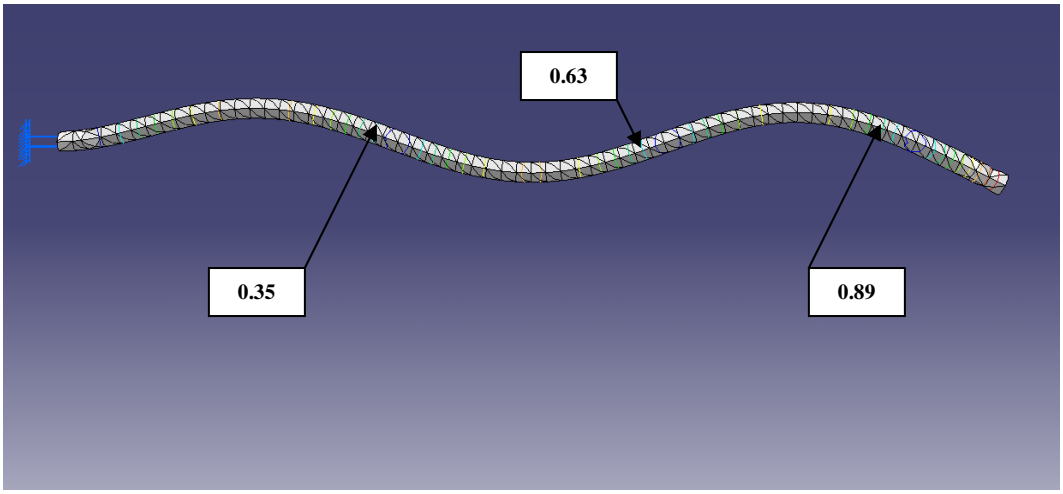

Figure 2.18 - Fourth mode shape of a cantilever beam using FEA

APPENDIX E

Data points for time history plots of a cantilever beam

Point	Time (sec)	UX (inch)	Point	Time (sec)	UX (inch)
1	0.0005	-0.00017782	50	0.2455	-0.00057937
2	0.0055	-0.00028827	51	0.2505	-0.00057691
3	0.0105	-0.00042702	52	0.2555	-0.00057991
4	0.0155	-0.00053317	53	0.2605	-0.00058643
5	0.0205	-0.00059457	54	0.2655	-0.00059262
6	0.0255	-0.00061925	55	0.2705	-0.00059496
7	0.0305	-0.00061918	56	0.2755	-0.00059225
8	0.0355	-0.00060633	57	0.2805	-0.00058627
9	0.0405	-0.00059121	58	0.2855	-0.00058055
10	0.0455	-0.00058052	59	0.2905	-0.00057835
11	0.0505	-0.00057677	60	0.2955	-0.00058077
12	0.0555	-0.00057985	61	0.3005	-0.00058624
13	0.0605	-0.00058738	62	0.3055	-0.0005915
14	0.0655	-0.00059466	63	0.3105	-0.00059356
15	0.0705	-0.00059683	64	0.3155	-0.00059139
16	0.0755	-0.00059225	65	0.3205	-0.00058642
17	0.0805	-0.00058372	66	0.3255	-0.00058161
18	0.0855	-0.0005764	67	0.3305	-0.0005797
19	0.0905	-0.0005746	68	0.3355	-0.00058163
20	0.0955	-0.00057944	69	0.3405	-0.00058612
21	0.1005	-0.00058838	70	0.3455	-0.0005905
22	0.1055	-0.00059639	71	0.3505	-0.00059228
23	0.1105	-0.00059873	72	0.3555	-0.00059056
24	0.1155	-0.00059386	73	0.3605	-0.00058651
25	0.1205	-0.00058455	74	0.3655	-0.00058253
26	0.1255	-0.00057625	75	0.3705	-0.00058089
27	0.1305	-0.00057377	76	0.3755	-0.00058241
28	0.1355	-0.0005785	77	0.3805	-0.00058606
29	0.1405	-0.00058768	78	0.3855	-0.00058966
30	0.1455	-0.00059599	79	0.3905	-0.00059116
31	0.1505	-0.00059865	80	0.3955	-0.00058982
32	0.1555	-0.00059416	81	0.4005	-0.00058655
33	0.1605	-0.00058521	82	0.4055	-0.0005833
34	0.1655	-0.00057703	83	0.4105	-0.00058193
35	0.1705	-0.00057433	84	0.4155	-0.0005831
36	0.1755	-0.00057856	85	0.4205	-0.00058603
37	0.1805	-0.00058713	86	0.4255	-0.00058895
38	0.1855	-0.00059502	87	0.4305	-0.00059021
39	0.1905	-0.00059772	88	0.4355	-0.00058918
40	0.1955	-0.0005938	89	0.4405	-0.00058657
41	0.2005	-0.00058569	90	0.4455	-0.00058394
42	0.2055	-0.00057815	91	0.4505	-0.0005828
43	0.2105	-0.0005755	92	0.4555	-0.0005837
44	0.2155	-0.00057911	93	0.4605	-0.00058603
45	0.2205	-0.00058672	94	0.4655	-0.00058838
46	0.2255	-0.00059383	95	0.4705	-0.00058942
47	0.2305	-0.0005964	96	0.4755	-0.00058863
48	0.2355	-0.0005931	97	0.4805	-0.00058656
49	0.2405	-0.00058603	98	0.4855	-0.00058446

Table 2.18– Data points for UX displacement time history plot of a cantilever beam

Point	Time (sec)	UY (inch)	Point	Time (sec)	UY (inch)
1	0.0005	-0.0037382	50	0.2455	-0.87582
2	0.0055	-0.31949	51	0.2505	-0.97072
3	0.0105	-0.98388	52	0.2555	-1.0658
4	0.0155	-1.5795	53	0.2605	-1.1075
5	0.0205	-1.7923	54	0.2655	-1.0765
6	0.0255	-1.545	55	0.2705	-0.99561
7	0.0305	-1.004	56	0.2755	-0.91415
8	0.0355	-0.48606	57	0.2805	-0.87796
9	0.0405	-0.28403	58	0.2855	-0.90397
10	0.0455	-0.49427	59	0.2905	-0.97287
11	0.0505	-0.96646	60	0.2955	-1.0427
12	0.0555	-1.411	61	0.3005	-1.074
13	0.0605	-1.5798	62	0.3055	-1.0523
14	0.0655	-1.4015	63	0.3105	-0.99355
15	0.0705	-1.003	64	0.3155	-0.93374
16	0.0755	-0.62334	65	0.3205	-0.90654
17	0.0805	-0.47414	66	0.3255	-0.9248
18	0.0855	-0.62284	67	0.3305	-0.97481
19	0.0905	-0.96386	68	0.3355	-1.0261
20	0.0955	-1.2904	69	0.3405	-1.0496
21	0.1005	-1.4195	70	0.3455	-1.0343
22	0.1055	-1.2937	71	0.3505	-0.99174
23	0.1105	-1.0032	72	0.3555	-0.94783
24	0.1155	-0.7238	73	0.3605	-0.92741
25	0.1205	-0.6115	74	0.3655	-0.9402
26	0.1255	-0.71694	75	0.3705	-0.97649
27	0.1305	-0.96452	76	0.3755	-1.0141
28	0.1355	-1.2043	77	0.3805	-1.0318
29	0.1405	-1.3019	78	0.3855	-1.0211
30	0.1455	-1.2131	79	0.3905	-0.99019
31	0.1505	-1.0021	80	0.3955	-0.95796
32	0.1555	-0.7966	81	0.4005	-0.94264
33	0.1605	-0.71186	82	0.4055	-0.95158
34	0.1655	-0.78638	83	0.4105	-0.97791
35	0.1705	-0.96627	84	0.4155	-1.0055
36	0.1755	-1.1424	85	0.4205	-1.0188
37	0.1805	-1.216	86	0.4255	-1.0113
38	0.1855	-1.1534	87	0.4305	-0.98889
39	0.1905	-1.0001	88	0.4355	-0.96524
40	0.1955	-0.84911	89	0.4405	-0.95376
41	0.2005	-0.78522	90	0.4455	-0.95999
42	0.2055	-0.83778	91	0.4505	-0.97909
43	0.2105	-0.96845	92	0.4555	-0.99935
44	0.2155	-1.0979	93	0.4605	-1.0093
45	0.2205	-1.1533	94	0.4655	-1.0041
46	0.2255	-1.1092	95	0.4705	-0.98782
47	0.2305	-0.99784	96	0.4755	-0.97047
48	0.2355	-0.88693	97	0.4805	-0.96187
49	0.2405	-0.83881	98	0.4855	-0.96621

Table 2.19 – Data points for UY displacement time history plot of a cantilever beam

Point	Time (sec)	UZ (inch)	Point	Time (sec)	UZ (inch)
1	0.0005	-0.0001634	50	0.2455	-0.013626
2	0.0055	-0.0053588	51	0.2505	-0.014987
3	0.0105	-0.015605	52	0.2555	-0.016351
4	0.0155	-0.023894	53	0.2605	-0.016949
5	0.0205	-0.026498	54	0.2655	-0.016504
6	0.0255	-0.023067	55	0.2705	-0.015344
7	0.0305	-0.01562	56	0.2755	-0.014176
8	0.0355	-0.0081699	57	0.2805	-0.013657
9	0.0405	-0.0050704	58	0.2855	-0.01403
10	0.0455	-0.008064	59	0.2905	-0.015018
11	0.0505	-0.014957	60	0.2955	-0.016019
12	0.0555	-0.021363	61	0.3005	-0.016469
13	0.0605	-0.023712	62	0.3055	-0.016157
14	0.0655	-0.021124	63	0.3105	-0.015315
15	0.0705	-0.015449	64	0.3155	-0.014457
16	0.0755	-0.010031	65	0.3205	-0.014067
17	0.0805	-0.00787	66	0.3255	-0.014329
18	0.0855	-0.009983	67	0.3305	-0.015046
19	0.0905	-0.014884	68	0.3355	-0.015781
20	0.0955	-0.019581	69	0.3405	-0.016119
21	0.1005	-0.021428	70	0.3455	-0.0159
22	0.1055	-0.019614	71	0.3505	-0.015289
23	0.1105	-0.01545	72	0.3555	-0.014659
24	0.1155	-0.011449	73	0.3605	-0.014366
25	0.1205	-0.0098384	74	0.3655	-0.01455
26	0.1255	-0.011347	75	0.3705	-0.01507
27	0.1305	-0.014897	76	0.3755	-0.01561
28	0.1355	-0.018338	77	0.3805	-0.015863
29	0.1405	-0.019738	78	0.3855	-0.01571
30	0.1455	-0.018464	79	0.3905	-0.015267
31	0.1505	-0.015436	80	0.3955	-0.014804
32	0.1555	-0.01249	81	0.4005	-0.014585
33	0.1605	-0.011275	82	0.4055	-0.014713
34	0.1655	-0.012344	83	0.4105	-0.015091
35	0.1705	-0.014923	84	0.4155	-0.015487
36	0.1755	-0.01745	85	0.4205	-0.015677
37	0.1805	-0.018506	86	0.4255	-0.01557
38	0.1855	-0.017608	87	0.4305	-0.015248
39	0.1905	-0.015409	88	0.4355	-0.014909
40	0.1955	-0.013243	89	0.4405	-0.014744
41	0.2005	-0.012327	90	0.4455	-0.014834
42	0.2055	-0.013081	91	0.4505	-0.015108
43	0.2105	-0.014955	92	0.4555	-0.015398
44	0.2155	-0.016811	93	0.4605	-0.015541
45	0.2205	-0.017606	94	0.4655	-0.015466
46	0.2255	-0.016973	95	0.4705	-0.015233
47	0.2305	-0.015376	96	0.4755	-0.014984
48	0.2355	-0.013786	97	0.4805	-0.014861
49	0.2405	-0.013096	98	0.4855	-0.014923

Table 2.20 – Data points for UZ displacement time history plot of the cantilever beam

APPENDIX F

Time history plots of a cantilever beam

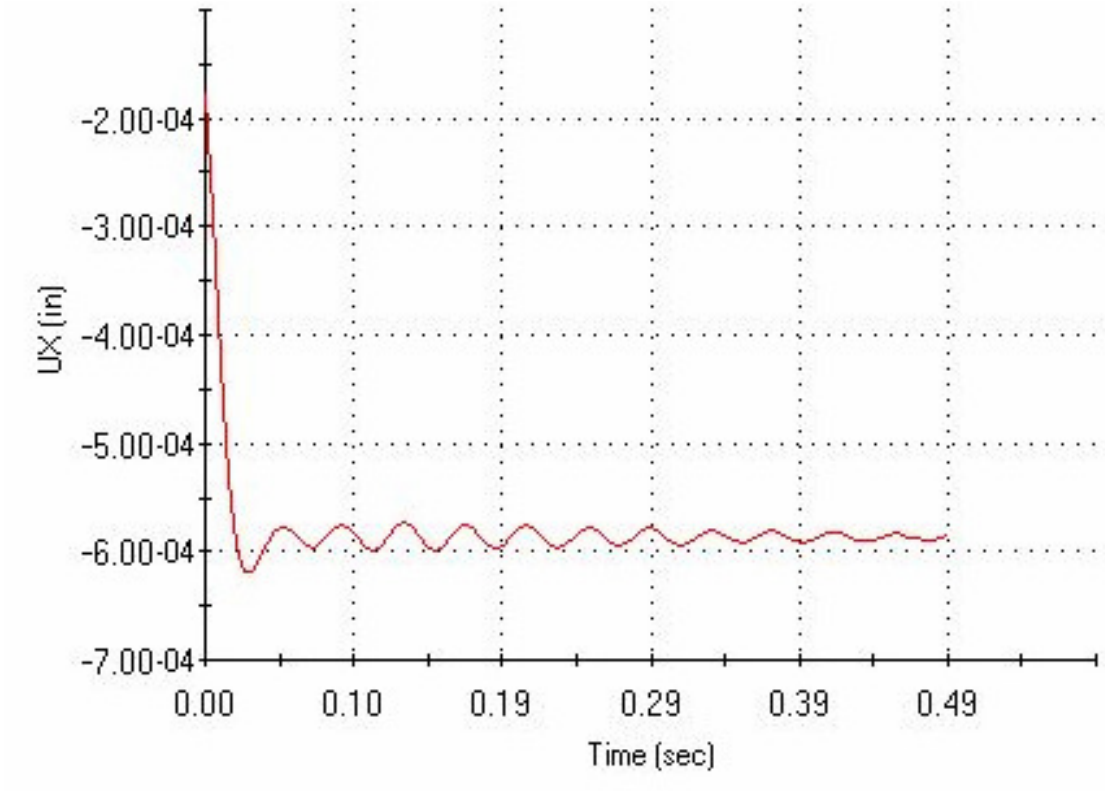

Figure 2.19 – UX displacement time history plot of a cantilever beam

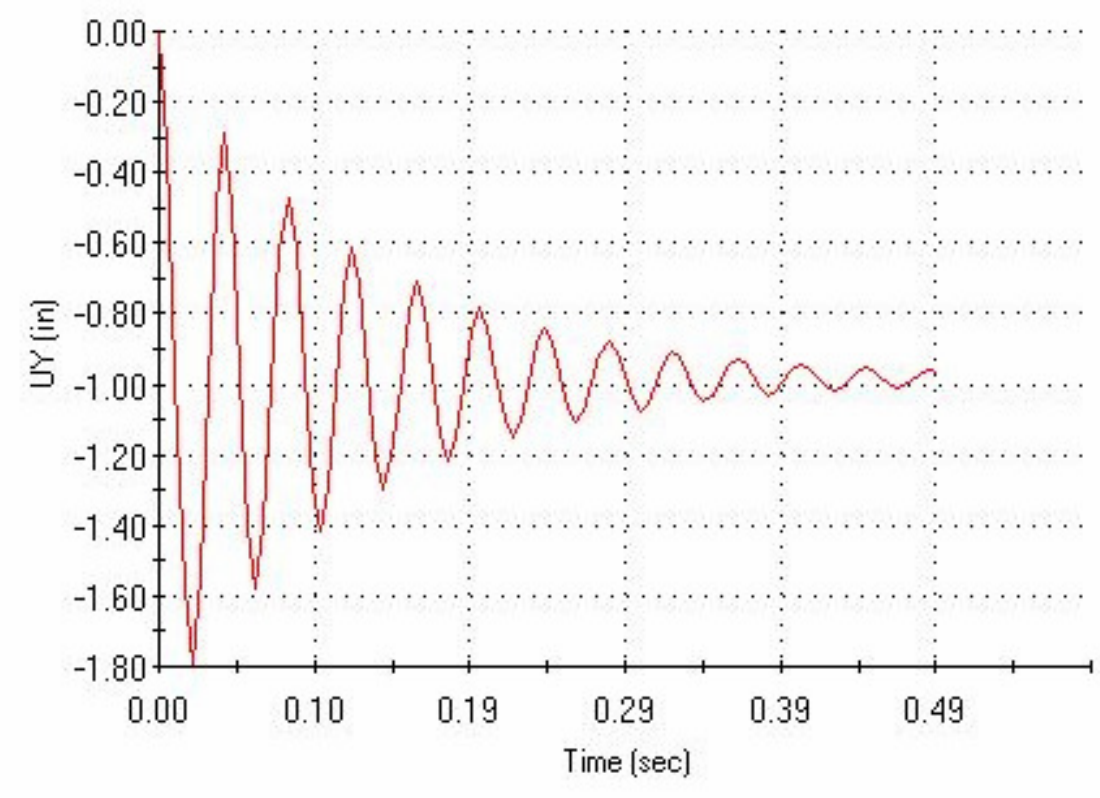

Figure 2.20 – UY displacement time history plot of a cantilever beam

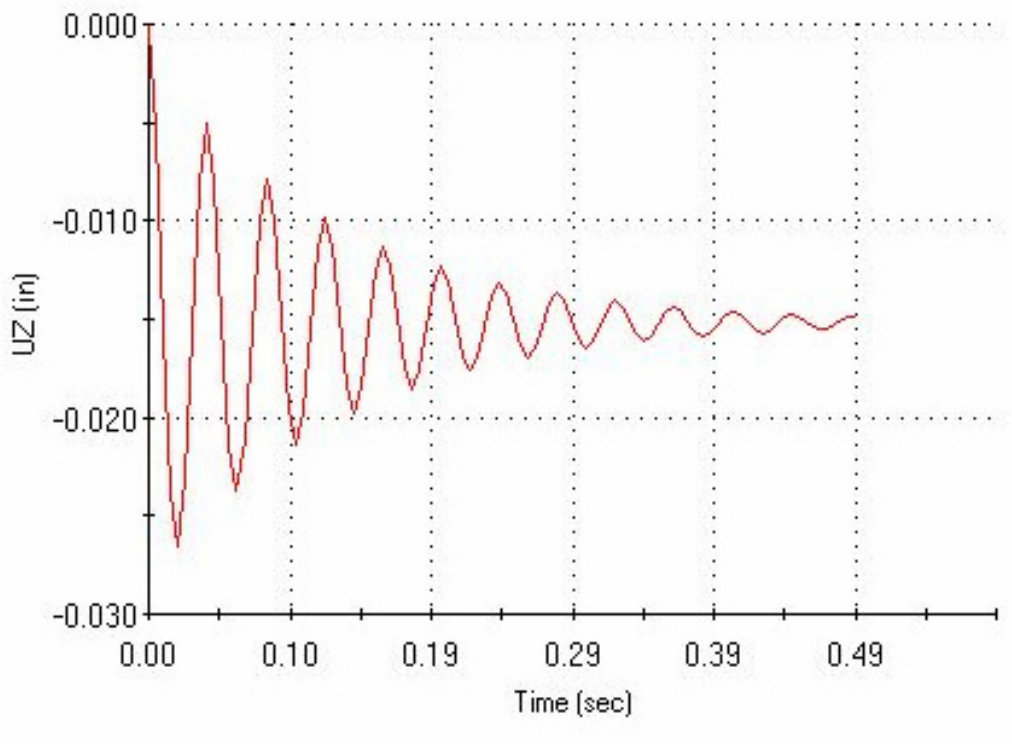

Figure 2.21 - UZ displacement time history plot of a cantilever beam

APPENDIX G

Data for time history plots of parametric study No.1

Point	Time (sec)	UX (inch)	Point	Time (sec)	UX (inch)	Point	Time (sec)	UX (inch)
1	0.0005	5.72E-07	49	0.1685	5.74E-07	97	0.3365	5.76E-07
2	0.004	5.97E-07	50	0.172	5.82E-07	98	0.34	5.77E-07
3	0.0075	5.50E-07	51	0.1755	5.70E-07	99	0.3435	5.76E-07
4	0.011	5.98E-07	52	0.179	5.81E-07	100	0.347	5.77E-07
5	0.0145	5.69E-07	53	0.1825	5.75E-07	101	0.3505	5.76E-07
6	0.018	5.68E-07	54	0.186	5.74E-07	102	0.354	5.76E-07
7	0.0215	5.97E-07	55	0.1895	5.81E-07	103	0.3575	5.77E-07
8	0.025	5.52E-07	56	0.193	5.72E-07	104	0.361	5.76E-07
9	0.0285	5.94E-07	57	0.1965	5.80E-07	105	0.3645	5.77E-07
10	0.032	5.72E-07	58	0.2	5.76E-07	106	0.368	5.77E-07
11	0.0355	5.67E-07	59	0.2035	5.74E-07	107	0.3715	5.76E-07
12	0.039	5.96E-07	60	0.207	5.80E-07	108	0.375	5.78E-07
13	0.0425	5.56E-07	61	0.2105	5.73E-07	109	0.3785	5.76E-07
14	0.046	5.90E-07	62	0.214	5.78E-07	110	0.382	5.77E-07
15	0.0495	5.74E-07	63	0.2175	5.77E-07	111	0.3855	5.77E-07
16	0.053	5.67E-07	64	0.221	5.74E-07	112	0.389	5.76E-07
17	0.0565	5.92E-07	65	0.2245	5.80E-07	113	0.3925	5.77E-07
18	0.06	5.61E-07	66	0.228	5.74E-07	114	0.396	5.76E-07
19	0.0635	5.85E-07	67	0.2315	5.77E-07	115	0.3995	5.77E-07
20	0.067	5.77E-07	68	0.235	5.78E-07	116	0.403	5.77E-07
21	0.0705	5.67E-07	69	0.2385	5.74E-07	117	0.4065	5.76E-07
22	0.074	5.90E-07	70	0.242	5.80E-07	118	0.41	5.77E-07
23	0.0775	5.65E-07	71	0.2455	5.74E-07	119	0.4135	5.76E-07
24	0.081	5.81E-07	72	0.249	5.77E-07	120	0.417	5.77E-07
25	0.0845	5.80E-07	73	0.2525	5.78E-07	121	0.4205	5.77E-07
26	0.088	5.66E-07	74	0.256	5.74E-07	122	0.424	5.76E-07
27	0.0915	5.89E-07	75	0.2595	5.79E-07	123	0.4275	5.77E-07
28	0.095	5.67E-07	76	0.263	5.75E-07	124	0.431	5.76E-07
29	0.0985	5.79E-07	77	0.2665	5.77E-07	125	0.4345	5.76E-07
30	0.102	5.81E-07	78	0.27	5.77E-07	126	0.438	5.77E-07
31	0.1055	5.66E-07	79	0.2735	5.75E-07	127	0.4415	5.76E-07
32	0.109	5.88E-07	80	0.277	5.78E-07	128	0.445	5.77E-07
33	0.1125	5.69E-07	81	0.2805	5.75E-07	129	0.4485	5.76E-07
34	0.116	5.78E-07	82	0.284	5.76E-07	130	0.452	5.76E-07
35	0.1195	5.81E-07	83	0.2875	5.78E-07	131	0.4555	5.77E-07
36	0.123	5.68E-07	84	0.291	5.75E-07	132	0.459	5.76E-07
37	0.1265	5.85E-07	85	0.2945	5.78E-07	133	0.4625	5.77E-07
38	0.13	5.71E-07	86	0.298	5.76E-07	134	0.466	5.76E-07
39	0.1335	5.77E-07	87	0.3015	5.76E-07	135	0.4695	5.76E-07
40	0.137	5.81E-07	88	0.305	5.78E-07	136	0.473	5.77E-07
41	0.1405	5.69E-07	89	0.3085	5.75E-07	137	0.4765	5.76E-07
42	0.144	5.83E-07	90	0.312	5.78E-07	138	0.48	5.77E-07
43	0.1475	5.74E-07	91	0.3155	5.76E-07	139	0.4835	5.76E-07
44	0.151	5.75E-07	92	0.319	5.76E-07	140	0.487	5.76E-07
45	0.1545	5.82E-07	93	0.3225	5.78E-07	141	0.4905	5.77E-07
46	0.158	5.70E-07	94	0.326	5.75E-07	142	0.494	5.76E-07
47	0.1615	5.82E-07	95	0.3295	5.78E-07	143	0.4975	5.77E-07
48	0.165	5.75E-07	96	0.333	5.76E-07			

Table 4.14 – Data points for UX displacement time history plot, parametric study No.1

Point	Time (sec)	UY (inch)	Point	Time (sec)	UY (inch)
1	0.0005	-2.83E-06	51	0.2505	-2.85E-06
2	0.0055	-2.74E-06	52	0.2555	-2.86E-06
3	0.0105	-2.74E-06	53	0.2605	-2.86E-06
4	0.0155	-2.83E-06	54	0.2655	-2.86E-06
5	0.0205	-2.93E-06	55	0.2705	-2.85E-06
6	0.0255	-2.96E-06	56	0.2755	-2.84E-06
7	0.0305	-2.90E-06	57	0.2805	-2.85E-06
8	0.0355	-2.81E-06	58	0.2855	-2.86E-06
9	0.0405	-2.76E-06	59	0.2905	-2.86E-06
10	0.0455	-2.79E-06	60	0.2955	-2.86E-06
11	0.0505	-2.86E-06	61	0.3005	-2.85E-06
12	0.0555	-2.92E-06	62	0.3055	-2.85E-06
13	0.0605	-2.92E-06	63	0.3105	-2.85E-06
14	0.0655	-2.87E-06	64	0.3155	-2.85E-06
15	0.0705	-2.81E-06	65	0.3205	-2.86E-06
16	0.0755	-2.79E-06	66	0.3255	-2.86E-06
17	0.0805	-2.82E-06	67	0.3305	-2.86E-06
18	0.0855	-2.88E-06	68	0.3355	-2.85E-06
19	0.0905	-2.91E-06	69	0.3405	-2.85E-06
20	0.0955	-2.89E-06	70	0.3455	-2.85E-06
21	0.1005	-2.85E-06	71	0.3505	-2.85E-06
22	0.1055	-2.81E-06	72	0.3555	-2.86E-06
23	0.1105	-2.81E-06	73	0.3605	-2.86E-06
24	0.1155	-2.84E-06	74	0.3655	-2.86E-06
25	0.1205	-2.88E-06	75	0.3705	-2.85E-06
26	0.1255	-2.90E-06	76	0.3755	-2.85E-06
27	0.1305	-2.87E-06	77	0.3805	-2.85E-06
28	0.1355	-2.84E-06	78	0.3855	-2.85E-06
29	0.1405	-2.82E-06	79	0.3905	-2.86E-06
30	0.1455	-2.83E-06	80	0.3955	-2.86E-06
31	0.1505	-2.86E-06	81	0.4005	-2.85E-06
32	0.1555	-2.88E-06	82	0.4055	-2.85E-06
33	0.1605	-2.88E-06	83	0.4105	-2.85E-06
34	0.1655	-2.86E-06	84	0.4155	-2.85E-06
35	0.1705	-2.84E-06	85	0.4205	-2.86E-06
36	0.1755	-2.83E-06	86	0.4255	-2.86E-06
37	0.1805	-2.84E-06	87	0.4305	-2.86E-06
38	0.1855	-2.86E-06	88	0.4355	-2.85E-06
39	0.1905	-2.88E-06	89	0.4405	-2.85E-06
40	0.1955	-2.87E-06	90	0.4455	-2.85E-06
41	0.2005	-2.85E-06	91	0.4505	-2.85E-06
42	0.2055	-2.84E-06	92	0.4555	-2.86E-06
43	0.2105	-2.84E-06	93	0.4605	-2.86E-06
44	0.2155	-2.85E-06	94	0.4655	-2.85E-06
45	0.2205	-2.86E-06	95	0.4705	-2.85E-06
46	0.2255	-2.87E-06	96	0.4755	-2.85E-06
47	0.2305	-2.86E-06	97	0.4805	-2.85E-06
48	0.2355	-2.85E-06	98	0.4855	-2.85E-06
49	0.2405	-2.84E-06	99	0.4905	-2.85E-06
50	0.2455	-2.84E-06	100	0.4955	-2.85E-06

Table 4.15 – Data points for UY displacement time history plot, parametric study No.1

Point	Time (sec)	UZ (inch)	Point	Time (sec)	UZ (inch)
1	0.0005	3.25E-09	51	0.2505	3.26E-09
2	0.0055	3.16E-09	52	0.2555	3.28E-09
3	0.0105	3.15E-09	53	0.2605	3.29E-09
4	0.0155	3.24E-09	54	0.2655	3.29E-09
5	0.0205	3.34E-09	55	0.2705	3.28E-09
6	0.0255	3.38E-09	56	0.2755	3.26E-09
7	0.0305	3.34E-09	57	0.2805	3.25E-09
8	0.0355	3.25E-09	58	0.2855	3.26E-09
9	0.0405	3.19E-09	59	0.2905	3.28E-09
10	0.0455	3.20E-09	60	0.2955	3.29E-09
11	0.0505	3.26E-09	61	0.3005	3.29E-09
12	0.0555	3.34E-09	62	0.3055	3.28E-09
13	0.0605	3.36E-09	63	0.3105	3.26E-09
14	0.0655	3.32E-09	64	0.3155	3.26E-09
15	0.0705	3.24E-09	65	0.3205	3.27E-09
16	0.0755	3.20E-09	66	0.3255	3.28E-09
17	0.0805	3.21E-09	67	0.3305	3.29E-09
18	0.0855	3.27E-09	68	0.3355	3.28E-09
19	0.0905	3.33E-09	69	0.3405	3.27E-09
20	0.0955	3.34E-09	70	0.3455	3.26E-09
21	0.1005	3.30E-09	71	0.3505	3.26E-09
22	0.1055	3.25E-09	72	0.3555	3.27E-09
23	0.1105	3.22E-09	73	0.3605	3.28E-09
24	0.1155	3.24E-09	74	0.3655	3.29E-09
25	0.1205	3.28E-09	75	0.3705	3.28E-09
26	0.1255	3.32E-09	76	0.3755	3.27E-09
27	0.1305	3.32E-09	77	0.3805	3.26E-09
28	0.1355	3.28E-09	78	0.3855	3.27E-09
29	0.1405	3.24E-09	79	0.3905	3.27E-09
30	0.1455	3.22E-09	80	0.3955	3.28E-09
31	0.1505	3.24E-09	81	0.4005	3.28E-09
32	0.1555	3.29E-09	82	0.4055	3.27E-09
33	0.1605	3.32E-09	83	0.4105	3.27E-09
34	0.1655	3.31E-09	84	0.4155	3.27E-09
35	0.1705	3.28E-09	85	0.4205	3.27E-09
36	0.1755	3.25E-09	86	0.4255	3.28E-09
37	0.1805	3.24E-09	87	0.4305	3.28E-09
38	0.1855	3.26E-09	88	0.4355	3.28E-09
39	0.1905	3.29E-09	89	0.4405	3.27E-09
40	0.1955	3.31E-09	90	0.4455	3.27E-09
41	0.2005	3.29E-09	91	0.4505	3.27E-09
42	0.2055	3.26E-09	92	0.4555	3.27E-09
43	0.2105	3.24E-09	93	0.4605	3.28E-09
44	0.2155	3.24E-09	94	0.4655	3.28E-09
45	0.2205	3.27E-09	95	0.4705	3.27E-09
46	0.2255	3.30E-09	96	0.4755	3.27E-09
47	0.2305	3.30E-09	97	0.4805	3.27E-09
48	0.2355	3.29E-09	98	0.4855	3.27E-09
49	0.2405	3.27E-09	99	0.4905	3.28E-09
50	0.2455	3.25E-09	100	0.4955	3.28E-09

Table 4.16 – Data points for UZ displacement time history plot, parametric study No.1

APPENDIX H

Time history plots of parametric study No.1

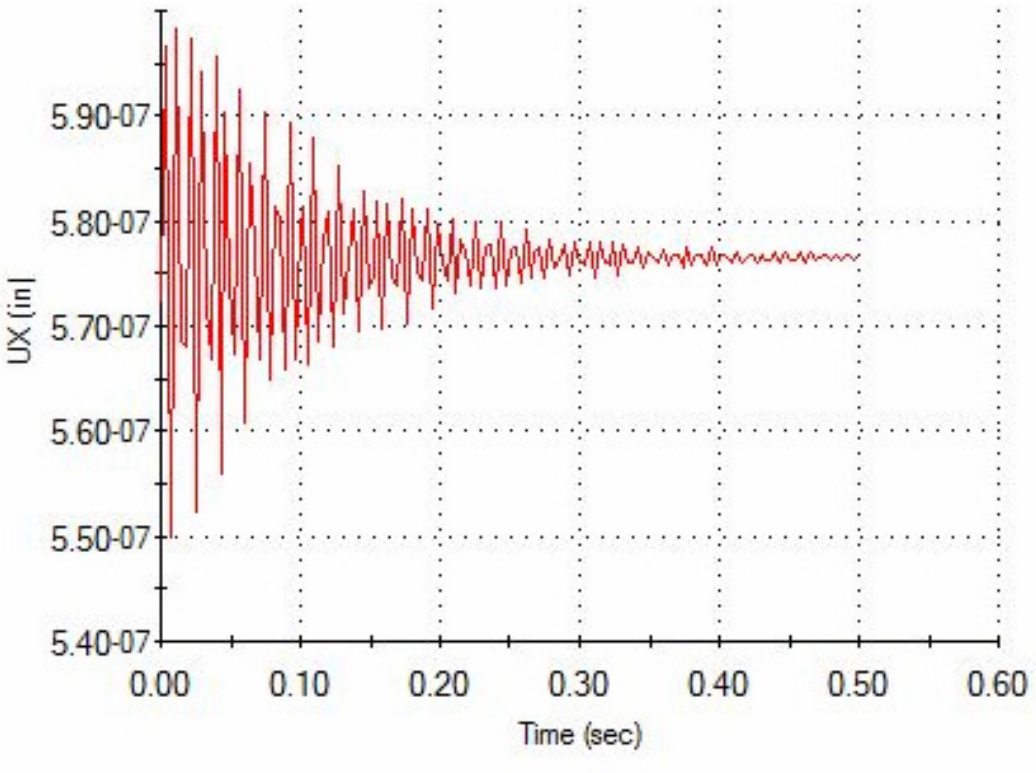

Figure 4.8 - UX displacement time history plot, Parametric Study No.1

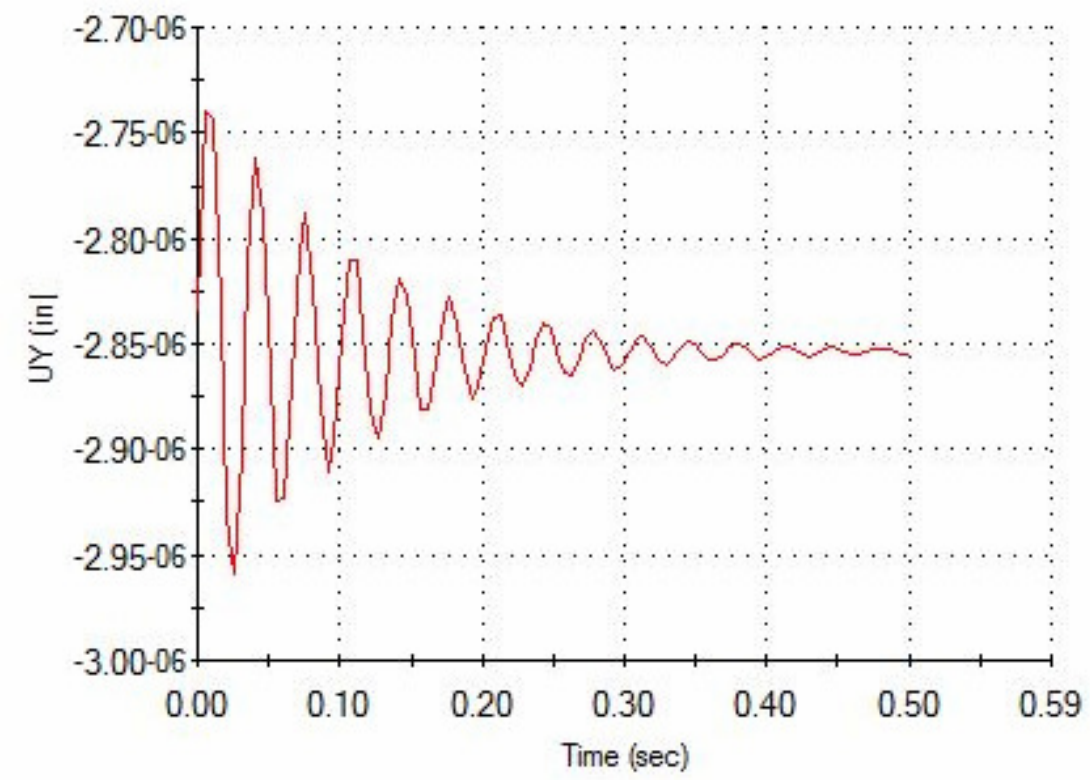

Figure 4.9 – UY displacement time history plot, Parametric Study No.1

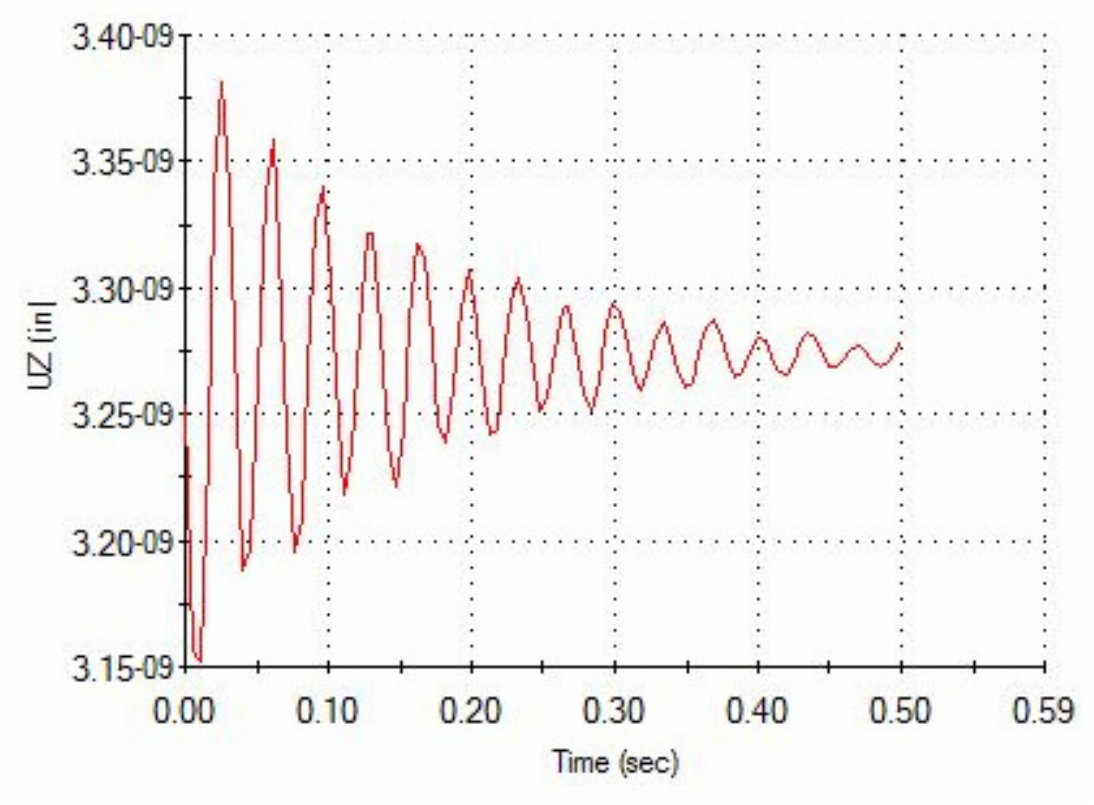

Figure 4.10 – UZ displacement time history plot, Parametric Study No.1

APPENDIX I

Mode shapes of parametric study No.1

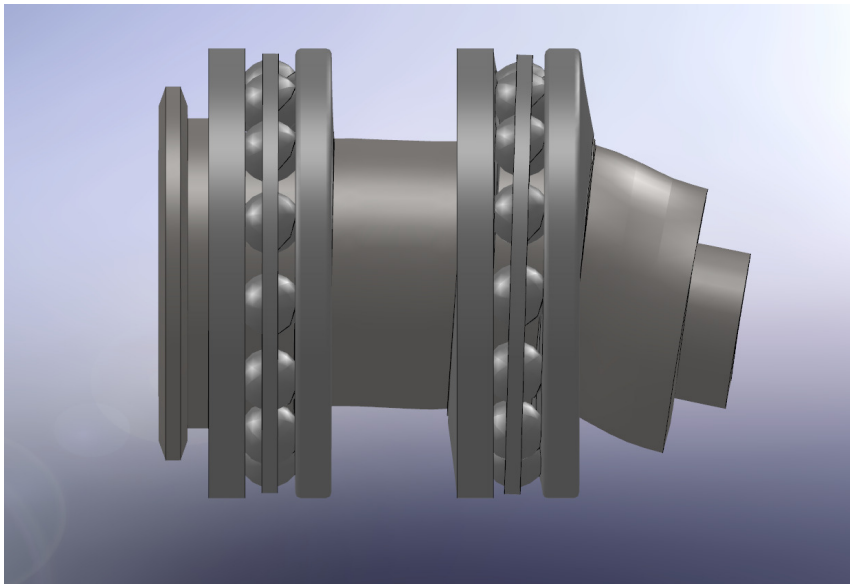

Figure 4.11 - First mode shape, parametric study No.1

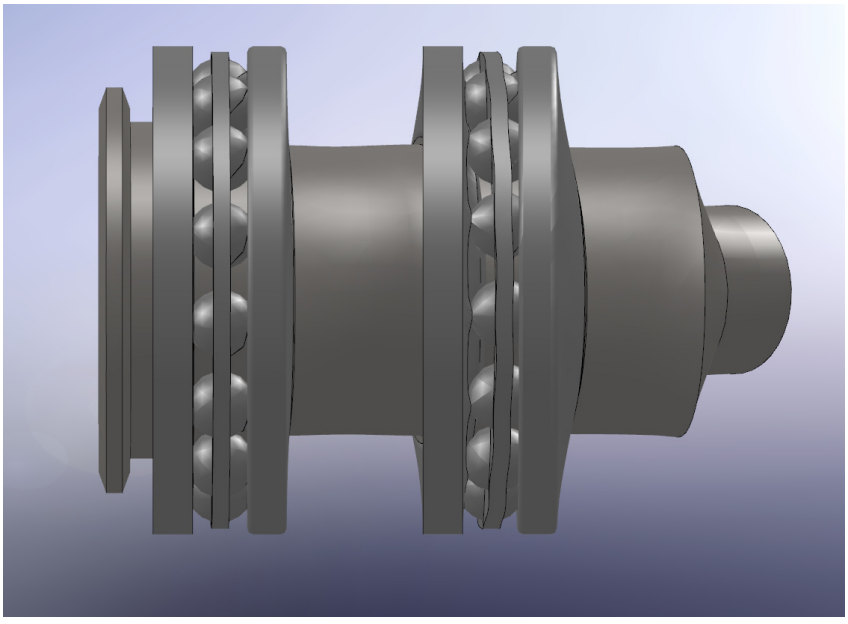

Figure 4.12 - Second mode shape, parametric study No.1

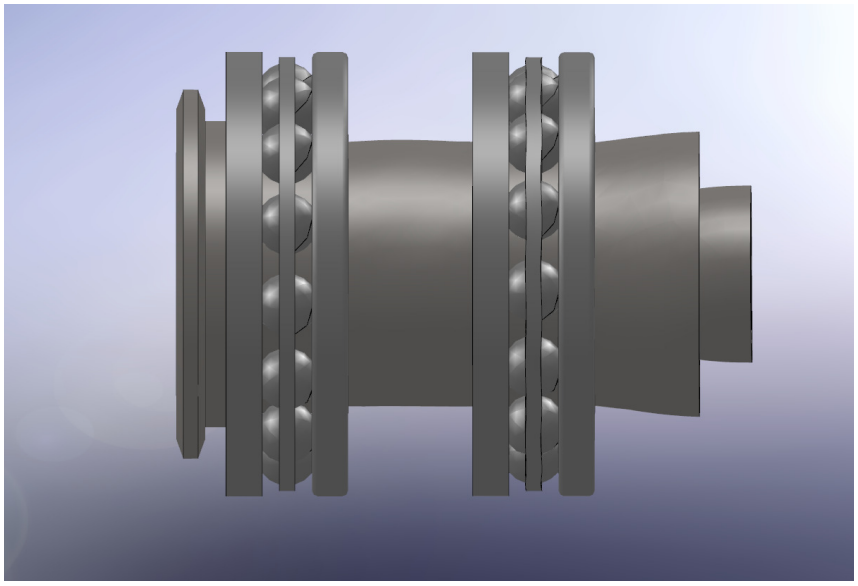

Figure 4.13 - Third mode shape, parametric study No.1

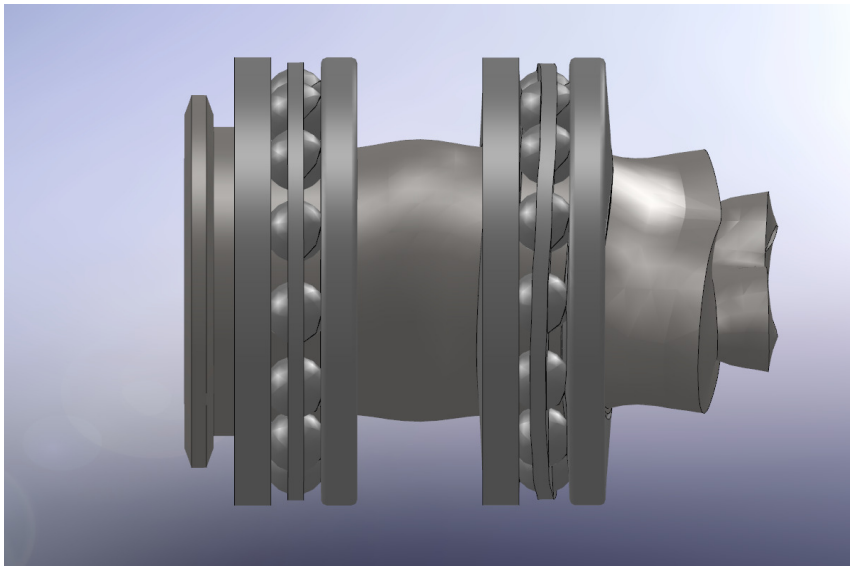

Figure 4.14 - Fourth mode shape, parametric study No.1

APPENDIX J

Data points for time history plots of parametric study No.2

Point	Time (sec)	UX (inch)	Point	Time (sec)	UX (inch)	Point	Time (sec)	UX (inch)
1	0.0005	1.78E-06	49	0.1685	1.80E-06	97	0.3365	1.80E-06
2	0.004	1.93E-06	50	0.172	1.81E-06	98	0.34	1.81E-06
3	0.0075	1.74E-06	51	0.1755	1.81E-06	99	0.3435	1.80E-06
4	0.011	1.74E-06	52	0.179	1.80E-06	100	0.347	1.81E-06
5	0.0145	1.90E-06	53	0.1825	1.80E-06	101	0.3505	1.80E-06
6	0.018	1.80E-06	54	0.186	1.81E-06	102	0.354	1.81E-06
7	0.0215	1.72E-06	55	0.1895	1.80E-06	103	0.3575	1.81E-06
8	0.025	1.87E-06	56	0.193	1.80E-06	104	0.361	1.81E-06
9	0.0285	1.84E-06	57	0.1965	1.81E-06	105	0.3645	1.81E-06
10	0.032	1.72E-06	58	0.2	1.80E-06	106	0.368	1.81E-06
11	0.0355	1.83E-06	59	0.2035	1.80E-06	107	0.3715	1.81E-06
12	0.039	1.85E-06	60	0.207	1.81E-06	108	0.375	1.80E-06
13	0.0425	1.75E-06	61	0.2105	1.81E-06	109	0.3785	1.81E-06
14	0.046	1.79E-06	62	0.214	1.80E-06	110	0.382	1.80E-06
15	0.0495	1.87E-06	63	0.2175	1.81E-06	111	0.3855	1.81E-06
16	0.053	1.78E-06	64	0.221	1.81E-06	112	0.389	1.81E-06
17	0.0565	1.77E-06	65	0.2245	1.80E-06	113	0.3925	1.81E-06
18	0.06	1.85E-06	66	0.228	1.81E-06	114	0.396	1.81E-06
19	0.0635	1.80E-06	67	0.2315	1.81E-06	115	0.3995	1.80E-06
20	0.067	1.77E-06	68	0.235	1.81E-06	116	0.403	1.81E-06
21	0.0705	1.83E-06	69	0.2385	1.80E-06	117	0.4065	1.80E-06
22	0.074	1.82E-06	70	0.242	1.81E-06	118	0.41	1.81E-06
23	0.0775	1.77E-06	71	0.2455	1.80E-06	119	0.4135	1.81E-06
24	0.081	1.82E-06	72	0.249	1.80E-06	120	0.417	1.81E-06
25	0.0845	1.83E-06	73	0.2525	1.81E-06	121	0.4205	1.81E-06
26	0.088	1.78E-06	74	0.256	1.80E-06	122	0.424	1.81E-06
27	0.0915	1.80E-06	75	0.2595	1.81E-06	123	0.4275	1.81E-06
28	0.095	1.83E-06	76	0.263	1.80E-06	124	0.431	1.80E-06
29	0.0985	1.80E-06	77	0.2665	1.81E-06	125	0.4345	1.81E-06
30	0.102	1.79E-06	78	0.27	1.80E-06	126	0.438	1.81E-06
31	0.1055	1.83E-06	79	0.2735	1.81E-06	127	0.4415	1.81E-06
32	0.109	1.80E-06	80	0.277	1.81E-06	128	0.445	1.81E-06
33	0.1125	1.79E-06	81	0.2805	1.80E-06	129	0.4485	1.81E-06
34	0.116	1.82E-06	82	0.284	1.81E-06	130	0.452	1.81E-06
35	0.1195	1.81E-06	83	0.2875	1.81E-06	131	0.4555	1.80E-06
36	0.123	1.79E-06	84	0.291	1.81E-06	132	0.459	1.81E-06
37	0.1265	1.81E-06	85	0.2945	1.80E-06	133	0.4625	1.81E-06
38	0.13	1.82E-06	86	0.298	1.81E-06	134	0.466	1.81E-06
39	0.1335	1.79E-06	87	0.3015	1.81E-06	135	0.4695	1.81E-06
40	0.137	1.80E-06	88	0.305	1.80E-06	136	0.473	1.81E-06
41	0.1405	1.82E-06	89	0.3085	1.81E-06	137	0.4765	1.81E-06
42	0.144	1.80E-06	90	0.312	1.81E-06	138	0.48	1.81E-06
43	0.1475	1.80E-06	91	0.3155	1.81E-06	139	0.4835	1.81E-06
44	0.151	1.81E-06	92	0.319	1.80E-06	140	0.487	1.81E-06
45	0.1545	1.81E-06	93	0.3225	1.81E-06	141	0.4905	1.81E-06
46	0.158	1.80E-06	94	0.326	1.80E-06	142	0.494	1.81E-06
47	0.1615	1.81E-06	95	0.3295	1.81E-06	143	0.4975	1.81E-06
48	0.165	1.81E-06	96	0.333	1.81E-06			

Table 4.17 – Data points for UX displacement time history Plot, parametric study No.2

Point	Time (sec)	UY (inch)	Point	Time (sec)	UY (inch)
1	0.0005	-7.49E-06	51	0.2505	-7.62E-06
2	0.0055	-7.05E-06	52	0.2555	-7.61E-06
3	0.0105	-7.86E-06	53	0.2605	-7.60E-06
4	0.0155	-8.00E-06	54	0.2655	-7.61E-06
5	0.0205	-7.28E-06	55	0.2705	-7.62E-06
6	0.0255	-7.37E-06	56	0.2755	-7.61E-06
7	0.0305	-7.95E-06	57	0.2805	-7.61E-06
8	0.0355	-7.72E-06	58	0.2855	-7.61E-06
9	0.0405	-7.30E-06	59	0.2905	-7.61E-06
10	0.0455	-7.61E-06	60	0.2955	-7.61E-06
11	0.0505	-7.88E-06	61	0.3005	-7.61E-06
12	0.0555	-7.54E-06	62	0.3055	-7.61E-06
13	0.0605	-7.40E-06	63	0.3105	-7.61E-06
14	0.0655	-7.73E-06	64	0.3155	-7.61E-06
15	0.0705	-7.75E-06	65	0.3205	-7.61E-06
16	0.0755	-7.47E-06	66	0.3255	-7.61E-06
17	0.0805	-7.53E-06	67	0.3305	-7.61E-06
18	0.0855	-7.75E-06	68	0.3355	-7.61E-06
19	0.0905	-7.64E-06	69	0.3405	-7.61E-06
20	0.0955	-7.49E-06	70	0.3455	-7.61E-06
21	0.1005	-7.62E-06	71	0.3505	-7.61E-06
22	0.1055	-7.71E-06	72	0.3555	-7.61E-06
23	0.1105	-7.57E-06	73	0.3605	-7.61E-06
24	0.1155	-7.53E-06	74	0.3655	-7.61E-06
25	0.1205	-7.66E-06	75	0.3705	-7.61E-06
26	0.1255	-7.66E-06	76	0.3755	-7.61E-06
27	0.1305	-7.55E-06	77	0.3805	-7.61E-06
28	0.1355	-7.59E-06	78	0.3855	-7.61E-06
29	0.1405	-7.67E-06	79	0.3905	-7.61E-06
30	0.1455	-7.62E-06	80	0.3955	-7.61E-06
31	0.1505	-7.56E-06	81	0.4005	-7.61E-06
32	0.1555	-7.62E-06	82	0.4055	-7.61E-06
33	0.1605	-7.65E-06	83	0.4105	-7.61E-06
34	0.1655	-7.59E-06	84	0.4155	-7.61E-06
35	0.1705	-7.58E-06	85	0.4205	-7.61E-06
36	0.1755	-7.63E-06	86	0.4255	-7.61E-06
37	0.1805	-7.62E-06	87	0.4305	-7.61E-06
38	0.1855	-7.58E-06	88	0.4355	-7.61E-06
39	0.1905	-7.60E-06	89	0.4405	-7.61E-06
40	0.1955	-7.63E-06	90	0.4455	-7.61E-06
41	0.2005	-7.61E-06	91	0.4505	-7.61E-06
42	0.2055	-7.59E-06	92	0.4555	-7.61E-06
43	0.2105	-7.62E-06	93	0.4605	-7.61E-06
44	0.2155	-7.63E-06	94	0.4655	-7.61E-06
45	0.2205	-7.60E-06	95	0.4705	-7.61E-06
46	0.2255	-7.60E-06	96	0.4755	-7.61E-06
47	0.2305	-7.62E-06	97	0.4805	-7.61E-06
48	0.2355	-7.61E-06	98	0.4855	-7.61E-06
49	0.2405	-7.60E-06	99	0.4905	-7.61E-06
50	0.2455	-7.61E-06	100	0.4955	-7.61E-06

Table 4.18 – Data points for UY displacement time history Plot, parametric study No.2

Point	Time (sec)	UZ (inch)	Point	Time (sec)	UZ (inch)
1	0.0005	4.28E-09	51	0.2505	4.41E-09
2	0.0055	4.00E-09	52	0.2555	4.09E-09
3	0.0105	5.54E-09	53	0.2605	4.54E-09
4	0.0155	4.11E-09	54	0.2655	4.69E-09
5	0.0205	3.06E-09	55	0.2705	4.27E-09
6	0.0255	5.65E-09	56	0.2755	4.26E-09
7	0.0305	5.61E-09	57	0.2805	4.65E-09
8	0.0355	2.55E-09	58	0.2855	4.55E-09
9	0.0405	3.82E-09	59	0.2905	4.24E-09
10	0.0455	6.65E-09	60	0.2955	4.41E-09
11	0.0505	4.28E-09	61	0.3005	4.62E-09
12	0.0555	2.19E-09	62	0.3055	4.40E-09
13	0.0605	5.34E-09	63	0.3105	4.28E-09
14	0.0655	6.40E-09	64	0.3155	4.50E-09
15	0.0705	2.98E-09	65	0.3205	4.55E-09
16	0.0755	3.04E-09	66	0.3255	4.35E-09
17	0.0805	6.31E-09	67	0.3305	4.37E-09
18	0.0855	5.20E-09	68	0.3355	4.54E-09
19	0.0905	2.41E-09	69	0.3405	4.48E-09
20	0.0955	4.30E-09	70	0.3455	4.35E-09
21	0.1005	6.34E-09	71	0.3505	4.44E-09
22	0.1055	3.96E-09	72	0.3555	4.52E-09
23	0.1105	2.82E-09	73	0.3605	4.41E-09
24	0.1155	5.38E-09	74	0.3655	4.36E-09
25	0.1205	5.68E-09	75	0.3705	4.47E-09
26	0.1255	3.24E-09	76	0.3755	4.48E-09
27	0.1305	3.69E-09	77	0.3805	4.39E-09
28	0.1355	5.76E-09	78	0.3855	4.41E-09
29	0.1405	4.73E-09	79	0.3905	4.49E-09
30	0.1455	3.14E-09	80	0.3955	4.45E-09
31	0.1505	4.54E-09	81	0.4005	4.40E-09
32	0.1555	5.55E-09	82	0.4055	4.44E-09
33	0.1605	4.01E-09	83	0.4105	4.47E-09
34	0.1655	3.56E-09	84	0.4155	4.42E-09
35	0.1705	5.09E-09	85	0.4205	4.40E-09
36	0.1755	5.05E-09	86	0.4255	4.45E-09
37	0.1805	3.70E-09	87	0.4305	4.45E-09
38	0.1855	4.13E-09	88	0.4355	4.42E-09
39	0.1905	5.20E-09	89	0.4405	4.43E-09
40	0.1955	4.50E-09	90	0.4455	4.46E-09
41	0.2005	3.74E-09	91	0.4505	4.44E-09
42	0.2055	4.57E-09	92	0.4555	4.42E-09
43	0.2105	4.99E-09	93	0.4605	4.44E-09
44	0.2155	4.14E-09	94	0.4655	4.45E-09
45	0.2205	4.03E-09	95	0.4705	4.43E-09
46	0.2255	4.82E-09	96	0.4755	4.42E-09
47	0.2305	4.71E-09	97	0.4805	4.44E-09
48	0.2355	4.04E-09	98	0.4855	4.44E-09
49	0.2405	4.33E-09	99	0.4905	4.43E-09
50	0.2455	4.82E-09	100	0.4955	4.44E-09

Table 4.19 – Data points for UZ displacement time history Plot, parametric study No.2

APPENDIX K

Time history plots of parametric study No.2

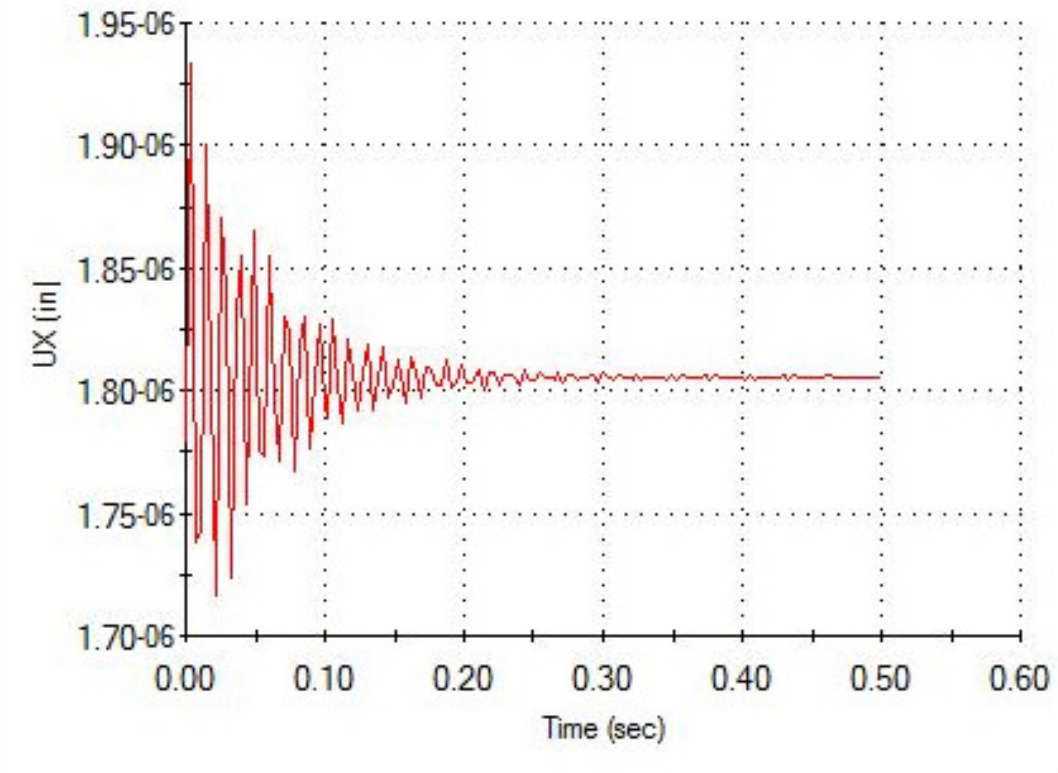

Figure 4.15 - UX displacement time history plot, parametric study No.2

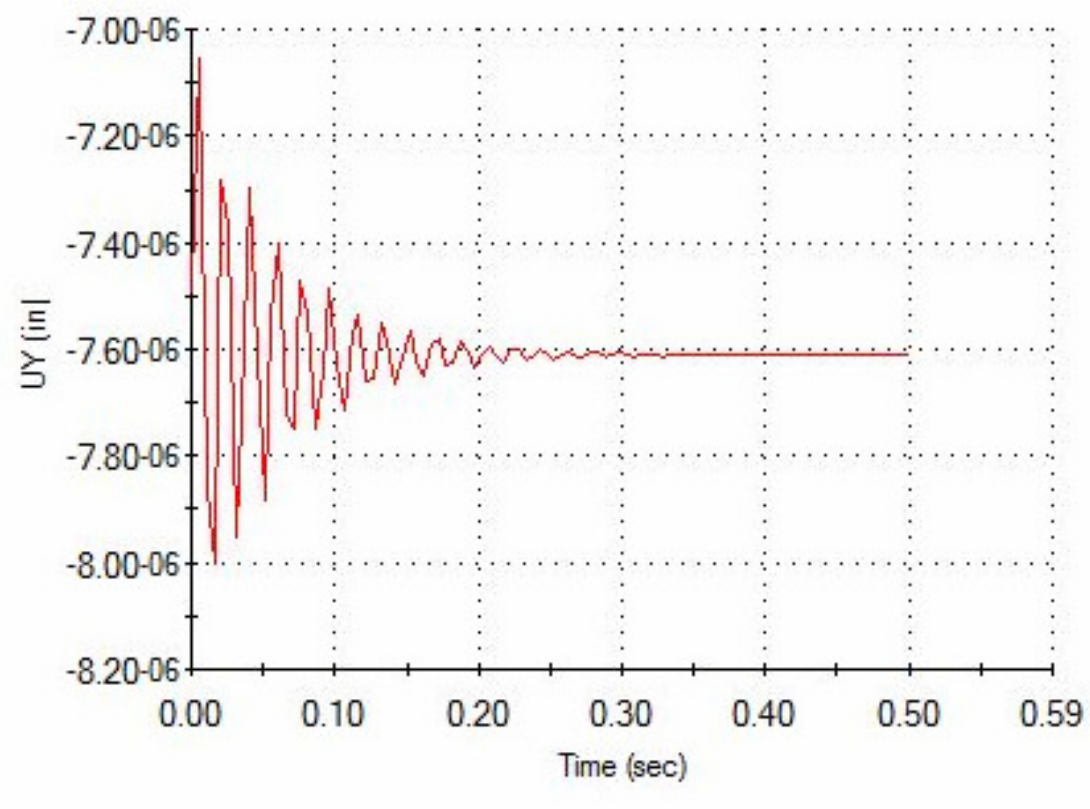

Figure 4.16 - UY displacement time history plot, parametric study No.2

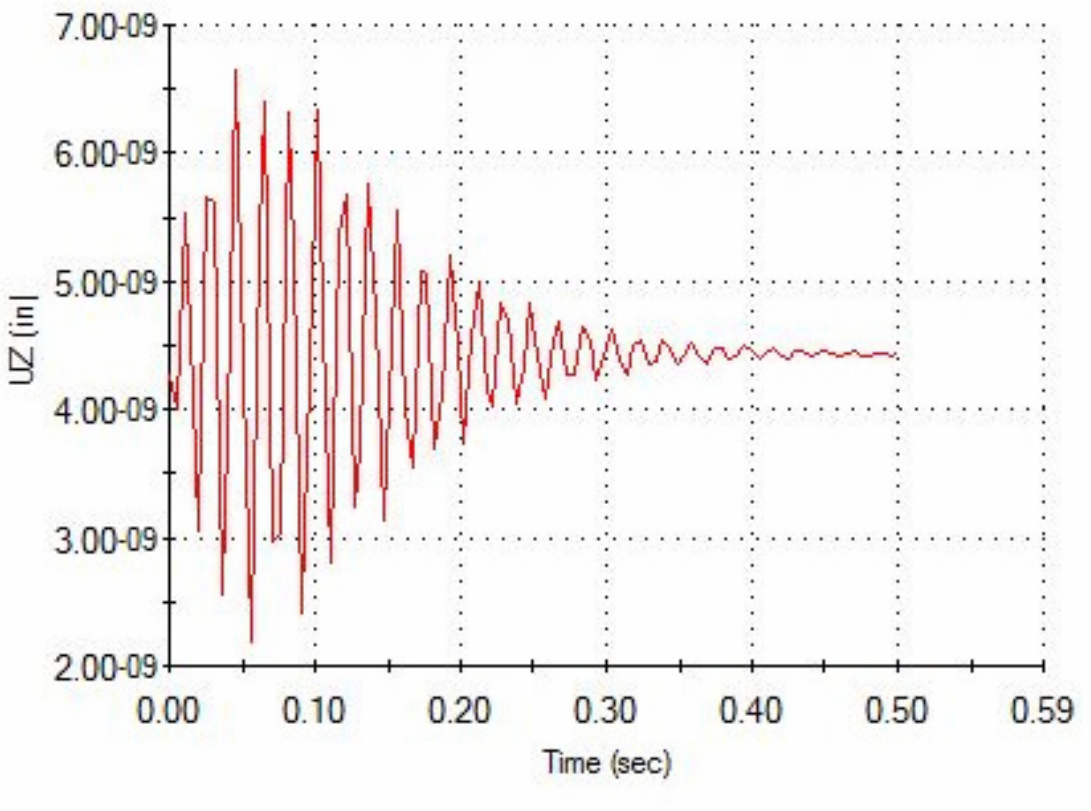

Figure 4.17 – UZ displacement time history plot, parametric study No.2

APPENDIX L

Mode shape plots of parametric study No.2

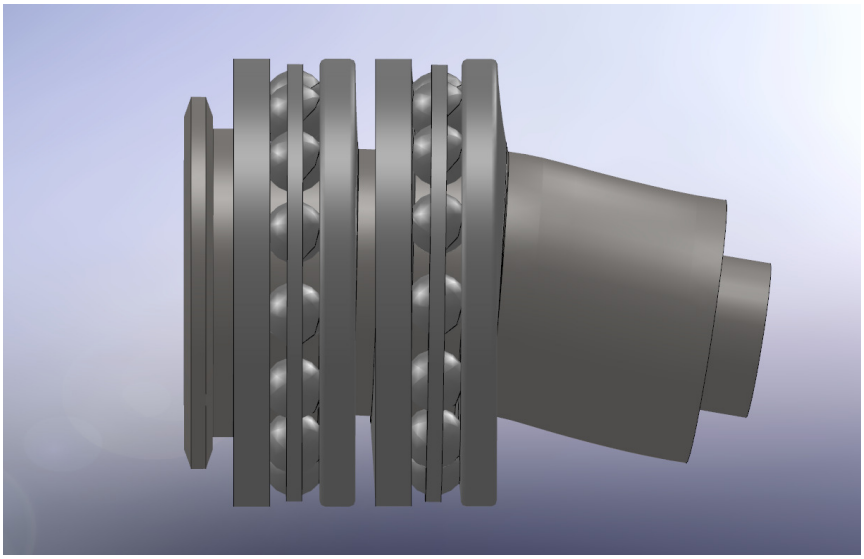

Figure 4.18 - First mode shape, parametric study No.2

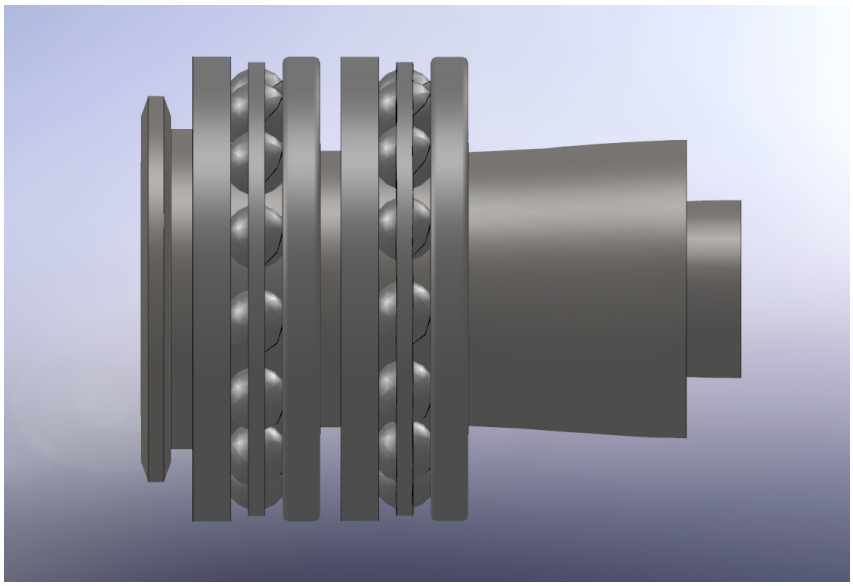

Figure 4.19 - Second mode shape, parametric study No.2

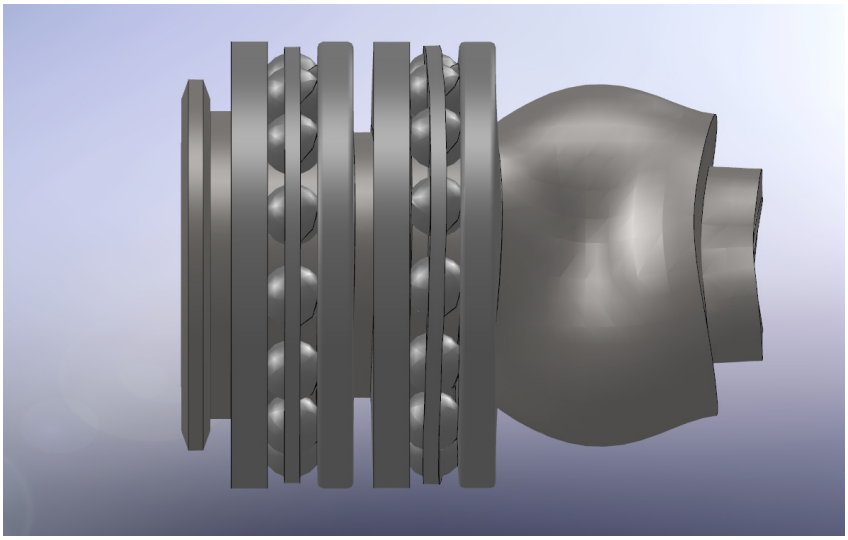

Figure 4.20 - Third mode shape, parametric study No.2

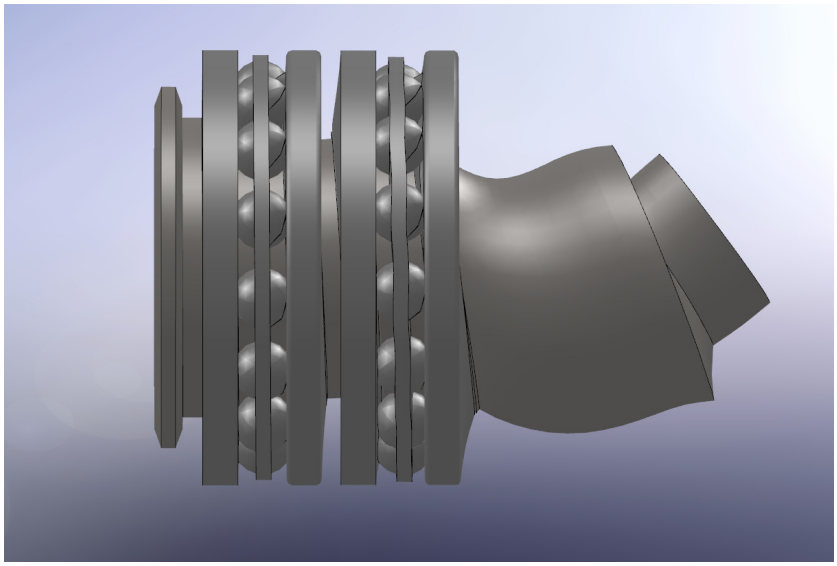

Figure 4.21 - Fourth mode shape, parametric study No.2

APPENDIX M

Data points for time history plots of parametric study No.3

Point	Time (sec)	UX (inch)	Point	Time (sec)	UX (inch)	Point	Time (sec)	UX (inch)
1	0.0005	3.96E-07	49	0.1685	3.95E-07	97	0.3365	3.96E-07
2	0.004	4.03E-07	50	0.172	4.01E-07	98	0.34	3.99E-07
3	0.0075	3.89E-07	51	0.1755	3.94E-07	99	0.3435	3.96E-07
4	0.011	4.08E-07	52	0.179	4.02E-07	100	0.347	3.99E-07
5	0.0145	3.87E-07	53	0.1825	3.95E-07	101	0.3505	3.97E-07
6	0.018	4.07E-07	54	0.186	4.00E-07	102	0.354	3.98E-07
7	0.0215	3.92E-07	55	0.1895	3.97E-07	103	0.3575	3.98E-07
8	0.025	4.00E-07	56	0.193	3.97E-07	104	0.361	3.97E-07
9	0.0285	4.00E-07	57	0.1965	4.00E-07	105	0.3645	3.99E-07
10	0.032	3.92E-07	58	0.2	3.95E-07	106	0.368	3.96E-07
11	0.0355	4.06E-07	59	0.2035	4.01E-07	107	0.3715	3.99E-07
12	0.039	3.89E-07	60	0.207	3.95E-07	108	0.375	3.97E-07
13	0.0425	4.07E-07	61	0.2105	4.00E-07	109	0.3785	3.98E-07
14	0.046	3.91E-07	62	0.214	3.96E-07	110	0.382	3.98E-07
15	0.0495	4.02E-07	63	0.2175	3.98E-07	111	0.3855	3.97E-07
16	0.053	3.97E-07	64	0.221	3.99E-07	112	0.389	3.99E-07
17	0.0565	3.96E-07	65	0.2245	3.96E-07	113	0.3925	3.97E-07
18	0.06	4.03E-07	66	0.228	4.01E-07	114	0.396	3.99E-07
19	0.0635	3.91E-07	67	0.2315	3.95E-07	115	0.3995	3.97E-07
20	0.067	4.06E-07	68	0.235	4.01E-07	116	0.403	3.99E-07
21	0.0705	3.91E-07	69	0.2385	3.96E-07	117	0.4065	3.97E-07
22	0.074	4.03E-07	70	0.242	3.99E-07	118	0.41	3.98E-07
23	0.0775	3.95E-07	71	0.2455	3.98E-07	119	0.4135	3.98E-07
24	0.081	3.98E-07	72	0.249	3.97E-07	120	0.417	3.97E-07
25	0.0845	4.00E-07	73	0.2525	4.00E-07	121	0.4205	3.99E-07
26	0.088	3.93E-07	74	0.256	3.95E-07	122	0.424	3.97E-07
27	0.0915	4.04E-07	75	0.2595	4.00E-07	123	0.4275	3.99E-07
28	0.095	3.91E-07	76	0.263	3.96E-07	124	0.431	3.97E-07
29	0.0985	4.04E-07	77	0.2665	3.99E-07	125	0.4345	3.98E-07
30	0.102	3.93E-07	78	0.27	3.97E-07	126	0.438	3.98E-07
31	0.1055	4.00E-07	79	0.2735	3.98E-07	127	0.4415	3.97E-07
32	0.109	3.98E-07	80	0.277	3.99E-07	128	0.445	3.99E-07
33	0.1125	3.95E-07	81	0.2805	3.96E-07	129	0.4485	3.97E-07
34	0.116	4.02E-07	82	0.284	4.00E-07	130	0.452	3.99E-07
35	0.1195	3.92E-07	83	0.2875	3.96E-07	131	0.4555	3.97E-07
36	0.123	4.03E-07	84	0.291	4.00E-07	132	0.459	3.98E-07
37	0.1265	3.93E-07	85	0.2945	3.97E-07	133	0.4625	3.98E-07
38	0.13	4.01E-07	86	0.298	3.98E-07	134	0.466	3.98E-07
39	0.1335	3.96E-07	87	0.3015	3.98E-07	135	0.4695	3.98E-07
40	0.137	3.97E-07	88	0.305	3.97E-07	136	0.473	3.97E-07
41	0.1405	4.00E-07	89	0.3085	3.99E-07	137	0.4765	3.99E-07
42	0.144	3.94E-07	90	0.312	3.96E-07	138	0.48	3.97E-07
43	0.1475	4.03E-07	91	0.3155	4.00E-07	139	0.4835	3.98E-07
44	0.151	3.93E-07	92	0.319	3.96E-07	140	0.487	3.97E-07
45	0.1545	4.02E-07	93	0.3225	3.99E-07	141	0.4905	3.98E-07
46	0.158	3.95E-07	94	0.326	3.98E-07	142	0.494	3.98E-07
47	0.1615	3.99E-07	95	0.3295	3.97E-07	143	0.4975	3.97E-07
48	0.165	3.99E-07	96	0.333	3.99E-07			

Table 4.20 – Data points for UX displacement time history plot, parametric study No.3

Point	Time (sec)	UY (inch)	Point	Time (sec)	UY (inch)
1	0.0005	-6.19E-07	51	0.2505	-6.24E-07
2	0.0055	-6.11E-07	52	0.2555	-6.25E-07
3	0.0105	-6.06E-07	53	0.2605	-6.25E-07
4	0.0155	-6.06E-07	54	0.2655	-6.24E-07
5	0.0205	-6.11E-07	55	0.2705	-6.22E-07
6	0.0255	-6.19E-07	56	0.2755	-6.20E-07
7	0.0305	-6.27E-07	57	0.2805	-6.18E-07
8	0.0355	-6.33E-07	58	0.2855	-6.18E-07
9	0.0405	-6.35E-07	59	0.2905	-6.18E-07
10	0.0455	-6.33E-07	60	0.2955	-6.20E-07
11	0.0505	-6.27E-07	61	0.3005	-6.22E-07
12	0.0555	-6.21E-07	62	0.3055	-6.23E-07
13	0.0605	-6.14E-07	63	0.3105	-6.24E-07
14	0.0655	-6.11E-07	64	0.3155	-6.24E-07
15	0.0705	-6.11E-07	65	0.3205	-6.24E-07
16	0.0755	-6.14E-07	66	0.3255	-6.22E-07
17	0.0805	-6.19E-07	67	0.3305	-6.21E-07
18	0.0855	-6.25E-07	68	0.3355	-6.19E-07
19	0.0905	-6.29E-07	69	0.3405	-6.19E-07
20	0.0955	-6.30E-07	70	0.3455	-6.19E-07
21	0.1005	-6.29E-07	71	0.3505	-6.20E-07
22	0.1055	-6.25E-07	72	0.3555	-6.21E-07
23	0.1105	-6.21E-07	73	0.3605	-6.23E-07
24	0.1155	-6.17E-07	74	0.3655	-6.23E-07
25	0.1205	-6.15E-07	75	0.3705	-6.23E-07
26	0.1255	-6.15E-07	76	0.3755	-6.23E-07
27	0.1305	-6.17E-07	77	0.3805	-6.22E-07
28	0.1355	-6.21E-07	78	0.3855	-6.21E-07
29	0.1405	-6.24E-07	79	0.3905	-6.20E-07
30	0.1455	-6.27E-07	80	0.3955	-6.20E-07
31	0.1505	-6.27E-07	81	0.4005	-6.20E-07
32	0.1555	-6.26E-07	82	0.4055	-6.21E-07
33	0.1605	-6.23E-07	83	0.4105	-6.21E-07
34	0.1655	-6.20E-07	84	0.4155	-6.22E-07
35	0.1705	-6.17E-07	85	0.4205	-6.23E-07
36	0.1755	-6.16E-07	86	0.4255	-6.23E-07
37	0.1805	-6.17E-07	87	0.4305	-6.22E-07
38	0.1855	-6.19E-07	88	0.4355	-6.22E-07
39	0.1905	-6.22E-07	89	0.4405	-6.21E-07
40	0.1955	-6.24E-07	90	0.4455	-6.21E-07
41	0.2005	-6.26E-07	91	0.4505	-6.20E-07
42	0.2055	-6.26E-07	92	0.4555	-6.21E-07
43	0.2105	-6.24E-07	93	0.4605	-6.21E-07
44	0.2155	-6.22E-07	94	0.4655	-6.22E-07
45	0.2205	-6.20E-07	95	0.4705	-6.22E-07
46	0.2255	-6.18E-07	96	0.4755	-6.22E-07
47	0.2305	-6.17E-07	97	0.4805	-6.22E-07
48	0.2355	-6.18E-07	98	0.4855	-6.22E-07
49	0.2405	-6.20E-07	99	0.4905	-6.21E-07
50	0.2455	-6.22E-07	100	0.4955	-6.21E-07

Table 4.21 – Data points for UY displacement time history plot, parametric study No.3

Point	Time (sec)	UZ (inch)	Point	Time (sec)	UZ (inch)
1	0.0005	9.45E-08	51	0.2505	9.54E-08
2	0.0055	9.35E-08	52	0.2555	9.53E-08
3	0.0105	9.29E-08	53	0.2605	9.51E-08
4	0.0155	9.27E-08	54	0.2655	9.48E-08
5	0.0205	9.29E-08	55	0.2705	9.45E-08
6	0.0255	9.35E-08	56	0.2755	9.42E-08
7	0.0305	9.43E-08	57	0.2805	9.41E-08
8	0.0355	9.52E-08	58	0.2855	9.42E-08
9	0.0405	9.60E-08	59	0.2905	9.43E-08
10	0.0455	9.64E-08	60	0.2955	9.45E-08
11	0.0505	9.65E-08	61	0.3005	9.48E-08
12	0.0555	9.62E-08	62	0.3055	9.50E-08
13	0.0605	9.56E-08	63	0.3105	9.52E-08
14	0.0655	9.48E-08	64	0.3155	9.52E-08
15	0.0705	9.41E-08	65	0.3205	9.52E-08
16	0.0755	9.35E-08	66	0.3255	9.50E-08
17	0.0805	9.32E-08	67	0.3305	9.48E-08
18	0.0855	9.33E-08	68	0.3355	9.46E-08
19	0.0905	9.36E-08	69	0.3405	9.44E-08
20	0.0955	9.42E-08	70	0.3455	9.43E-08
21	0.1005	9.48E-08	71	0.3505	9.43E-08
22	0.1055	9.54E-08	72	0.3555	9.44E-08
23	0.1105	9.59E-08	73	0.3605	9.45E-08
24	0.1155	9.60E-08	74	0.3655	9.47E-08
25	0.1205	9.59E-08	75	0.3705	9.48E-08
26	0.1255	9.56E-08	76	0.3755	9.50E-08
27	0.1305	9.50E-08	77	0.3805	9.51E-08
28	0.1355	9.45E-08	78	0.3855	9.51E-08
29	0.1405	9.40E-08	79	0.3905	9.50E-08
30	0.1455	9.37E-08	80	0.3955	9.49E-08
31	0.1505	9.36E-08	81	0.4005	9.47E-08
32	0.1555	9.38E-08	82	0.4055	9.46E-08
33	0.1605	9.41E-08	83	0.4105	9.45E-08
34	0.1655	9.46E-08	84	0.4155	9.44E-08
35	0.1705	9.51E-08	85	0.4205	9.44E-08
36	0.1755	9.55E-08	86	0.4255	9.45E-08
37	0.1805	9.57E-08	87	0.4305	9.46E-08
38	0.1855	9.57E-08	88	0.4355	9.48E-08
39	0.1905	9.55E-08	89	0.4405	9.49E-08
40	0.1955	9.51E-08	90	0.4455	9.50E-08
41	0.2005	9.47E-08	91	0.4505	9.50E-08
42	0.2055	9.43E-08	92	0.4555	9.50E-08
43	0.2105	9.40E-08	93	0.4605	9.49E-08
44	0.2155	9.39E-08	94	0.4655	9.48E-08
45	0.2205	9.39E-08	95	0.4705	9.47E-08
46	0.2255	9.42E-08	96	0.4755	9.46E-08
47	0.2305	9.45E-08	97	0.4805	9.45E-08
48	0.2355	9.49E-08	98	0.4855	9.45E-08
49	0.2405	9.52E-08	99	0.4905	9.45E-08
50	0.2455	9.54E-08	100	0.4955	9.46E-08

Table 4.22 – Data points for UZ displacement time history plot, parametric study No.3

APPENDIX N

Time history plots of parametric study No.3

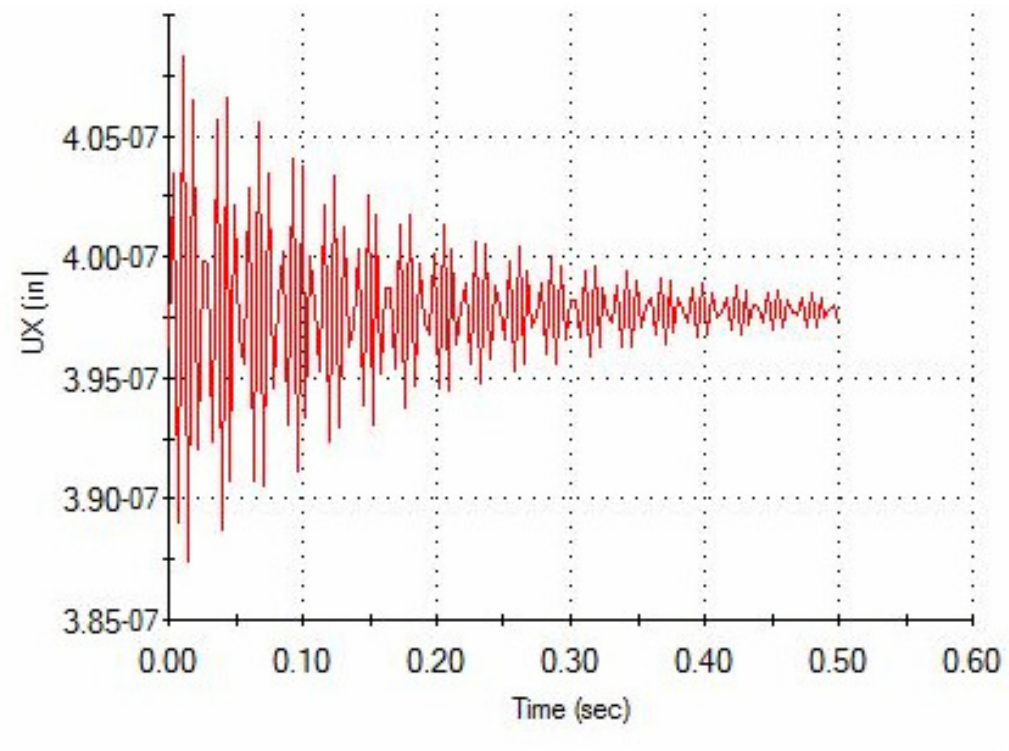

Figure 4.22 – UX displacement time history plot, parametric study No.3

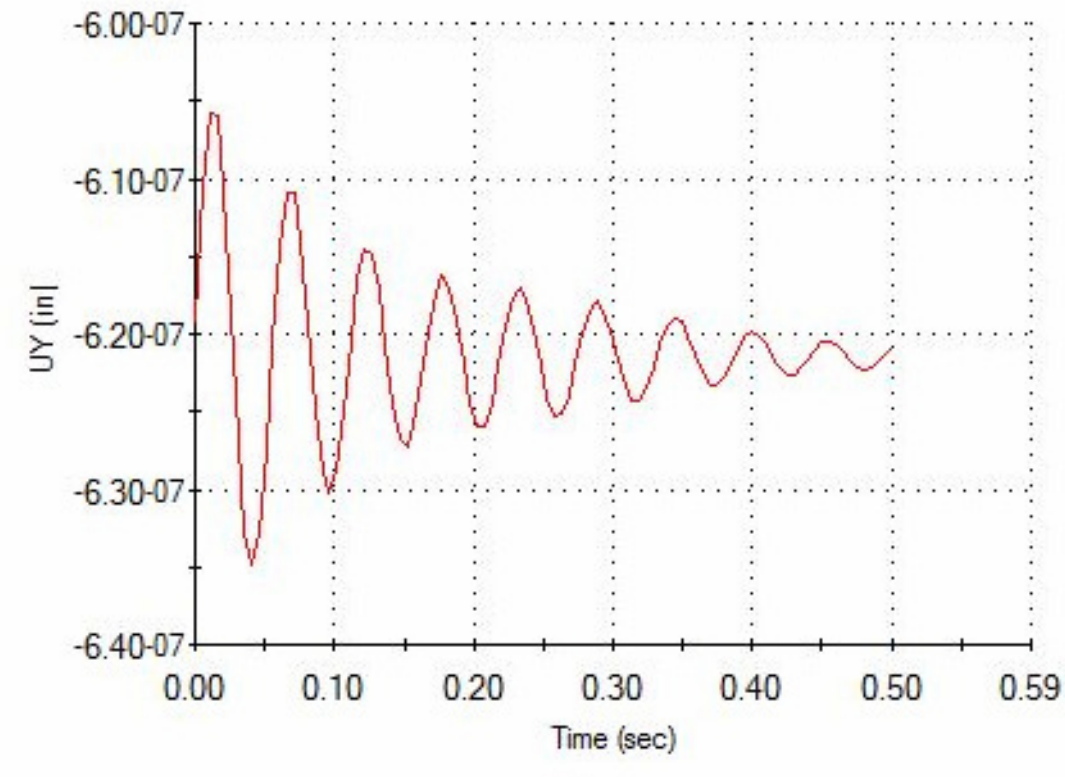

Figure 4.23 – UY displacement time history plot, parametric study No.3

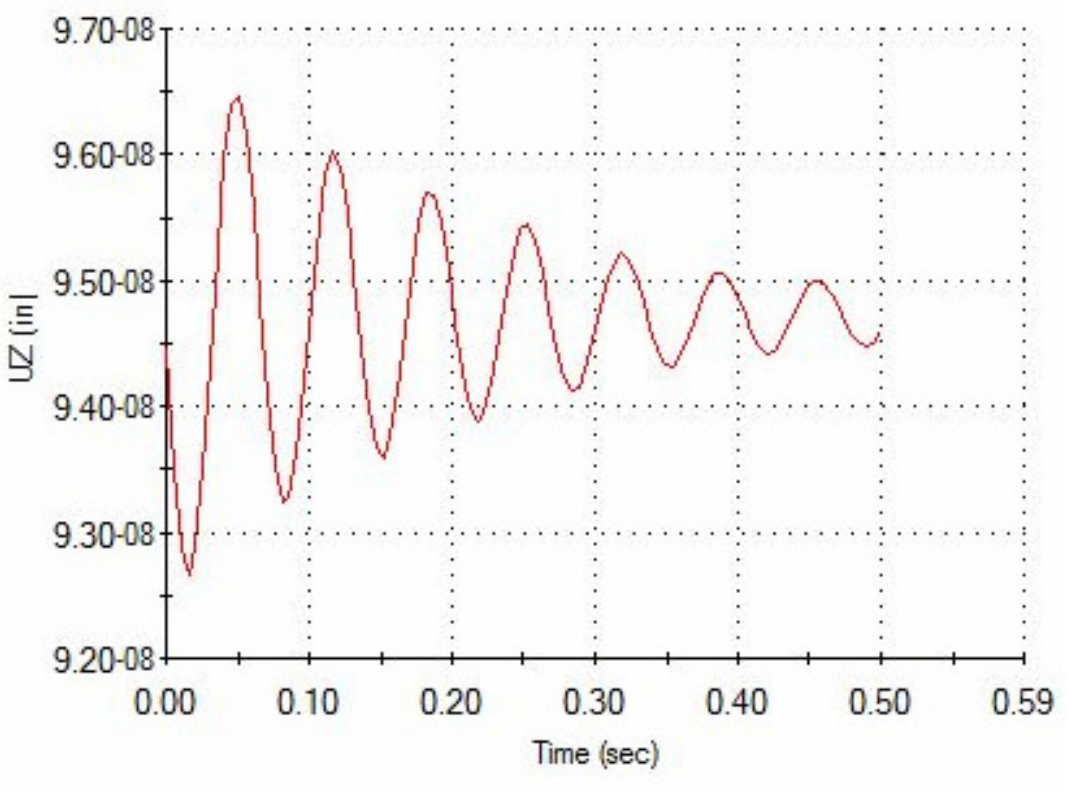

Figure 4.24 – UZ displacement time history plot, parametric study No.3

APPENDIX P

Mode shape plots of parametric study No.3

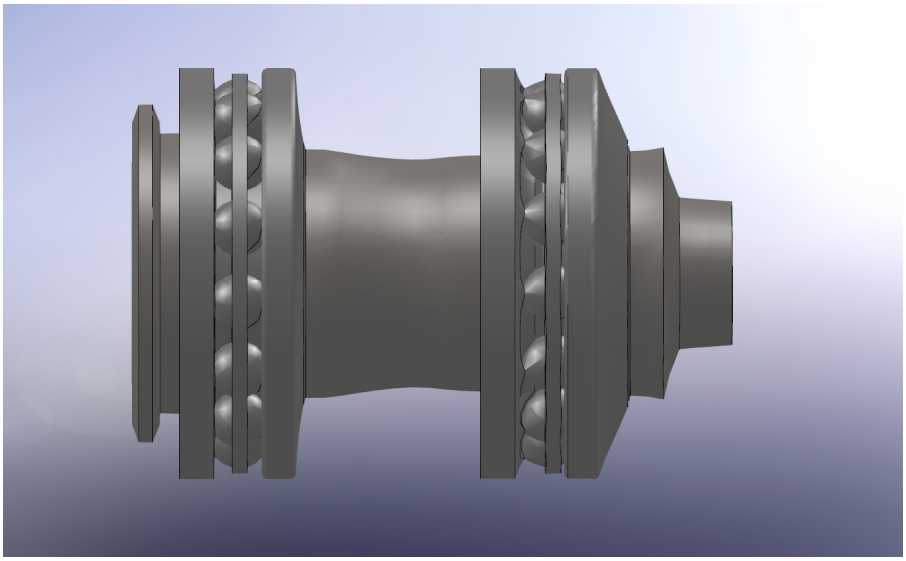

Figure 4.25 - First mode shape, parametric study No.3

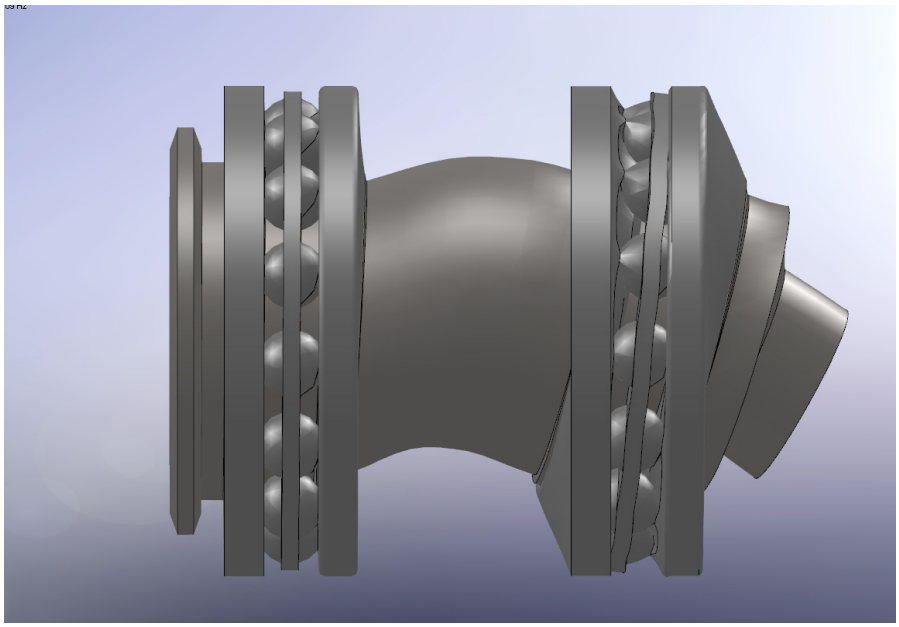

Figure 4.26 - Second mode shape, parametric study No.3

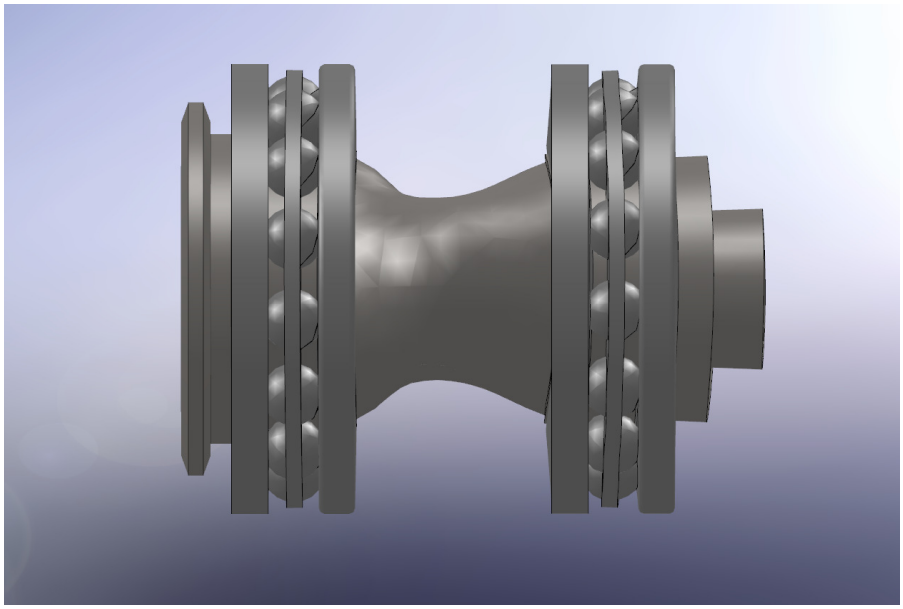

Figure 4.27 - Third mode shape, parametric study No.3

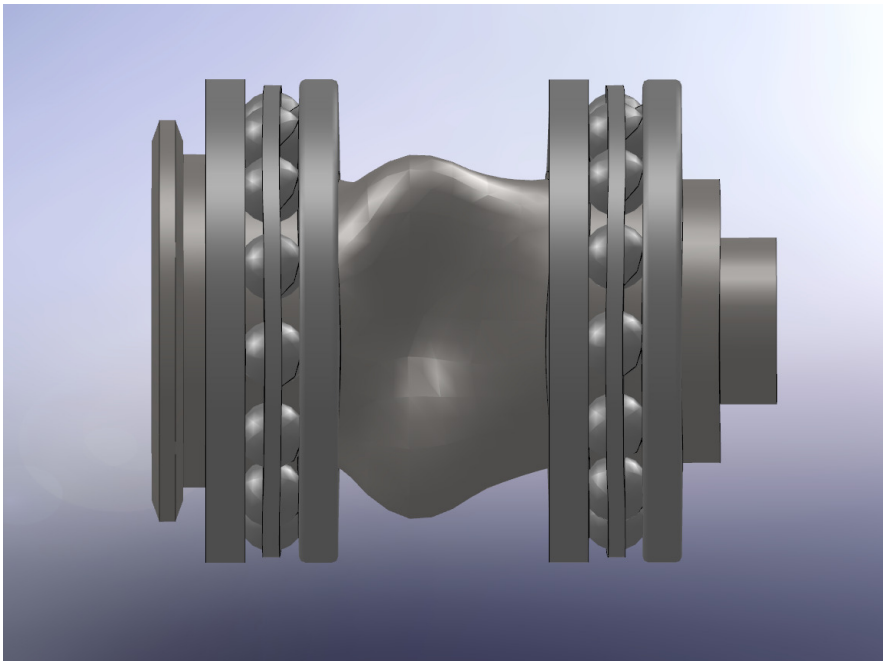

Figure 4.28 - Fourth mode shape, parametric study No.3

APPENDIX Q

Data points for time history plots of parametric study No.4

Point	Time (sec)	UX (inch)	Point	Time (sec)	UX (inch)	Point	Time (sec)	UX (inch)
1	0.0005	5.10E-07	49	0.1685	5.11E-07	97	0.3365	5.14E-07
2	0.004	5.26E-07	50	0.172	5.11E-07	98	0.34	5.13E-07
3	0.0075	4.94E-07	51	0.1755	5.16E-07	99	0.3435	5.12E-07
4	0.011	5.31E-07	52	0.179	5.08E-07	100	0.347	5.14E-07
5	0.0145	5.01E-07	53	0.1825	5.17E-07	101	0.3505	5.12E-07
6	0.018	5.15E-07	54	0.186	5.10E-07	102	0.354	5.14E-07
7	0.0215	5.21E-07	55	0.1895	5.13E-07	103	0.3575	5.12E-07
8	0.025	4.98E-07	56	0.193	5.15E-07	104	0.361	5.13E-07
9	0.0285	5.29E-07	57	0.1965	5.09E-07	105	0.3645	5.13E-07
10	0.032	5.00E-07	58	0.2	5.17E-07	106	0.368	5.12E-07
11	0.0355	5.18E-07	59	0.2035	5.10E-07	107	0.3715	5.14E-07
12	0.039	5.16E-07	60	0.207	5.14E-07	108	0.375	5.12E-07
13	0.0425	5.02E-07	61	0.2105	5.14E-07	109	0.3785	5.13E-07
14	0.046	5.27E-07	62	0.214	5.10E-07	110	0.382	5.13E-07
15	0.0495	5.00E-07	63	0.2175	5.16E-07	111	0.3855	5.12E-07
16	0.053	5.20E-07	64	0.221	5.10E-07	112	0.389	5.14E-07
17	0.0565	5.13E-07	65	0.2245	5.14E-07	113	0.3925	5.12E-07
18	0.06	5.06E-07	66	0.228	5.13E-07	114	0.396	5.13E-07
19	0.0635	5.24E-07	67	0.2315	5.11E-07	115	0.3995	5.13E-07
20	0.067	5.01E-07	68	0.235	5.16E-07	116	0.403	5.12E-07
21	0.0705	5.21E-07	69	0.2385	5.10E-07	117	0.4065	5.13E-07
22	0.074	5.10E-07	70	0.242	5.15E-07	118	0.41	5.12E-07
23	0.0775	5.09E-07	71	0.2455	5.12E-07	119	0.4135	5.13E-07
24	0.081	5.21E-07	72	0.249	5.12E-07	120	0.417	5.13E-07
25	0.0845	5.02E-07	73	0.2525	5.15E-07	121	0.4205	5.12E-07
26	0.088	5.22E-07	74	0.256	5.10E-07	122	0.424	5.13E-07
27	0.0915	5.08E-07	75	0.2595	5.15E-07	123	0.4275	5.12E-07
28	0.095	5.12E-07	76	0.263	5.12E-07	124	0.431	5.13E-07
29	0.0985	5.18E-07	77	0.2665	5.12E-07	125	0.4345	5.13E-07
30	0.102	5.04E-07	78	0.27	5.14E-07	126	0.438	5.13E-07
31	0.1055	5.21E-07	79	0.2735	5.11E-07	127	0.4415	5.13E-07
32	0.109	5.07E-07	80	0.277	5.15E-07	128	0.445	5.12E-07
33	0.1125	5.14E-07	81	0.2805	5.12E-07	129	0.4485	5.13E-07
34	0.116	5.16E-07	82	0.284	5.13E-07	130	0.452	5.13E-07
35	0.1195	5.06E-07	83	0.2875	5.14E-07	131	0.4555	5.13E-07
36	0.123	5.20E-07	84	0.291	5.11E-07	132	0.459	5.13E-07
37	0.1265	5.07E-07	85	0.2945	5.14E-07	133	0.4625	5.12E-07
38	0.13	5.16E-07	86	0.298	5.11E-07	134	0.466	5.13E-07
39	0.1335	5.14E-07	87	0.3015	5.13E-07	135	0.4695	5.12E-07
40	0.137	5.08E-07	88	0.305	5.13E-07	136	0.473	5.13E-07
41	0.1405	5.19E-07	89	0.3085	5.12E-07	137	0.4765	5.13E-07
42	0.144	5.07E-07	90	0.312	5.14E-07	138	0.48	5.12E-07
43	0.1475	5.17E-07	91	0.3155	5.11E-07	139	0.4835	5.13E-07
44	0.151	5.12E-07	92	0.319	5.13E-07	140	0.487	5.12E-07
45	0.1545	5.10E-07	93	0.3225	5.13E-07	141	0.4905	5.13E-07
46	0.158	5.18E-07	94	0.326	5.12E-07	142	0.494	5.13E-07
47	0.1615	5.07E-07	95	0.3295	5.14E-07	143	0.4975	5.13E-07
48	0.165	5.17E-07	96	0.333	5.11E-07			

Table 4.23 – Data points for UX displacement time history plot, parametric study No.4

Point	Time (sec)	UY (inch)	Point	Time (sec)	UY (inch)
1	0.0005	-2.24E-06	51	0.2505	-2.26E-06
2	0.0055	-2.18E-06	52	0.2555	-2.26E-06
3	0.0105	-2.17E-06	53	0.2605	-2.26E-06
4	0.0155	-2.21E-06	54	0.2655	-2.25E-06
5	0.0205	-2.27E-06	55	0.2705	-2.24E-06
6	0.0255	-2.32E-06	56	0.2755	-2.24E-06
7	0.0305	-2.32E-06	57	0.2805	-2.24E-06
8	0.0355	-2.27E-06	58	0.2855	-2.25E-06
9	0.0405	-2.22E-06	59	0.2905	-2.26E-06
10	0.0455	-2.19E-06	60	0.2955	-2.26E-06
11	0.0505	-2.20E-06	61	0.3005	-2.25E-06
12	0.0555	-2.24E-06	62	0.3055	-2.25E-06
13	0.0605	-2.28E-06	63	0.3105	-2.24E-06
14	0.0655	-2.30E-06	64	0.3155	-2.24E-06
15	0.0705	-2.29E-06	65	0.3205	-2.25E-06
16	0.0755	-2.25E-06	66	0.3255	-2.25E-06
17	0.0805	-2.21E-06	67	0.3305	-2.26E-06
18	0.0855	-2.20E-06	68	0.3355	-2.25E-06
19	0.0905	-2.22E-06	69	0.3405	-2.25E-06
20	0.0955	-2.26E-06	70	0.3455	-2.25E-06
21	0.1005	-2.28E-06	71	0.3505	-2.24E-06
22	0.1055	-2.29E-06	72	0.3555	-2.25E-06
23	0.1105	-2.27E-06	73	0.3605	-2.25E-06
24	0.1155	-2.24E-06	74	0.3655	-2.25E-06
25	0.1205	-2.22E-06	75	0.3705	-2.25E-06
26	0.1255	-2.22E-06	76	0.3755	-2.25E-06
27	0.1305	-2.24E-06	77	0.3805	-2.25E-06
28	0.1355	-2.26E-06	78	0.3855	-2.25E-06
29	0.1405	-2.28E-06	79	0.3905	-2.25E-06
30	0.1455	-2.27E-06	80	0.3955	-2.25E-06
31	0.1505	-2.25E-06	81	0.4005	-2.25E-06
32	0.1555	-2.23E-06	82	0.4055	-2.25E-06
33	0.1605	-2.23E-06	83	0.4105	-2.25E-06
34	0.1655	-2.23E-06	84	0.4155	-2.25E-06
35	0.1705	-2.25E-06	85	0.4205	-2.25E-06
36	0.1755	-2.27E-06	86	0.4255	-2.25E-06
37	0.1805	-2.27E-06	87	0.4305	-2.25E-06
38	0.1855	-2.26E-06	88	0.4355	-2.25E-06
39	0.1905	-2.25E-06	89	0.4405	-2.25E-06
40	0.1955	-2.23E-06	90	0.4455	-2.25E-06
41	0.2005	-2.23E-06	91	0.4505	-2.25E-06
42	0.2055	-2.24E-06	92	0.4555	-2.25E-06
43	0.2105	-2.26E-06	93	0.4605	-2.25E-06
44	0.2155	-2.26E-06	94	0.4655	-2.25E-06
45	0.2205	-2.26E-06	95	0.4705	-2.25E-06
46	0.2255	-2.25E-06	96	0.4755	-2.25E-06
47	0.2305	-2.24E-06	97	0.4805	-2.25E-06
48	0.2355	-2.24E-06	98	0.4855	-2.25E-06
49	0.2405	-2.24E-06	99	0.4905	-2.25E-06
50	0.2455	-2.25E-06	100	0.4955	-2.25E-06

Table 4.24 – Data points for UY displacement time history plot, parametric study No.4

Point	Time (sec)	UZ (inch)	Point	Time (sec)	UZ (inch)
1	0.0005	-1.26E-09	51	0.2505	-1.08E-09
2	0.0055	-1.32E-09	52	0.2555	-1.23E-09
3	0.0105	-1.28E-09	53	0.2605	-1.39E-09
4	0.0155	-1.14E-09	54	0.2655	-1.46E-09
5	0.0205	-1.04E-09	55	0.2705	-1.39E-09
6	0.0255	-1.07E-09	56	0.2755	-1.25E-09
7	0.0305	-1.24E-09	57	0.2805	-1.12E-09
8	0.0355	-1.44E-09	58	0.2855	-1.09E-09
9	0.0405	-1.55E-09	59	0.2905	-1.17E-09
10	0.0455	-1.47E-09	60	0.2955	-1.30E-09
11	0.0505	-1.26E-09	61	0.3005	-1.39E-09
12	0.0555	-1.05E-09	62	0.3055	-1.39E-09
13	0.0605	-9.91E-10	63	0.3105	-1.30E-09
14	0.0655	-1.11E-09	64	0.3155	-1.18E-09
15	0.0705	-1.31E-09	65	0.3205	-1.11E-09
16	0.0755	-1.46E-09	66	0.3255	-1.14E-09
17	0.0805	-1.45E-09	67	0.3305	-1.24E-09
18	0.0855	-1.28E-09	68	0.3355	-1.35E-09
19	0.0905	-1.09E-09	69	0.3405	-1.39E-09
20	0.0955	-1.01E-09	70	0.3455	-1.35E-09
21	0.1005	-1.11E-09	71	0.3505	-1.25E-09
22	0.1055	-1.33E-09	72	0.3555	-1.16E-09
23	0.1105	-1.52E-09	73	0.3605	-1.13E-09
24	0.1155	-1.54E-09	74	0.3655	-1.18E-09
25	0.1205	-1.38E-09	75	0.3705	-1.27E-09
26	0.1255	-1.12E-09	76	0.3755	-1.35E-09
27	0.1305	-9.38E-10	77	0.3805	-1.36E-09
28	0.1355	-9.45E-10	78	0.3855	-1.31E-09
29	0.1405	-1.14E-09	79	0.3905	-1.22E-09
30	0.1455	-1.40E-09	80	0.3955	-1.17E-09
31	0.1505	-1.56E-09	81	0.4005	-1.17E-09
32	0.1555	-1.53E-09	82	0.4055	-1.23E-09
33	0.1605	-1.33E-09	83	0.4105	-1.30E-09
34	0.1655	-1.10E-09	84	0.4155	-1.33E-09
35	0.1705	-9.89E-10	85	0.4205	-1.32E-09
36	0.1755	-1.05E-09	86	0.4255	-1.26E-09
37	0.1805	-1.24E-09	87	0.4305	-1.20E-09
38	0.1855	-1.43E-09	88	0.4355	-1.18E-09
39	0.1905	-1.48E-09	89	0.4405	-1.20E-09
40	0.1955	-1.38E-09	90	0.4455	-1.26E-09
41	0.2005	-1.19E-09	91	0.4505	-1.31E-09
42	0.2055	-1.05E-09	92	0.4555	-1.32E-09
43	0.2105	-1.04E-09	93	0.4605	-1.29E-09
44	0.2155	-1.18E-09	94	0.4655	-1.24E-09
45	0.2205	-1.37E-09	95	0.4705	-1.20E-09
46	0.2255	-1.49E-09	96	0.4755	-1.19E-09
47	0.2305	-1.45E-09	97	0.4805	-1.23E-09
48	0.2355	-1.30E-09	98	0.4855	-1.28E-09
49	0.2405	-1.11E-09	99	0.4905	-1.31E-09
50	0.2455	-1.02E-09	100	0.4955	-1.30E-09

Table 4.25 – Data points for UZ displacement time history plot, parametric study No.4

APPENDIX R

Time history plots of parametric study No.4

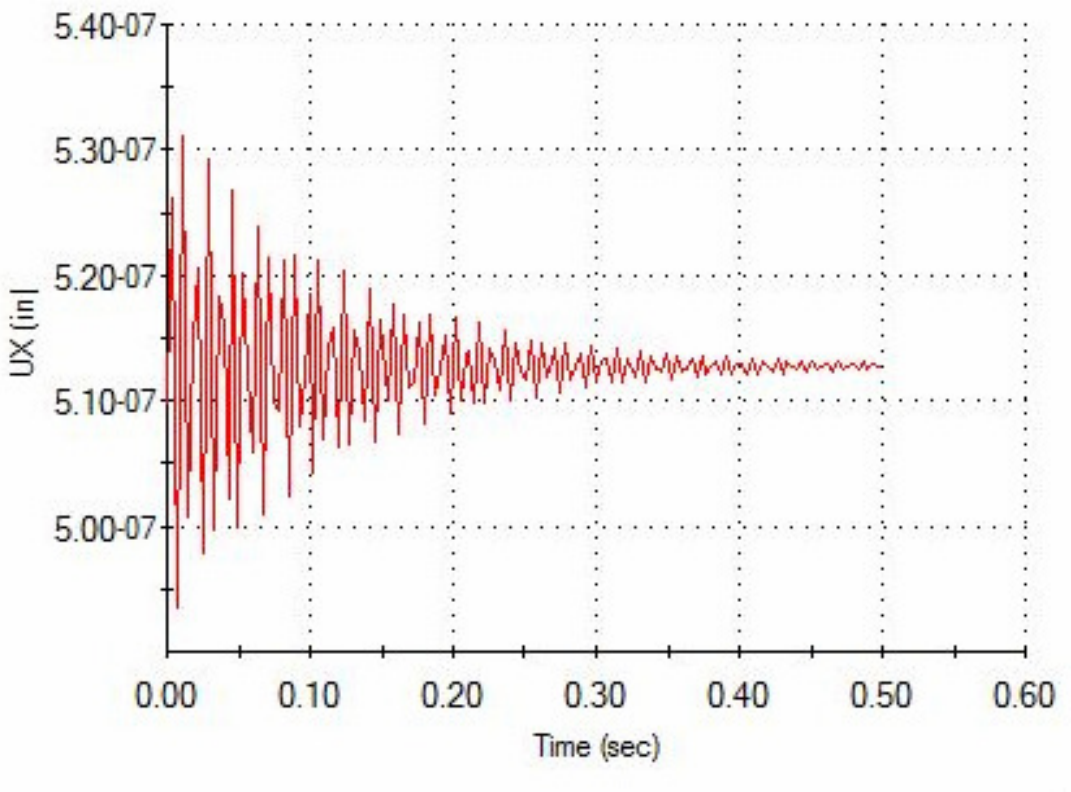

Figure 4.29 – UX displacement time history plot, parametric study No.4

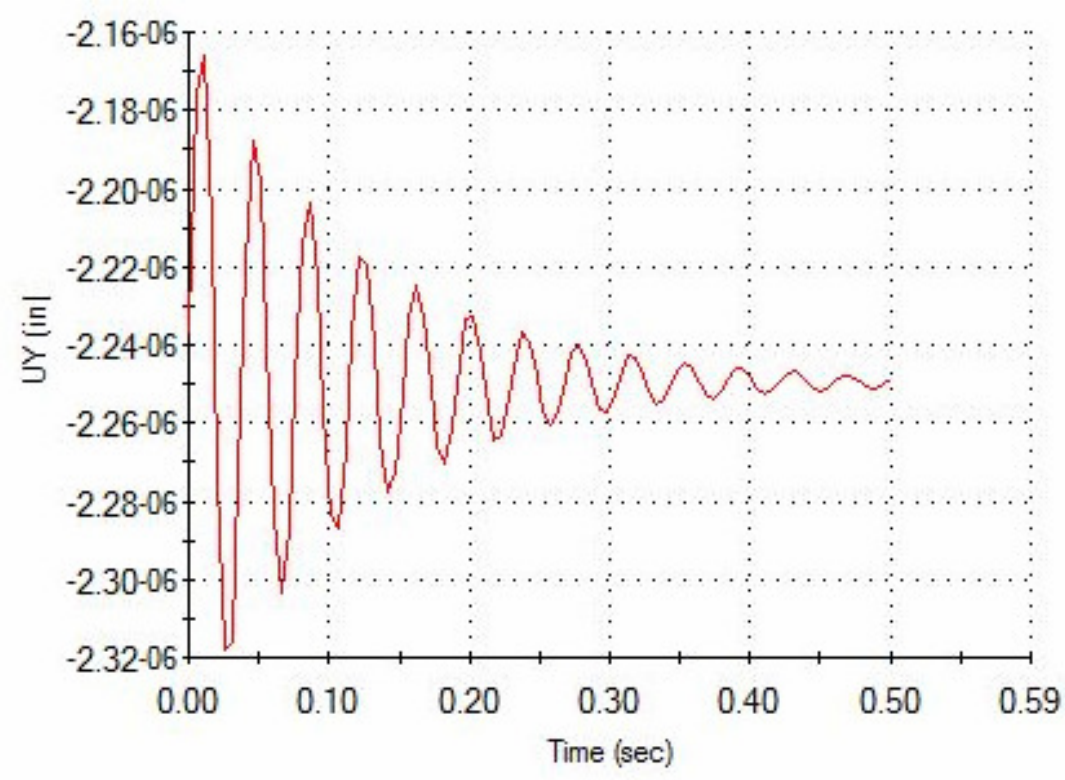

Figure 4.30 – UY displacement time history plot, parametric study No.4

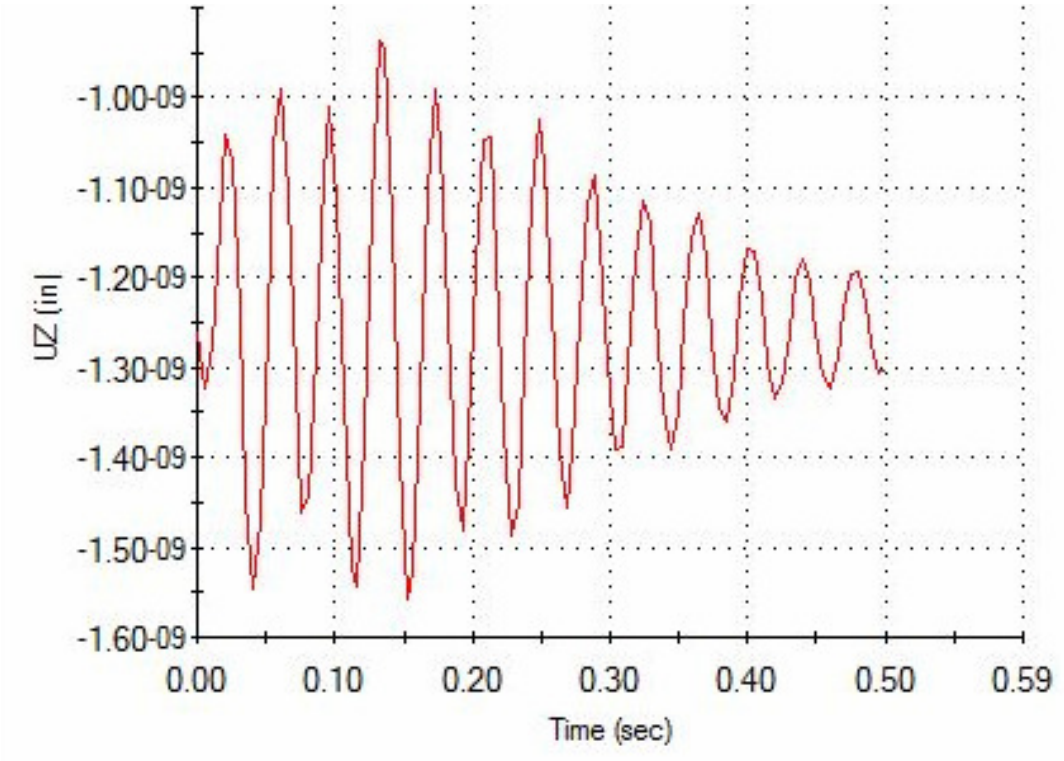

Figure 4.31 – UZ displacement time history plot, parametric study No.4

APPENDIX S

Mode shapes of parametric study No.4

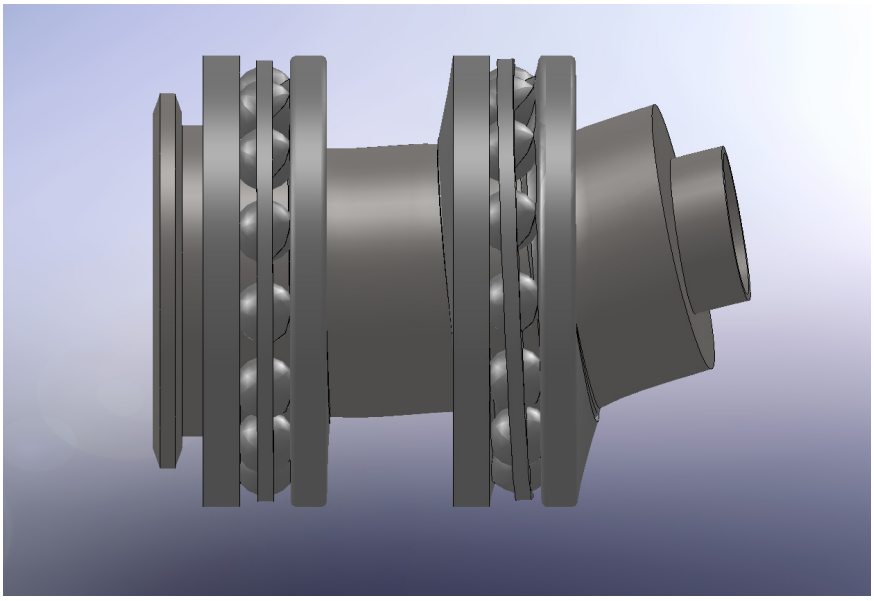

Figure 4.32 - first mode shape, parametric study No.4

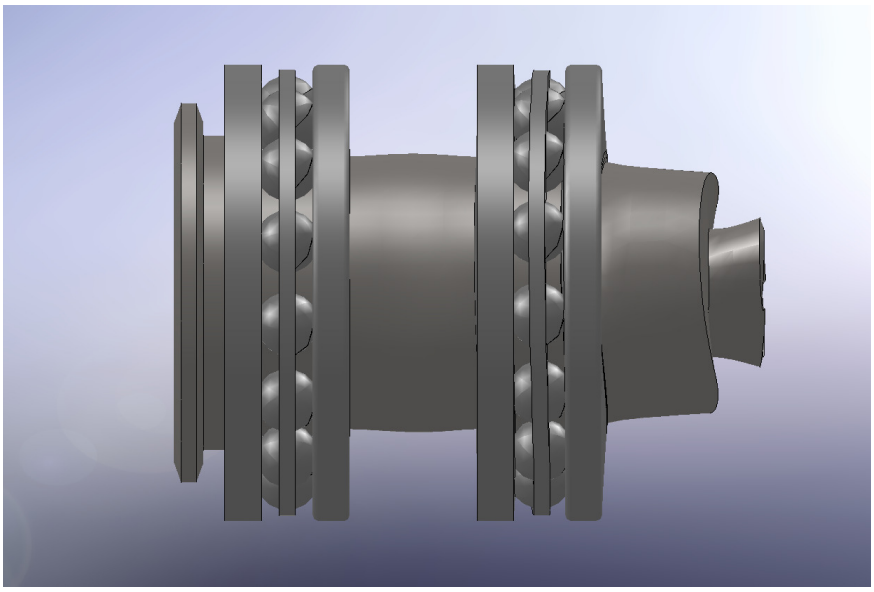

Figure 4.33 - Second mode shape, parametric study No.4

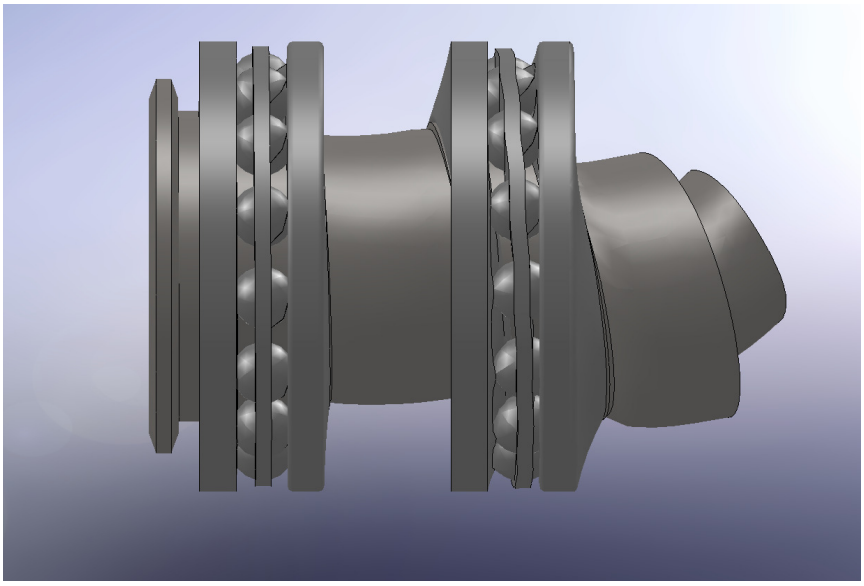

Figure 4.34 - Third mode shape, parametric study No.4

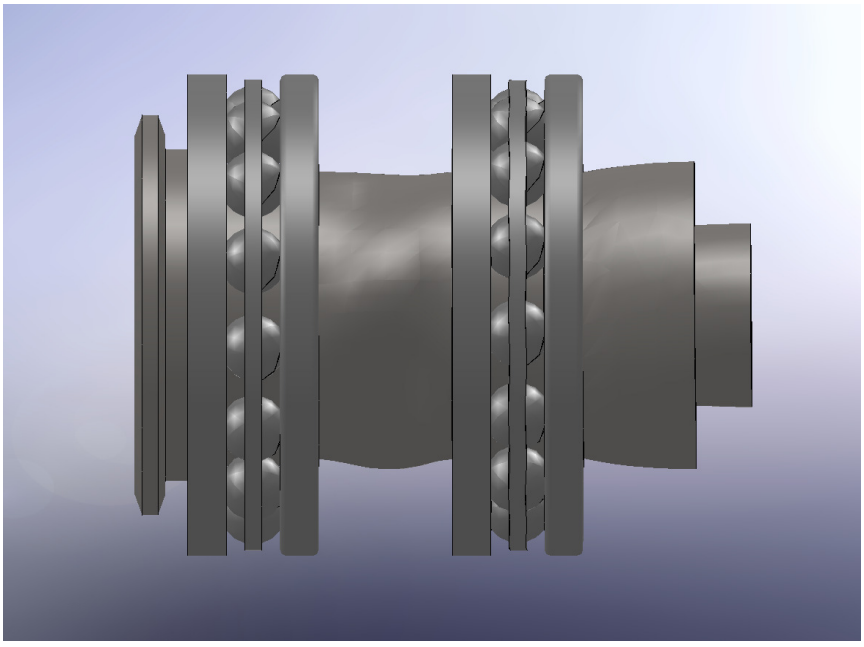

Figure 4.35 - Fourth mode shape, parametric study No.4

APPENDIX T

Data for time history plots of parametric study No.5

Point	Time (sec)	UX (inch)	Point	Time (sec)	UX (inch)	Point	Time (sec)	UX (inch)
1	0.0005	2.31E-06	49	0.1685	2.35E-06	97	0.3365	2.35E-06
2	0.004	2.55E-06	50	0.172	2.35E-06	98	0.34	2.35E-06
3	0.0075	2.35E-06	51	0.1755	2.36E-06	99	0.3435	2.35E-06
4	0.011	2.20E-06	52	0.179	2.35E-06	100	0.347	2.35E-06
5	0.0145	2.36E-06	53	0.1825	2.35E-06	101	0.3505	2.35E-06
6	0.018	2.50E-06	54	0.186	2.35E-06	102	0.354	2.35E-06
7	0.0215	2.31E-06	55	0.1895	2.35E-06	103	0.3575	2.35E-06
8	0.025	2.24E-06	56	0.193	2.36E-06	104	0.361	2.35E-06
9	0.0285	2.42E-06	57	0.1965	2.35E-06	105	0.3645	2.35E-06
10	0.032	2.43E-06	58	0.2	2.36E-06	106	0.368	2.35E-06
11	0.0355	2.30E-06	59	0.2035	2.36E-06	107	0.3715	2.35E-06
12	0.039	2.28E-06	60	0.207	2.35E-06	108	0.375	2.35E-06
13	0.0425	2.42E-06	61	0.2105	2.35E-06	109	0.3785	2.35E-06
14	0.046	2.40E-06	62	0.214	2.35E-06	110	0.382	2.35E-06
15	0.0495	2.29E-06	63	0.2175	2.36E-06	111	0.3855	2.35E-06
16	0.053	2.33E-06	64	0.221	2.35E-06	112	0.389	2.35E-06
17	0.0565	2.40E-06	65	0.2245	2.35E-06	113	0.3925	2.35E-06
18	0.06	2.38E-06	66	0.228	2.35E-06	114	0.396	2.35E-06
19	0.0635	2.29E-06	67	0.2315	2.35E-06	115	0.3995	2.35E-06
20	0.067	2.35E-06	68	0.235	2.35E-06	116	0.403	2.35E-06
21	0.0705	2.40E-06	69	0.2385	2.35E-06	117	0.4065	2.35E-06
22	0.074	2.35E-06	70	0.242	2.36E-06	118	0.41	2.35E-06
23	0.0775	2.32E-06	71	0.2455	2.35E-06	119	0.4135	2.35E-06
24	0.081	2.35E-06	72	0.249	2.35E-06	120	0.417	2.35E-06
25	0.0845	2.39E-06	73	0.2525	2.35E-06	121	0.4205	2.35E-06
26	0.088	2.34E-06	74	0.256	2.35E-06	122	0.424	2.35E-06
27	0.0915	2.33E-06	75	0.2595	2.36E-06	123	0.4275	2.35E-06
28	0.095	2.37E-06	76	0.263	2.35E-06	124	0.431	2.35E-06
29	0.0985	2.37E-06	77	0.2665	2.36E-06	125	0.4345	2.35E-06
30	0.102	2.34E-06	78	0.27	2.35E-06	126	0.438	2.35E-06
31	0.1055	2.33E-06	79	0.2735	2.35E-06	127	0.4415	2.35E-06
32	0.109	2.38E-06	80	0.277	2.35E-06	128	0.445	2.35E-06
33	0.1125	2.36E-06	81	0.2805	2.35E-06	129	0.4485	2.35E-06
34	0.116	2.34E-06	82	0.284	2.36E-06	130	0.452	2.35E-06
35	0.1195	2.35E-06	83	0.2875	2.35E-06	131	0.4555	2.35E-06
36	0.123	2.36E-06	84	0.291	2.36E-06	132	0.459	2.35E-06
37	0.1265	2.36E-06	85	0.2945	2.35E-06	133	0.4625	2.35E-06
38	0.13	2.34E-06	86	0.298	2.35E-06	134	0.466	2.35E-06
39	0.1335	2.36E-06	87	0.3015	2.35E-06	135	0.4695	2.35E-06
40	0.137	2.36E-06	88	0.305	2.35E-06	136	0.473	2.35E-06
41	0.1405	2.35E-06	89	0.3085	2.36E-06	137	0.4765	2.35E-06
42	0.144	2.35E-06	90	0.312	2.35E-06	138	0.48	2.35E-06
43	0.1475	2.35E-06	91	0.3155	2.35E-06	139	0.4835	2.35E-06
44	0.151	2.37E-06	92	0.319	2.35E-06	140	0.487	2.35E-06
45	0.1545	2.35E-06	93	0.3225	2.35E-06	141	0.4905	2.35E-06
46	0.158	2.35E-06	94	0.326	2.35E-06	142	0.494	2.35E-06
47	0.1615	2.36E-06	95	0.3295	2.35E-06	143	0.4975	2.35E-06
48	0.165	2.36E-06	96	0.333	2.36E-06			

Table 4.26 – Data points for UX displacement time history plot, parametric study No.5

Point	Time (sec)	UY (inch)	Point	Time (sec)	UY (inch)
1	0.0005	-1.04E-05	51	0.2505	-1.06E-05
2	0.0055	-9.89E-06	52	0.2555	-1.06E-05
3	0.0105	-1.14E-05	53	0.2605	-1.06E-05
4	0.0155	-1.04E-05	54	0.2655	-1.06E-05
5	0.0205	-1.01E-05	55	0.2705	-1.06E-05
6	0.0255	-1.12E-05	56	0.2755	-1.06E-05
7	0.0305	-1.04E-05	57	0.2805	-1.06E-05
8	0.0355	-1.03E-05	58	0.2855	-1.06E-05
9	0.0405	-1.11E-05	59	0.2905	-1.06E-05
10	0.0455	-1.04E-05	60	0.2955	-1.06E-05
11	0.0505	-1.04E-05	61	0.3005	-1.06E-05
12	0.0555	-1.09E-05	62	0.3055	-1.06E-05
13	0.0605	-1.05E-05	63	0.3105	-1.06E-05
14	0.0655	-1.05E-05	64	0.3155	-1.06E-05
15	0.0705	-1.09E-05	65	0.3205	-1.06E-05
16	0.0755	-1.05E-05	66	0.3255	-1.06E-05
17	0.0805	-1.05E-05	67	0.3305	-1.06E-05
18	0.0855	-1.08E-05	68	0.3355	-1.06E-05
19	0.0905	-1.05E-05	69	0.3405	-1.06E-05
20	0.0955	-1.05E-05	70	0.3455	-1.06E-05
21	0.1005	-1.07E-05	71	0.3505	-1.06E-05
22	0.1055	-1.05E-05	72	0.3555	-1.06E-05
23	0.1105	-1.06E-05	73	0.3605	-1.06E-05
24	0.1155	-1.07E-05	74	0.3655	-1.06E-05
25	0.1205	-1.06E-05	75	0.3705	-1.06E-05
26	0.1255	-1.06E-05	76	0.3755	-1.06E-05
27	0.1305	-1.07E-05	77	0.3805	-1.06E-05
28	0.1355	-1.06E-05	78	0.3855	-1.06E-05
29	0.1405	-1.06E-05	79	0.3905	-1.06E-05
30	0.1455	-1.06E-05	80	0.3955	-1.06E-05
31	0.1505	-1.06E-05	81	0.4005	-1.06E-05
32	0.1555	-1.06E-05	82	0.4055	-1.06E-05
33	0.1605	-1.06E-05	83	0.4105	-1.06E-05
34	0.1655	-1.06E-05	84	0.4155	-1.06E-05
35	0.1705	-1.06E-05	85	0.4205	-1.06E-05
36	0.1755	-1.06E-05	86	0.4255	-1.06E-05
37	0.1805	-1.06E-05	87	0.4305	-1.06E-05
38	0.1855	-1.06E-05	88	0.4355	-1.06E-05
39	0.1905	-1.06E-05	89	0.4405	-1.06E-05
40	0.1955	-1.06E-05	90	0.4455	-1.06E-05
41	0.2005	-1.06E-05	91	0.4505	-1.06E-05
42	0.2055	-1.06E-05	92	0.4555	-1.06E-05
43	0.2105	-1.06E-05	93	0.4605	-1.06E-05
44	0.2155	-1.06E-05	94	0.4655	-1.06E-05
45	0.2205	-1.06E-05	95	0.4705	-1.06E-05
46	0.2255	-1.06E-05	96	0.4755	-1.06E-05
47	0.2305	-1.06E-05	97	0.4805	-1.06E-05
48	0.2355	-1.06E-05	98	0.4855	-1.06E-05
49	0.2405	-1.06E-05	99	0.4905	-1.06E-05
50	0.2455	-1.06E-05	100	0.4955	-1.06E-05

Table 4.27 – Data points for UY displacement time history plot, parametric study No.5

Point	Time (sec)	UZ (inch)	Point	Time (sec)	UZ (inch)
1	0.0005	1.59E-08	51	0.2505	1.61E-08
2	0.0055	1.58E-08	52	0.2555	1.63E-08
3	0.0105	1.76E-08	53	0.2605	1.65E-08
4	0.0155	1.37E-08	54	0.2655	1.61E-08
5	0.0205	1.76E-08	55	0.2705	1.63E-08
6	0.0255	1.77E-08	56	0.2755	1.64E-08
7	0.0305	1.32E-08	57	0.2805	1.61E-08
8	0.0355	1.87E-08	58	0.2855	1.63E-08
9	0.0405	1.72E-08	59	0.2905	1.64E-08
10	0.0455	1.29E-08	60	0.2955	1.62E-08
11	0.0505	1.89E-08	61	0.3005	1.63E-08
12	0.0555	1.66E-08	62	0.3055	1.64E-08
13	0.0605	1.31E-08	63	0.3105	1.62E-08
14	0.0655	1.90E-08	64	0.3155	1.63E-08
15	0.0705	1.64E-08	65	0.3205	1.63E-08
16	0.0755	1.37E-08	66	0.3255	1.62E-08
17	0.0805	1.90E-08	67	0.3305	1.63E-08
18	0.0855	1.61E-08	68	0.3355	1.63E-08
19	0.0905	1.41E-08	69	0.3405	1.62E-08
20	0.0955	1.86E-08	70	0.3455	1.63E-08
21	0.1005	1.58E-08	71	0.3505	1.63E-08
22	0.1055	1.45E-08	72	0.3555	1.62E-08
23	0.1105	1.83E-08	73	0.3605	1.63E-08
24	0.1155	1.58E-08	74	0.3655	1.63E-08
25	0.1205	1.51E-08	75	0.3705	1.62E-08
26	0.1255	1.81E-08	76	0.3755	1.63E-08
27	0.1305	1.57E-08	77	0.3805	1.63E-08
28	0.1355	1.53E-08	78	0.3855	1.63E-08
29	0.1405	1.77E-08	79	0.3905	1.63E-08
30	0.1455	1.56E-08	80	0.3955	1.63E-08
31	0.1505	1.55E-08	81	0.4005	1.63E-08
32	0.1555	1.74E-08	82	0.4055	1.63E-08
33	0.1605	1.58E-08	83	0.4105	1.63E-08
34	0.1655	1.58E-08	84	0.4155	1.62E-08
35	0.1705	1.73E-08	85	0.4205	1.63E-08
36	0.1755	1.58E-08	86	0.4255	1.63E-08
37	0.1805	1.59E-08	87	0.4305	1.63E-08
38	0.1855	1.70E-08	88	0.4355	1.63E-08
39	0.1905	1.58E-08	89	0.4405	1.63E-08
40	0.1955	1.60E-08	90	0.4455	1.63E-08
41	0.2005	1.68E-08	91	0.4505	1.63E-08
42	0.2055	1.59E-08	92	0.4555	1.63E-08
43	0.2105	1.62E-08	93	0.4605	1.63E-08
44	0.2155	1.68E-08	94	0.4655	1.63E-08
45	0.2205	1.60E-08	95	0.4705	1.63E-08
46	0.2255	1.62E-08	96	0.4755	1.63E-08
47	0.2305	1.66E-08	97	0.4805	1.63E-08
48	0.2355	1.60E-08	98	0.4855	1.63E-08
49	0.2405	1.62E-08	99	0.4905	1.63E-08
50	0.2455	1.65E-08	100	0.4955	1.63E-08

Table 4.28 – Data points for UZ displacement time history plot, parametric study No.5

APPENDIX U

Time history plots of parametric study No.5

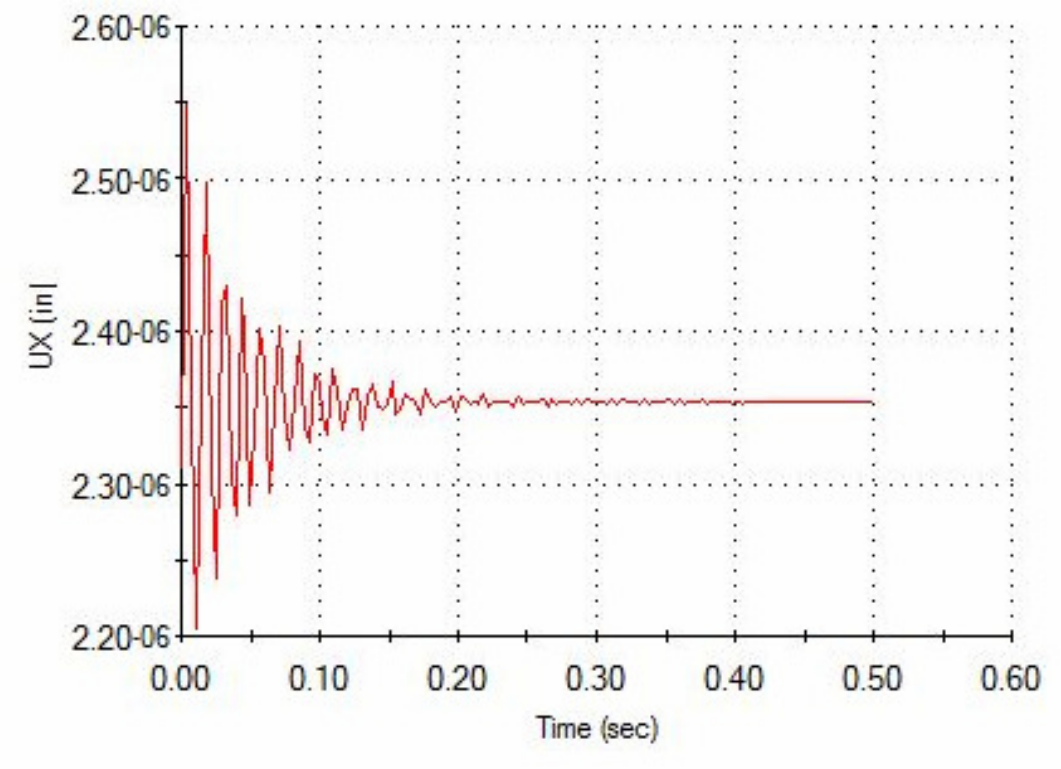

Figure 4.36 – UX displacement time history plot, parametric study No.5

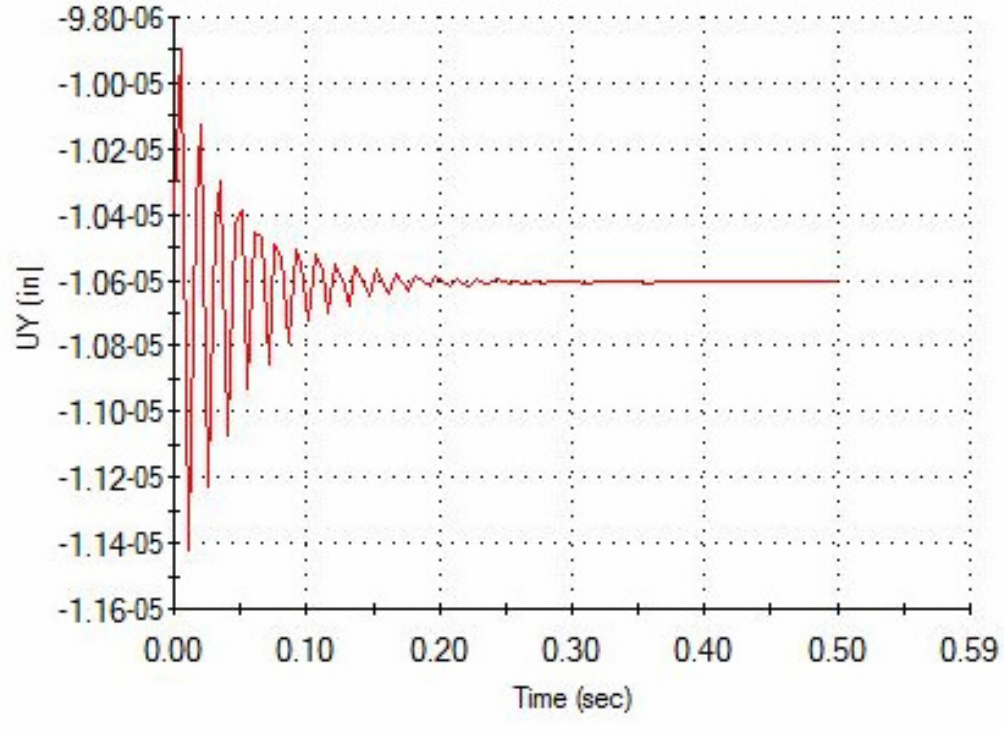

Figure 4.37 – UY displacement time history plot, parametric study No.5

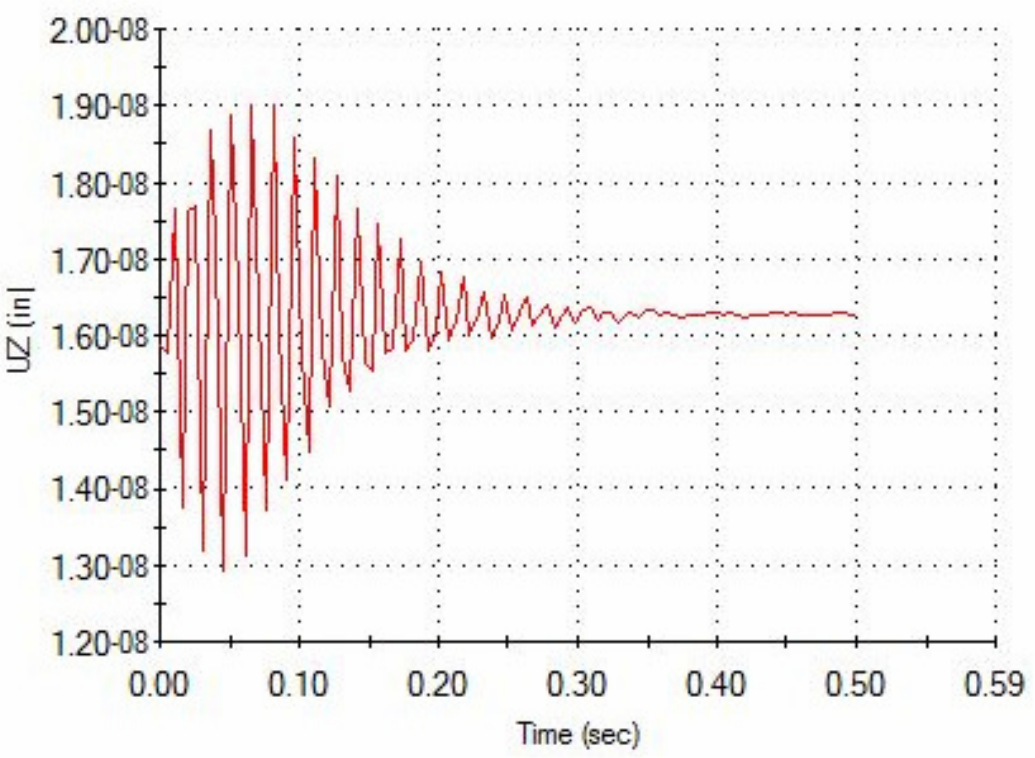

Figure 4.38 – UZ displacement time history plot, parametric study No.5

APPENDIX V

Mode shapes of parametric study No.5

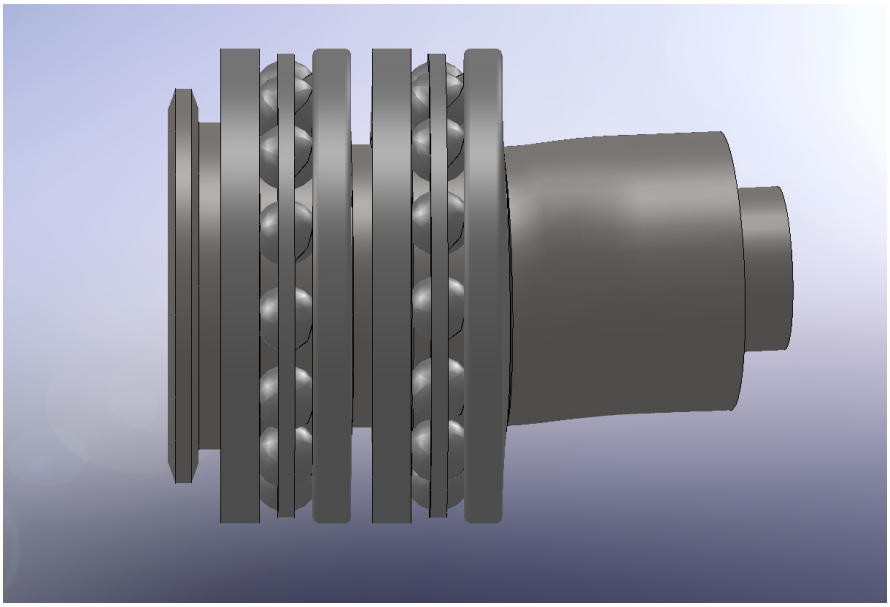

Figure 4.39 – First mode shape, parametric study No.5

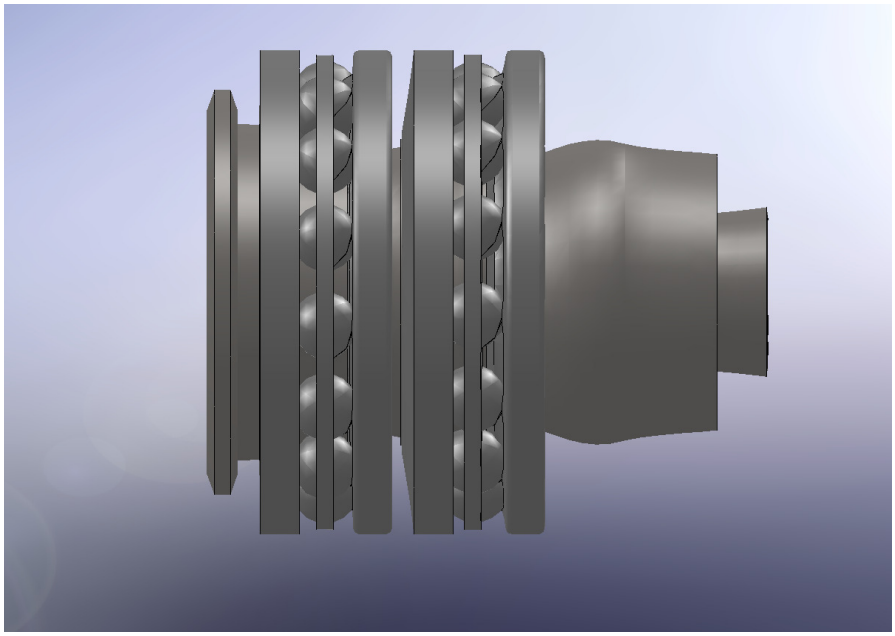

Figure 4.40 – Second mode shape, parametric study No.5

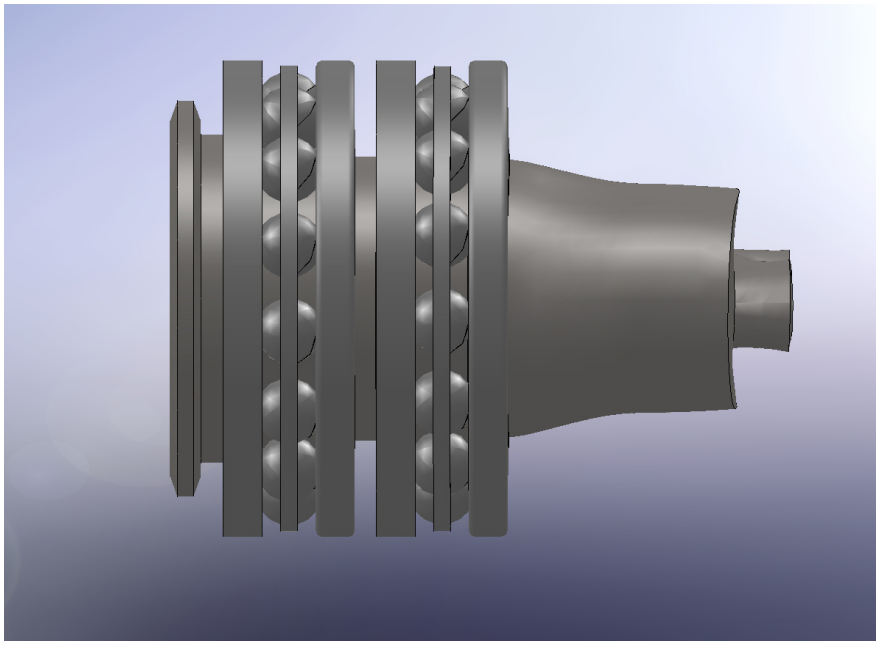

Figure 4.41 – Third mode shape, parametric study No.5

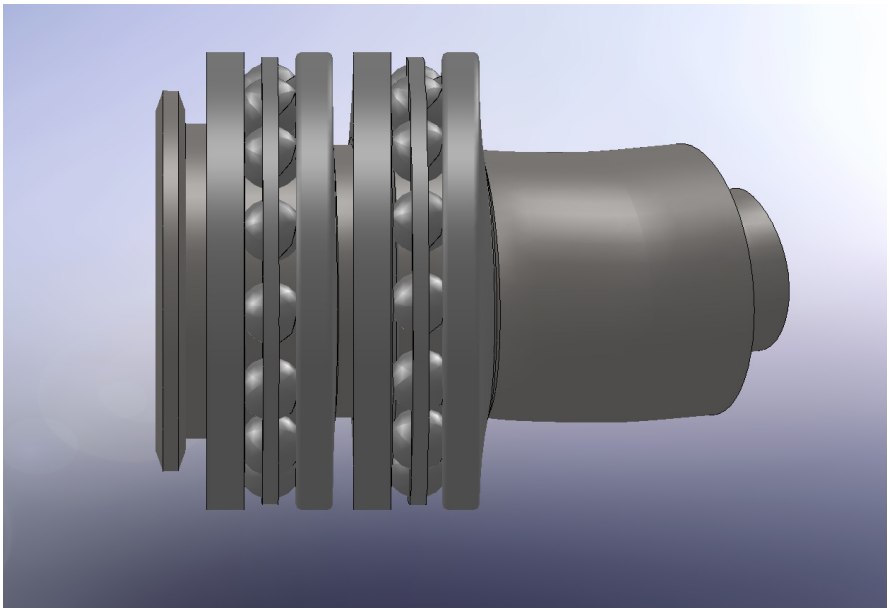

Figure 4.42 – Fourth mode shape, parametric study No.5

APPENDIX W

Data points for time history plots of parametric study No.6

Point	Time (sec)	UX (inch)	Point	Time (sec)	UX (inch)	Point	Time (sec)	UX (inch)
1	0.0005	1.91E-07	49	0.1685	1.92E-07	97	0.3365	1.92E-07
2	0.004	1.94E-07	50	0.172	1.92E-07	98	0.34	1.91E-07
3	0.0075	1.88E-07	51	0.1755	1.91E-07	99	0.3435	1.92E-07
4	0.011	1.96E-07	52	0.179	1.93E-07	100	0.347	1.92E-07
5	0.0145	1.87E-07	53	0.1825	1.90E-07	101	0.3505	1.91E-07
6	0.018	1.96E-07	54	0.186	1.94E-07	102	0.354	1.92E-07
7	0.0215	1.89E-07	55	0.1895	1.90E-07	103	0.3575	1.91E-07
8	0.025	1.93E-07	56	0.193	1.93E-07	104	0.361	1.92E-07
9	0.0285	1.92E-07	57	0.1965	1.91E-07	105	0.3645	1.91E-07
10	0.032	1.90E-07	58	0.2	1.92E-07	106	0.368	1.92E-07
11	0.0355	1.95E-07	59	0.2035	1.92E-07	107	0.3715	1.92E-07
12	0.039	1.88E-07	60	0.207	1.91E-07	108	0.375	1.91E-07
13	0.0425	1.96E-07	61	0.2105	1.93E-07	109	0.3785	1.92E-07
14	0.046	1.88E-07	62	0.214	1.90E-07	110	0.382	1.91E-07
15	0.0495	1.95E-07	63	0.2175	1.93E-07	111	0.3855	1.92E-07
16	0.053	1.90E-07	64	0.221	1.90E-07	112	0.389	1.91E-07
17	0.0565	1.92E-07	65	0.2245	1.92E-07	113	0.3925	1.92E-07
18	0.06	1.93E-07	66	0.228	1.91E-07	114	0.396	1.91E-07
19	0.0635	1.89E-07	67	0.2315	1.91E-07	115	0.3995	1.92E-07
20	0.067	1.95E-07	68	0.235	1.93E-07	116	0.403	1.92E-07
21	0.0705	1.88E-07	69	0.2385	1.90E-07	117	0.4065	1.91E-07
22	0.074	1.95E-07	70	0.242	1.93E-07	118	0.41	1.92E-07
23	0.0775	1.89E-07	71	0.2455	1.90E-07	119	0.4135	1.91E-07
24	0.081	1.93E-07	72	0.249	1.93E-07	120	0.417	1.92E-07
25	0.0845	1.91E-07	73	0.2525	1.91E-07	121	0.4205	1.91E-07
26	0.088	1.91E-07	74	0.256	1.92E-07	122	0.424	1.92E-07
27	0.0915	1.94E-07	75	0.2595	1.92E-07	123	0.4275	1.92E-07
28	0.095	1.89E-07	76	0.263	1.91E-07	124	0.431	1.92E-07
29	0.0985	1.95E-07	77	0.2665	1.93E-07	125	0.4345	1.92E-07
30	0.102	1.89E-07	78	0.27	1.90E-07	126	0.438	1.91E-07
31	0.1055	1.94E-07	79	0.2735	1.93E-07	127	0.4415	1.92E-07
32	0.109	1.90E-07	80	0.277	1.91E-07	128	0.445	1.91E-07
33	0.1125	1.92E-07	81	0.2805	1.92E-07	129	0.4485	1.92E-07
34	0.116	1.92E-07	82	0.284	1.91E-07	130	0.452	1.91E-07
35	0.1195	1.90E-07	83	0.2875	1.92E-07	131	0.4555	1.92E-07
36	0.123	1.94E-07	84	0.291	1.92E-07	132	0.459	1.92E-07
37	0.1265	1.89E-07	85	0.2945	1.91E-07	133	0.4625	1.91E-07
38	0.13	1.94E-07	86	0.298	1.93E-07	134	0.466	1.92E-07
39	0.1335	1.89E-07	87	0.3015	1.91E-07	135	0.4695	1.91E-07
40	0.137	1.93E-07	88	0.305	1.93E-07	136	0.473	1.92E-07
41	0.1405	1.91E-07	89	0.3085	1.91E-07	137	0.4765	1.91E-07
42	0.144	1.91E-07	90	0.312	1.92E-07	138	0.48	1.92E-07
43	0.1475	1.93E-07	91	0.3155	1.92E-07	139	0.4835	1.91E-07
44	0.151	1.90E-07	92	0.319	1.91E-07	140	0.487	1.92E-07
45	0.1545	1.94E-07	93	0.3225	1.92E-07	141	0.4905	1.92E-07
46	0.158	1.89E-07	94	0.326	1.91E-07	142	0.494	1.91E-07
47	0.1615	1.94E-07	95	0.3295	1.93E-07	143	0.4975	1.92E-07
48	0.165	1.90E-07	96	0.333	1.91E-07			

Table 4.29 – Data points for UX displacement time history plot, parametric study No.6

Point	Time (sec)	UY (inch)	Point	Time (sec)	UY (inch)
1	0.0005	-1.99E-07	51	0.2505	-1.99E-07
2	0.0055	-1.96E-07	52	0.2555	-1.99E-07
3	0.0105	-1.95E-07	53	0.2605	-2.00E-07
4	0.0155	-1.95E-07	54	0.2655	-2.00E-07
5	0.0205	-1.96E-07	55	0.2705	-2.01E-07
6	0.0255	-1.98E-07	56	0.2755	-2.01E-07
7	0.0305	-2.01E-07	57	0.2805	-2.00E-07
8	0.0355	-2.03E-07	58	0.2855	-2.00E-07
9	0.0405	-2.04E-07	59	0.2905	-1.99E-07
10	0.0455	-2.04E-07	60	0.2955	-1.99E-07
11	0.0505	-2.02E-07	61	0.3005	-1.98E-07
12	0.0555	-2.00E-07	62	0.3055	-1.99E-07
13	0.0605	-1.98E-07	63	0.3105	-1.99E-07
14	0.0655	-1.96E-07	64	0.3155	-2.00E-07
15	0.0705	-1.96E-07	65	0.3205	-2.00E-07
16	0.0755	-1.96E-07	66	0.3255	-2.00E-07
17	0.0805	-1.98E-07	67	0.3305	-2.00E-07
18	0.0855	-2.00E-07	68	0.3355	-2.00E-07
19	0.0905	-2.01E-07	69	0.3405	-2.00E-07
20	0.0955	-2.02E-07	70	0.3455	-1.99E-07
21	0.1005	-2.03E-07	71	0.3505	-1.99E-07
22	0.1055	-2.02E-07	72	0.3555	-1.99E-07
23	0.1105	-2.01E-07	73	0.3605	-1.99E-07
24	0.1155	-1.99E-07	74	0.3655	-1.99E-07
25	0.1205	-1.98E-07	75	0.3705	-1.99E-07
26	0.1255	-1.97E-07	76	0.3755	-2.00E-07
27	0.1305	-1.97E-07	77	0.3805	-2.00E-07
28	0.1355	-1.98E-07	78	0.3855	-2.00E-07
29	0.1405	-1.99E-07	79	0.3905	-2.00E-07
30	0.1455	-2.00E-07	80	0.3955	-2.00E-07
31	0.1505	-2.01E-07	81	0.4005	-2.00E-07
32	0.1555	-2.02E-07	82	0.4055	-1.99E-07
33	0.1605	-2.02E-07	83	0.4105	-1.99E-07
34	0.1655	-2.01E-07	84	0.4155	-1.99E-07
35	0.1705	-2.00E-07	85	0.4205	-1.99E-07
36	0.1755	-1.99E-07	86	0.4255	-1.99E-07
37	0.1805	-1.98E-07	87	0.4305	-2.00E-07
38	0.1855	-1.98E-07	88	0.4355	-2.00E-07
39	0.1905	-1.98E-07	89	0.4405	-2.00E-07
40	0.1955	-1.99E-07	90	0.4455	-2.00E-07
41	0.2005	-2.00E-07	91	0.4505	-2.00E-07
42	0.2055	-2.00E-07	92	0.4555	-2.00E-07
43	0.2105	-2.01E-07	93	0.4605	-1.99E-07
44	0.2155	-2.01E-07	94	0.4655	-1.99E-07
45	0.2205	-2.01E-07	95	0.4705	-1.99E-07
46	0.2255	-2.00E-07	96	0.4755	-1.99E-07
47	0.2305	-1.99E-07	97	0.4805	-1.99E-07
48	0.2355	-1.99E-07	98	0.4855	-1.99E-07
49	0.2405	-1.98E-07	99	0.4905	-2.00E-07
50	0.2455	-1.98E-07	100	0.4955	-2.00E-07

Table 4.30 – Data points for UY displacement time history plot, parametric study No.6

Point	Time (sec)	UZ (inch)	Point	Time (sec)	UZ (inch)
1	0.0005	-2.51E-07	51	0.2505	-2.51E-07
2	0.0055	-2.48E-07	52	0.2555	-2.51E-07
3	0.0105	-2.46E-07	53	0.2605	-2.52E-07
4	0.0155	-2.46E-07	54	0.2655	-2.53E-07
5	0.0205	-2.47E-07	55	0.2705	-2.53E-07
6	0.0255	-2.50E-07	56	0.2755	-2.53E-07
7	0.0305	-2.53E-07	57	0.2805	-2.53E-07
8	0.0355	-2.56E-07	58	0.2855	-2.52E-07
9	0.0405	-2.57E-07	59	0.2905	-2.51E-07
10	0.0455	-2.57E-07	60	0.2955	-2.51E-07
11	0.0505	-2.55E-07	61	0.3005	-2.50E-07
12	0.0555	-2.53E-07	62	0.3055	-2.51E-07
13	0.0605	-2.50E-07	63	0.3105	-2.51E-07
14	0.0655	-2.48E-07	64	0.3155	-2.52E-07
15	0.0705	-2.47E-07	65	0.3205	-2.52E-07
16	0.0755	-2.48E-07	66	0.3255	-2.53E-07
17	0.0805	-2.49E-07	67	0.3305	-2.53E-07
18	0.0855	-2.52E-07	68	0.3355	-2.53E-07
19	0.0905	-2.54E-07	69	0.3405	-2.52E-07
20	0.0955	-2.55E-07	70	0.3455	-2.52E-07
21	0.1005	-2.56E-07	71	0.3505	-2.51E-07
22	0.1055	-2.55E-07	72	0.3555	-2.51E-07
23	0.1105	-2.53E-07	73	0.3605	-2.51E-07
24	0.1155	-2.51E-07	74	0.3655	-2.51E-07
25	0.1205	-2.50E-07	75	0.3705	-2.52E-07
26	0.1255	-2.49E-07	76	0.3755	-2.52E-07
27	0.1305	-2.48E-07	77	0.3805	-2.52E-07
28	0.1355	-2.49E-07	78	0.3855	-2.53E-07
29	0.1405	-2.51E-07	79	0.3905	-2.53E-07
30	0.1455	-2.53E-07	80	0.3955	-2.52E-07
31	0.1505	-2.54E-07	81	0.4005	-2.52E-07
32	0.1555	-2.55E-07	82	0.4055	-2.51E-07
33	0.1605	-2.54E-07	83	0.4105	-2.51E-07
34	0.1655	-2.54E-07	84	0.4155	-2.51E-07
35	0.1705	-2.52E-07	85	0.4205	-2.51E-07
36	0.1755	-2.51E-07	86	0.4255	-2.51E-07
37	0.1805	-2.50E-07	87	0.4305	-2.52E-07
38	0.1855	-2.49E-07	88	0.4355	-2.52E-07
39	0.1905	-2.50E-07	89	0.4405	-2.52E-07
40	0.1955	-2.51E-07	90	0.4455	-2.52E-07
41	0.2005	-2.52E-07	91	0.4505	-2.52E-07
42	0.2055	-2.53E-07	92	0.4555	-2.52E-07
43	0.2105	-2.54E-07	93	0.4605	-2.52E-07
44	0.2155	-2.54E-07	94	0.4655	-2.51E-07
45	0.2205	-2.53E-07	95	0.4705	-2.51E-07
46	0.2255	-2.53E-07	96	0.4755	-2.51E-07
47	0.2305	-2.51E-07	97	0.4805	-2.51E-07
48	0.2355	-2.51E-07	98	0.4855	-2.52E-07
49	0.2405	-2.50E-07	99	0.4905	-2.52E-07
50	0.2455	-2.50E-07	100	0.4955	-2.52E-07

Table 4.31 – Data points for UZ displacement time history plot, parametric study No.6

APPENDIX X

Time history plots of parametric study No.6

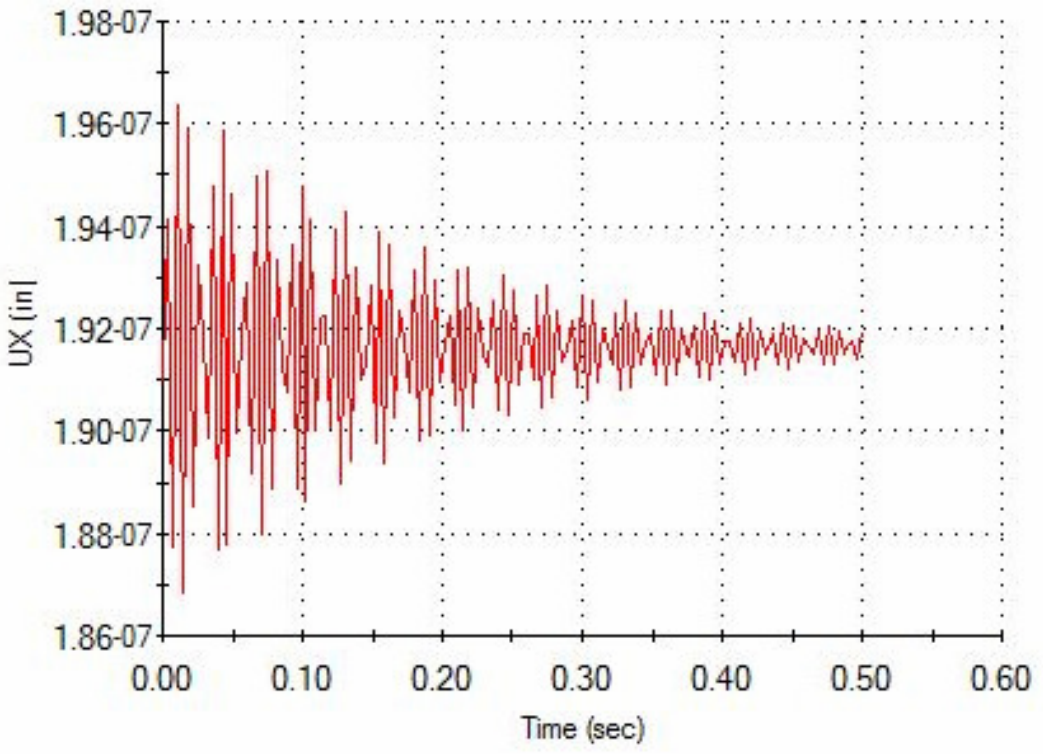

Figure 4.43 – UX displacement time history plot, parametric study No.6

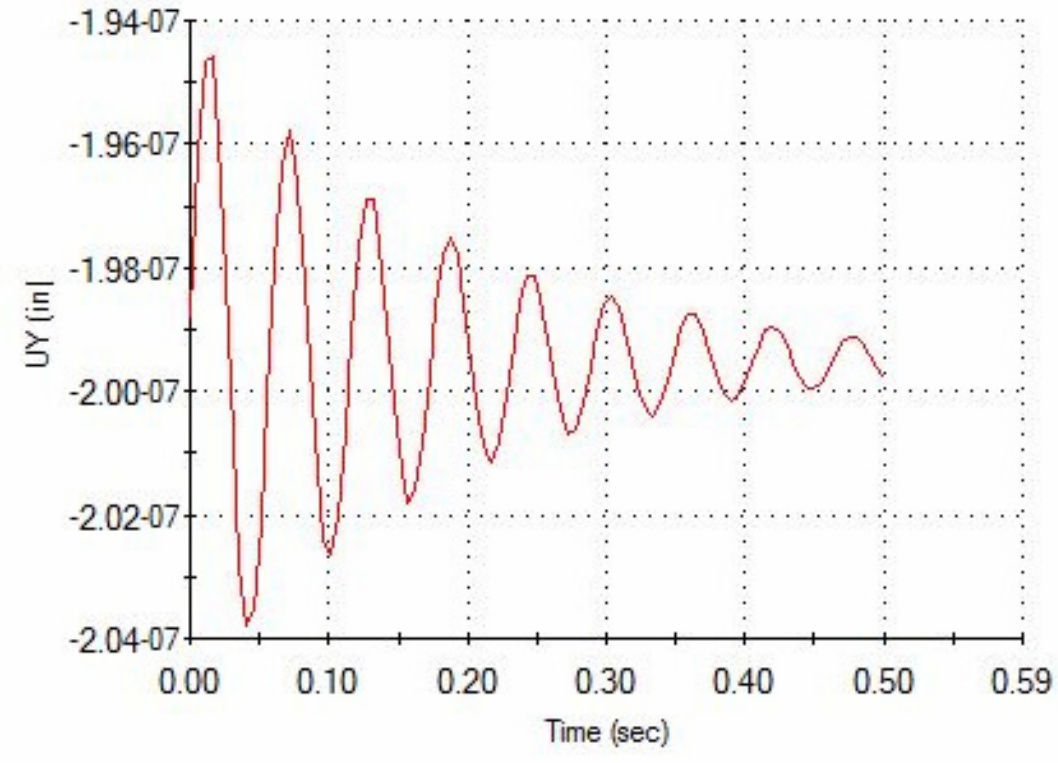

Figure 4.44 – UY displacement time history plot, parametric study No.6

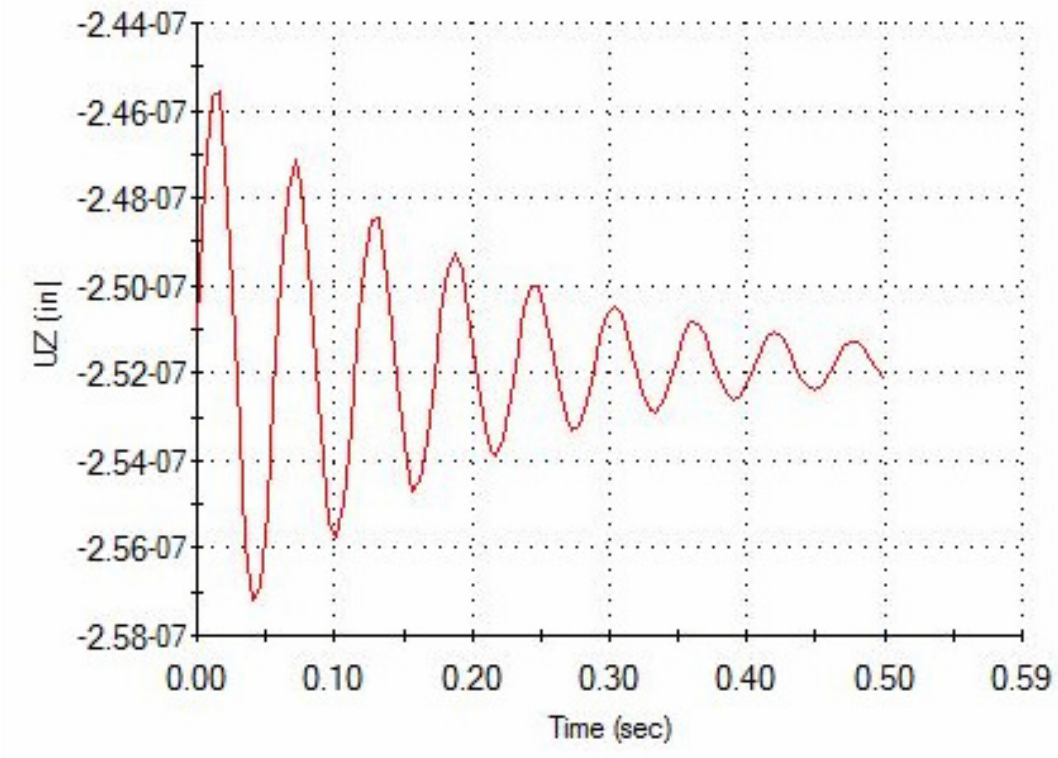

Figure 4.45 – UZ displacement time history plot, parametric study No.6

APPENDIX Y

Mode shapes of parametric study No.6

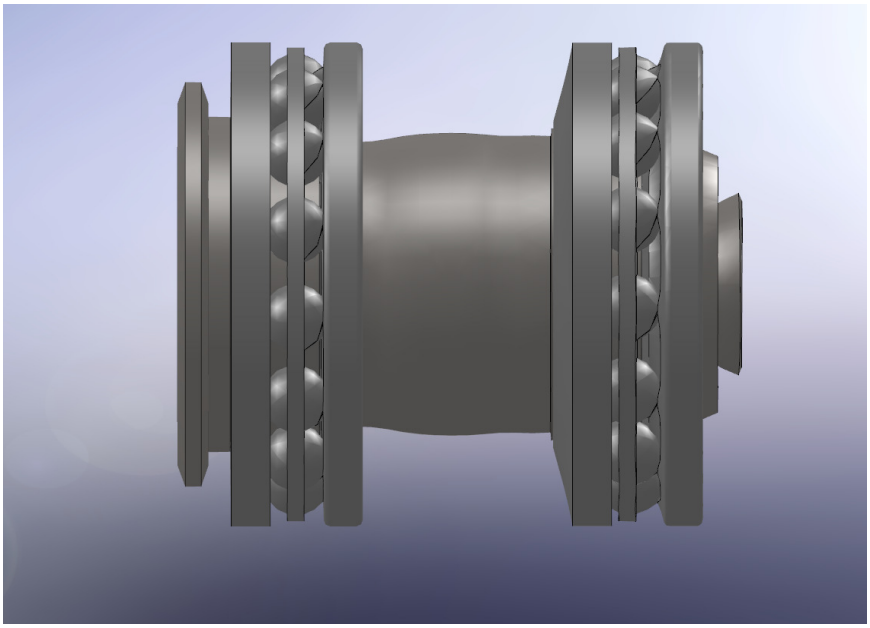

Figure 4.46 – First mode shape, parametric study No.6

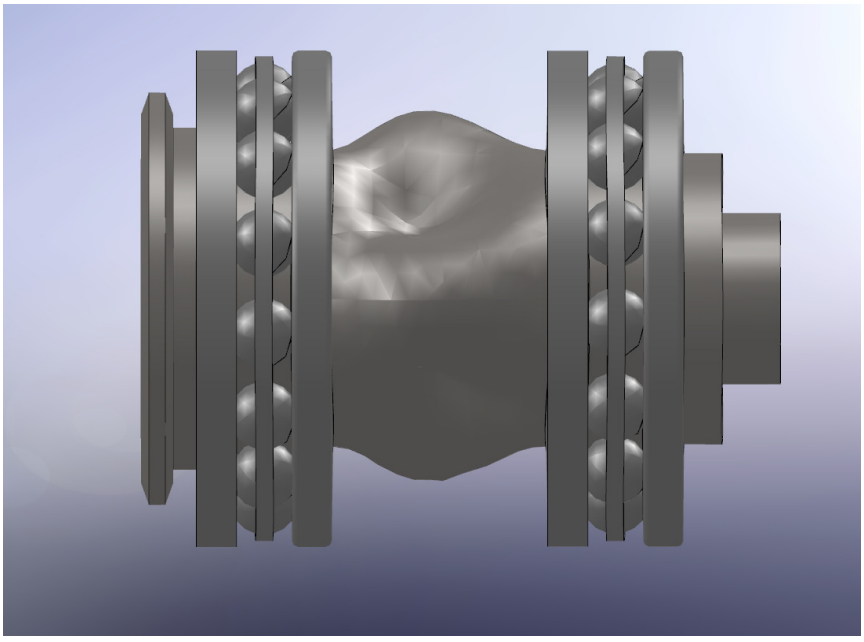

Figure 4.47 – Second mode shape, parametric study No.6

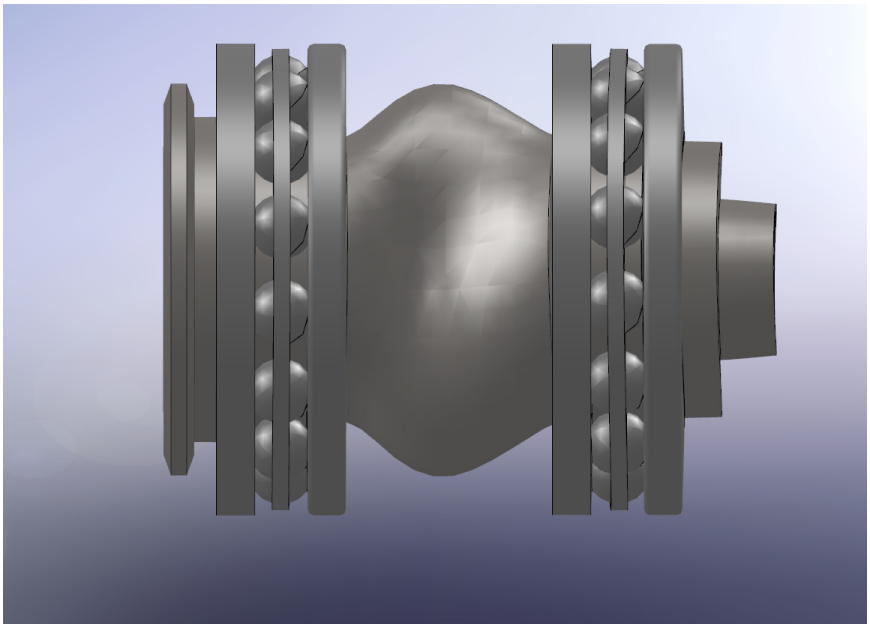

Figure 4.48 – Third mode shape, parametric study No.6

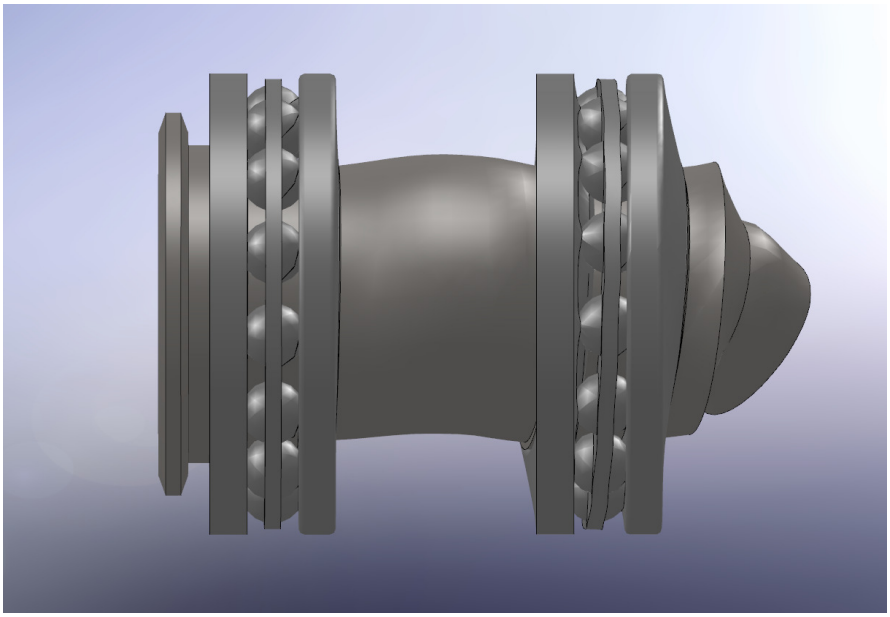

Figure 4.49– Fourth mode shape, parametric study No.6